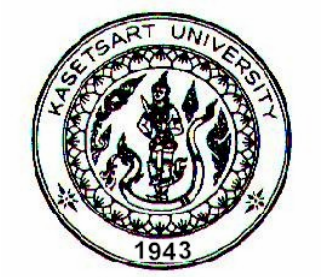

THESIS

DETERMINATION OF CADMIUM(II) AND ALUMINIUM(III) AS 8-HYDROXYQUINOLINE-5-SULPHONATE COMPLEXES BY SYNCHRONOUS-SCANNING FLUORESCENCE SPECTROMETRY

NISA NAUANGCHAMNONG

GRADUATE SCHOOL, KASETSART UNIVERSITY
2008

THESIS APPROVAL

GRADUATE SCHOOL, KASETSART UNIVERSITY

Master of Science (Chemistry)
DEGREE

Chemistry	Chemistry
FIELD	**DEPARTMENT**

TITLE: Determination of Cadmium(II) and Aluminium(III) as 8-Hydroxy-quinoline-5-sulphonate Complexes by Synchronous-scanning Fluorescence Spectrometry

NAME: Miss Nisa Nauangchamnong

THIS THESIS HAS BEEN ACCEPTED BY

P. Pornsinlapatip — **THESIS ADVISOR**
(Miss Pornpun Pornsinlapatip, Ph.D.)

L. Charnsethikul — **COMMITTEE MEMBER**
(Assistant Professor Saijai Charnsethikul, M.S.)

Apisit Songsasen — **COMMITTEE MEMBER**
(Associate Professor Apisit Songsasen, Ph.D.)

Noojaree Prasitpan — **DEPARTMENT HEAD**
(Assistant Professor Noojaree Prasitpan, Ph.D.)

APPROVED BY THE GRADUATE SCHOOL ON 5 June 2008

Gunjana Theeragool — **DEAN**
(Associate Professor Gunjana Theeragool, D.Agr.)

THESIS

DETERMINATION OF CADMIUM(II) AND ALUMINIUM(III) AS 8-HYDROXYQUINOLINE-5-SULPHONATE COMPLEXES BY SYNCHRONOUS-SCANNING FLUORESCENCE SPECTROMETRY

NISA NAUANGCHAMNONG

A Thesis Submitted in Partial Fulfillment of
the Requirements for the Degree of
Master of Science (Chemistry)
Graduate School, Kasetsart University
2008

Nisa Nuangchamnong 2008: Determination of Cadmium(II) and Aluminium(III) as 8-Hydroxyquinoline-5-sulphonate Complexes by Synchronous-scanning Fluorescence Spectrometry. Master of Science (Chemistry), Major Field: Chemistry, Department of Chemistry. Thesis Advisor: Miss Pornpun Pornsinlapatip, Ph.D. 113 pages.

A synchronous-scanning fluorescence (SSF) method was first developed for simultaneous determination of cadmium(II) and aluminium(III) based upon the formation of fluorescent chelates with 8-hydroxyquinoline-5-sulphonic acid (HQS). Under the optimised conditions Cd(II)-HQS and Al(III)-HQS emitted fluorescence at λ_{em} of 519 nm and 497 nm, respectively. Strong interference between the two metals was observed. SSF and derivative SSF methods were applied in an attempt to resolve the interference without prior chemical separation.

Instrumental parameters were optimised. Wavelength intervals of 120 nm and 115 nm were used in SSF of Cd(II)-HQS and Al(III)-HQS, respectively. The resolution of spectral peaks was improved but inadequate for use in binary mixture. Zero-crossing wavelengths in D1SSF and D2SSF spectra of Cd(II)-HQS were used for signal measurement of Al(III)-HQS, and vice versa. The D1SSF zero-crossing wavelengths of Cd(II) and Al(III) were 302 nm and 438 nm, and those of D2SSF were 400 nm and 443 nm, respectively. The resolution and the independence of signals were improved considerably compared to those obtained from conventional fluorimetry (CF). The determination of Cd(II) and Al(III) were accomplished by means of external calibration method. The calibration graphs of D1SSF and D2SSF were linear over 0-1000 $\mu g\ l^{-1}$ of metals. Good correlation coefficient was obtained: 0.9916 and 0.9628 for Cd(II); and 0.8909 and 0.9560 for Al(III), respectively. The analysis of synthetic samples yielded quite satisfactory results. The methods were simple, rapid, and cost-effective.

Nisa Nuangchamnong P. Pornsinlapatip 3 / 6 / 2008

Student's signature Thesis Advisor's signature

ACKNOWLEDGEMENTS

I would like to express my gratitude to my supervisor, Dr. Pornpun Pornsinlapatip for her kindness, encouragement and suggestion throughout this work; and to my thesis committee, Assistant Professor Saijai Charnsethikul and Associate Professor Dr. Apisit Songsasen, for their kind guidance and valuable comments.

I gratefully acknowledge the Center for Innovation in Chemistry: Postgraduate Education and Research Program in Chemistry (PERCH-CIC) for scholarship and financial support.

I wish to express my thanks to the Department of Chemistry, Faculty of Science, Kasetsart University for the research facilities, and to the staff for their help and co-operation.

I sincerely thank my colleagues and friends for their kind assistance in my work.

Finally, I would like to express my heartfelt gratitude to my parents and my family for their love and support which enable me to carry on throughout the cause of my work.

Nisa Nauangchamnong

May 2008

TABLE OF CONTENTS

LIST OF TABLES

LIST OF FIGURES

LIST OF FIGURES (Continued)

LIST OF ABBREVIATIONS

Al	=	Aluminium
Cd	=	Cadmium
HQS	=	8-Hydroxyquinoline-5-sulphonic acid
CF	=	Conventional Fluorescence
SSF	=	Synchronous-scanning fluorescence
DS	=	Derivative spectrophotometry
D1SSF	=	First-derivative synchronous-scanning fluorescence
D2SSF	=	Second-derivative synchronous-scanning fluorescence
ppm	=	parts per million
ppb	=	parts per billion
nm	=	nanometer

DETERMINATION OF CADMIUM(II) AND ALUMINIUM(III) AS 8-HYDROXYQUINOLINE-5-SULPHONATE COMPLEXES BY SYNCHRONOUS-SCANNING FLUORESCENCE SPECTROMETRY

INTRODUCTION

Metals are widely used in various industries ranging from metal-works to metallic alloys, electric appliances to electronic circuitry, medicines to cosmetics, plastics to fertilizers, paints and dyes, insecticides and herbicides, *etc.*. Each metal has its use in different ways, such as the aluminium is important material in can industry; whilst chromium, manganese, nickel and copper are used in alloys. Lead, cadmium, nickel and mercury are employed in battery production. Copper, nickel and mercury are found use in the electronic appliances and electrical industries. The release of metals and chemical wastes into the environment — water resources, soil and air — affects the ecological system and human health, directly and indirectly.

Living systems require trace amounts of some metals for proper biochemical functioning, for instance, copper is necessary to hemoglobin production, trace amounts of zinc and nickel are essential to maintain the metabolism in human body . Large amounts of metals, however, present a hazard to health. Metals may enter the body via ingestion, inhalation, or absorption through skin. The degree of toxicity depends on the metal species, the amount of intake, and the duration of exposure. A very high dose of intake, even for a short period, causes the acute effects on health. A long period of exposure results in accumulation of these metals in the body, leading to the malfunction of the organs.

The necessity for evaluating the concentration of metals in the environments has commanded a considerable attention in analytical chemistry. Several instrumental techniques employed for the purpose include electrothermal atomic absorption spectrometry (ETAAS), inductively-coupled plasma–mass spectrometry (ICP-MS), neutron activation analysis (NAA), and high performance liquid chromatography (HPLC). Although these analytical methods employ sophisticate and expensive

equipment, they still involve tedious sample preparation procedure, prior separation of interfering species, skilled personnel in operations, and provision for use and disposal of solvents. The search and development for new, simple, rapid, and low-cost methods are still widely studied.

Aluminium

Aluminium (Al; atomic number 13, atomic weight 26.98) is a silvery element in group IIIA of the periodic table (Lee, 1991; Greenwood and Earnshaw, 1995; Daintith, 1996). It occurs naturally and composes approximately 8% — the third most abundant element — in the earth's crust. Aluminium is soft, malleable and ductile. Its hardness on the Mohs' scale is 2.75. Aluminium is a poor metallic and light-weight element with the density ~2.7 times that of water and about one-third of copper and steel. It melts at 660.32 $^{\circ}$C and boils at 2519 $^{\circ}$C. The electron configuration of aluminium is $1s^2$, $2s^2$, $2p^6$, $3s^2$ and $3p^1$. Aluminium exhibits the oxidation state +3 in most of its compounds. The oxidation state of +2 is also found. Aluminium is paramagnetic.

Aluminum reacts with oxygen to form passivating oxide on the surface, hence, is resistant the corrosion. Aluminum is combined with small amounts of various elements (*e.g.* copper, manganese, magnesium, silicon, *etc.*) in forming alloys of different properties (Clyne and Withers, 1993). Because of the versatile properties, aluminum and its alloys form diverse products for the use in different industries, *e.g.* building, transportation, food packaging, beverage cans, cooking utensils, surgery materials, food additives, medicines, cosmetics, and water purification, *etc.*.

Aluminium is found naturally in human body about 35 to 50 mg which is most present in the lung ~50%, in soft tissues ~25%, and in the bone ~25%. The quantity of aluminium in daily diet ranges between 3 to 12 mg. Although small amount of aluminium can be excreted rapidly by the kidney, but it takes a long period for very high uptake to be released from the body (Williams, 2002). The accumulation of

excess aluminium can produce the neurotoxicity effects such as Alzheimer's disease and other neurodegenerative diseases.

Cadmium

Cadmium (Cd; atomic number 48, atomic weight 112.41) is a bluish-white transition metal in group IIB of the periodic table (Lee, 1991; Greenwood and Earnshaw, 1995; Daintith, 1996). Cadmium occurs mainly in the earth's crust in combination with zinc.

Cadmium is a soft metal with the hardness of 2.0 on the Mohs' scale. It is malleable, and ductile. Its density is about 8.65 times that of water. Cadmium melts at 321.07 $^{\circ}$C and has a boiling point of 767 $^{\circ}$C. The electron configuration of cadmium is [Kr] $4d^{10}$ $5s^{2}$. The normal oxidation state of cadmium is +2, but sometime Cd^{+1} can also be found. Cadmium is paramagnetic.

Three quarters of pure cadmium and its compounds used in industries involve in the production of Ni-Cd batteries. The rest quarter is mainly used in electroplating, alloys, pigments, *etc.*. Cadmium is considered an occupational poison because of its involvement in many industries. Inhaling of cadmium fume causes immediate effects on the respiratory tract, *e.g.* a dryness in the throat, and difficulty in breathing. Long-term exposure to cadmium causes kidney diseases, lung damage, and fragile bones. The other exposure is the oral intake via contaminated food and drinking water by which causes the deficiency of iron gastrointestinal absorption and may result in anemia. High dose of oral exposure causes severe irritation to the gastrointestinal epithelium (Berman, 1980).

Several methods have been used for the determination of these metals. Most of the methods involve separation of interfering species prior to the analysis. Spectrofluorimetry and related methods are known as being simple and sensitive methods for analysis of samples consisting of aromatic system. Vo-dinh (1978) used the synchronous excitation technique in luminescence spectrometry with several

advantages, including narrowing of spectral bands, resolving the spectral overlapping, enhancing the selectivity by spectral simplification, and decreasing in measurement time of multi-component analysis.

8-hydroxyquinoline-5-sulphonic acid (HQS, $C_9H_7NO_4S$), a derivative of 8-hydroxyquinoline (oxine, HQ; C_9H_7NO), is a univalent ligand with two co-ordination sites, N and O^-. HQS possesses a chelating behaviour similar to that of oxine with essentially the same formation constants (Hollingshead, 1954-56; Marczenko, 1986; Snell 1978). HQS is a water-soluble reagent whilst oxine is not. Consequently, the aqueous solubility of HQS complexes is greatly enhanced. From this standpoint, HQS is an alternative to oxine where problems arising from precipitation, at least in neutral and alkaline solutions (Soroka *et al.*, 1987). Although it does not show intrinsic fluorescence itself, HQS reacts with a large number of metal ions of which about 42 species form highly fluorescent complexes. On the account of its unique advantages, HQS has been widely used as fluorogenic reagent for spectrofluorimetric determination of various metal species including aluminium and cadmium. Since the reagent is not selective, separation step(s) prior to the analysis is often required.

The aim of this research is to study and develop a simple, rapid, and low-cost method for the determination of Cd(II) and Al(III) without prior separation step, based upon the formation of 8-hydroxyquinoline-5-sulphonate chelates and the use of synchronous-scanning fluorescence spectrometric technique.

1. Fluorescence Spectrophotometry

1.1 Principles of Fluorescence

Fluorescence is a photon emission phenomenon of fluorescent molecules, resulted from the return of electron in the electronic excited state to the electronic ground state of the same multiplicity. The partial energy-level diagram in Figure 1 (Jablonski diagram) shows the processes involving in photoluminescence. Electronic states are typically separated by gap of energy corresponding to wave-number in the order of 10^4 cm^{-1}. Each electronic state comprises multiple vibrational-levels with the energy difference ~10^3 cm^{-1} between the two levels. Several rotational energy levels are associated with each vibrational level. The rotational levels are separated with the energy difference of ~10^0-10^2 cm^{-1}, which is relatively small compared to those of vibrational levels. (Skoog *et al.*, 1998)

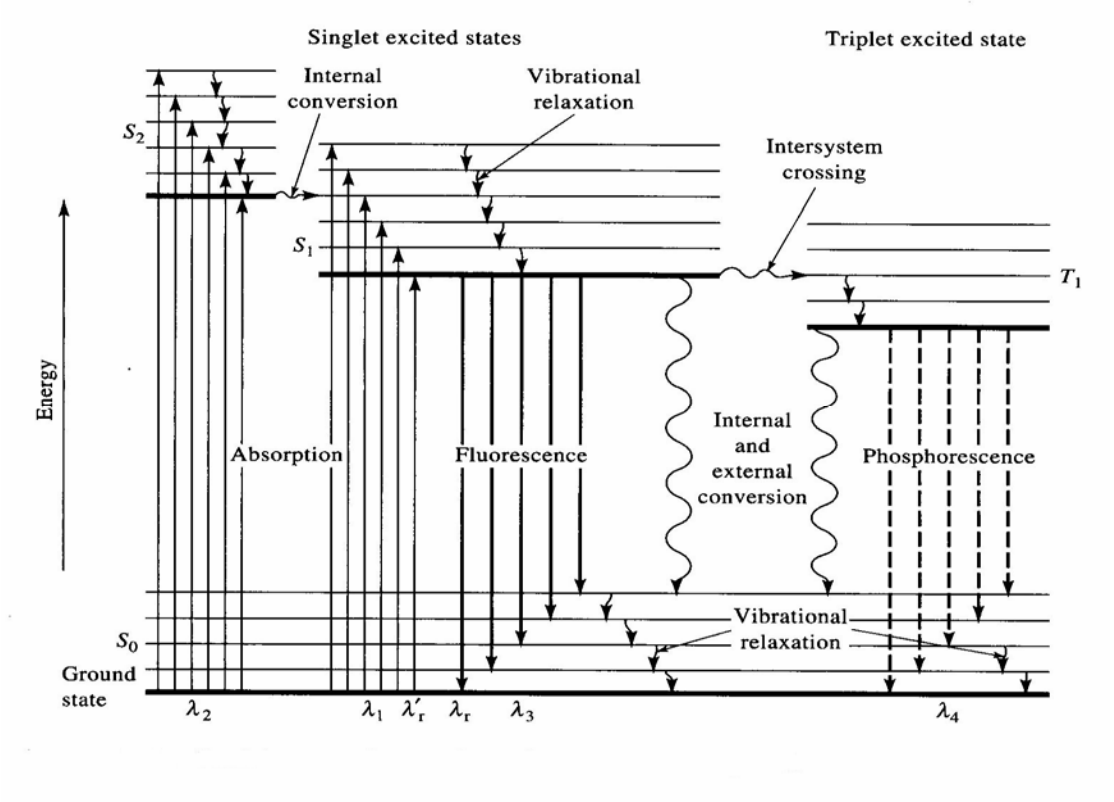

Figure 1 Partial energy diagram and processes involving in photoluminescence.

Source: Skoog *et al.* (1998)

A molecule at room temperature normally resides in the electronic ground state that is usually a singlet state (S_0) with the electrons occupying the same molecular orbital are paired. When the molecule in S_0 absorbs high-energy photons (*i.e.* the ultraviolet to the blue-green region of the visible spectrum) the molecule is promptly excited from the lowest vibrational energy level of S_0 to one of the vibrational levels of either the first, S_1, or the second, S_2, or higher electronic excited state of the same multiplicity (that is singlet state). The absorption and excitation of a molecule can occur in very short time, $\sim 10^{-15}$ seconds. In solution, the excited molecule is rapidly deactivated as a consequence of collisions between the molecules of the excited species and those of the solvent. The collisional process causes energy transfer, and the excess vibrational energy is lost as heat. Through this *vibrational relaxation*, the molecule then drops from the higher vibrational energy level to the lowest vibrational level of that electronic state. This relaxation process takes about 10^{-12} seconds or less to complete. With such rate the emission of fluorescence from solution, when it occurs, always involves a transition from the lowest vibrational level of an excited state.

For a molecule promoted to an electronic excited state higher than S_1, it may undergo an intramolecular process called *internal conversion*. The excited molecule passes from one electronic state of higher energy level to a lower energy electronic state through the overlapping vibrational levels without emission of radiation. The two electronic energy levels must be sufficiently close for the existence of an overlap in vibrational levels. Hence, the molecule proceeds from the higher electronic excited state to the lowest vibrational level of the lower electronic excited state via a series of vibrational relaxation, internal conversion, and further vibrational relaxation.

Radiationless deactivation of an excited molecule between two electronic excited states may also involve *external conversion* processes, *e.g.* interaction and energy transfer between the excited molecule and the solvent or other solutes. The excited molecule, thus, repeatedly loses the excess energy by these deactivation

processes along the pathway down to the lowest vibrational level of the first excited singlet state, S_1.

From the state S_1, the molecule descends back to the ground state S_0 by emitting the energy as a photon — a process called *fluorescence*. The emission of fluorescence generally occurs in ~10^{-9} to 10^{-6} s after the excitation.

While the molecule is in an excited state, the spin of one electron may be reversed resulting in a change in the multiplicity. The excited molecule is to undergo a singlet-triplet transition via the *intersystem crossing*, in which it passes from the singlet state to a triplet state through the overlapping vibrational levels. The molecule swiftly degrades through the series of non-radiation processes and attains the lowest vibrational level of the first excited triplet state, T_1, from which it returns to the ground state S_0 by emitting a photon. This photoemission process is referred to as *phosphorescence*. It takes longer time for a molecule to emit phosphorescence. Because transition between states of different multiplicity (*i.e.* $S \rightarrow T$ and $T \rightarrow S$) is forbidden, an excited molecule is thus retained in T_1 much longer than in S_1. The lifetime of phosphorescence is ~10^{-3} to 10 s, much longer than that of fluorescence.

Since fluorescence occurs from the lowest electronic excited state S_1, the wavelength of emitted radiation (*i.e.* fluorescence spectrum) is therefore independent of the wavelength of excitation radiation. The radiant power or intensity of emitted fluorescence (F) is, however, proportional to the intensity of the excitation radiation, and in turn, the number of photons absorbed.

$$F = \phi (P_0 - P) \tag{1}$$

where ϕ is a proportionality constant — the *quantum efficiency* of the fluorescence process, which is a measure of the fraction of absorbed photons that are converted into fluorescent photons;

P_0 is the intensity of the excitation radiation;

P is the intensity of the transmitted radiation.

The transmittance (T) as expressed in Beer's law is:

$$T = P/P_0 = 10^{-\varepsilon bc} = 10^{-A} \quad (2)$$

where ε is the *molar absorptivity* of the fluorescent species, in l mol^{-1} cm^{-1};
b is the path length of light traveling through the solution, in cm;
c is the concentration of the fluorescent species, in mol l^{-1}.

By substituting P from equation (2) into equation (1), hence:

$$F = \phi P_0(1 - 10^{-\varepsilon bc}) = \phi P_0(1 - 10^{-A}) \quad (3)$$

If the product $\varepsilon bc = A$ is large, the exponential term $10^{-\varepsilon bc}$ is then negligible compare to 1. Thus F is directly proportional only to the power of light source, P_0 .

$$F = \phi P_0 \quad (4)$$

When $\varepsilon bc = A$ is ≤ 0.05, a good approximation for F can be attained by the expansion of the exponential term $10^{-\varepsilon bc}$ in equation (3).

$$F = 2.303\phi P_0 \varepsilon bc \quad (5)$$

or at constant P_0 , $F = Kc$ (6)

That is the fluorescence intensity is directly proportional to the concentration of the fluorescent species. The equation (6) generally holds for the concentration up to a few parts per million depending on the fluorescent species. A graphic plot of F versus c should be linear. At high concentrations where the absorbance is greater than 0.05, the plot is then deviated from linearity.

1.2 Fluorescence Measurement

Fluorescence instruments are designed for fluorescence measurement. The major components, similar to those of UV-visible absorption measurements, include a light source, wavelength selectors, sample-cell holder, transducer/detector, and readout system. Schematic diagram in Figure 2 illustrates a simple design of a fluorimeter.

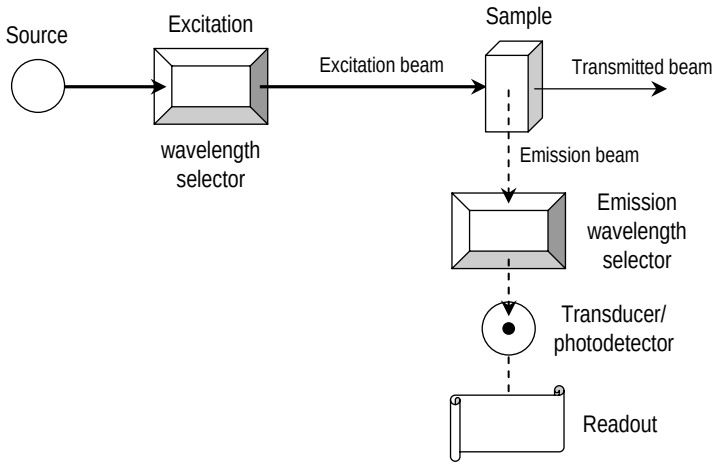

Figure 2 A simple design and components of a fluorimeter.

The polychromatic radiation from light source passes through a primary wavelength selector which serves to select and transmit only the wavelength of excitation radiation. For fluorescence measurement, it is necessary to separate the emitted radiation from the excitation radiation. The secondary wavelength selector isolates and passes only the wavelength of emission on to the detector. Because the fluorescent radiation is emitted from the sample in all directions whereas the excitation beam passes straight through the solution, therefore, the fluorescence is to be observed and measured at the right angles to the path of excitation radiation — so to minimize the interference of the stray excitation beam.

1.2.1 Excitation Sources

A high-power ultraviolet source, more intense than those used in absorption spectrophotometers, is required for most application. A mercury or a xenon arc lamp is commonly employed. The mercury arc lamps generate line spectrum with principle lines at 254, 302, 313, 405, 436, 546, 577, 691, and 773 nm. The xenon arc lamp provides continuous radiation over the range of ~300-1300 nm. A discharging capacitor is incorporated into some instruments, to provide flashes with regular interval of time which results in high intensity pulses. Various types of lasers are also used as excitation source.

Apart from the high power, a constant output and uniform radiant power of the excitation source is also desirable. Fluctuations in the output and power of the source certainly affect the fluorescence intensity.

1.2.2 Wavelength Selectors

Filters and monochromators are employed for selecting particular wavelength of the radiation in fluorescence measurements. Both interference and absorption filters are used to restrict the wavelengths of the beams, whilst the monochromators are used to disperse a broadband light to an array of wavelengths.

1.2.3 Cells and Cell Compartments

The solution of sample is to contain in a cell and placed in the cell compartment where it is excited. Both cylindrical and rectangular cells fabricated of glass or silica may be used. Glass cells, nevertheless, generate much background fluorescence than those made of silica or quartz. The most commonly employed is a 1-cm^2 rectangular, fused silica or quartz cell. The cell compartment must be carefully designed so to reduce the scattered radiation reaching the detector.

1.2.4 Transducers and Detectors

Several types of photo-transducer/detector, which convert the emitted light into an electrical signal, are used in fluorescence instruments. The detectors may be classified by the manner of detection as single- or multi-channel detectors. A single-channel detector measures the signal at one single point of the radiant spectrum at a given time. On the other hand, the multi-channel detectors measure the signals of the radiant spectrum simultaneously.

Four types of detectors are found in commercial fluorescence instruments: photo-emissive; semiconductor; photodiode-array; and charge-transfer detectors. Photomultiplier tubes (PMT) are the most common transducers in sensitive fluorescence measurements. Multi-channel detectors, *e.g.* photodiode arrays, are increasingly used as they permit the rapid recording of both excitation and emission spectra.

1.2.5 Signal Processors and Readouts

The electrical signal from the transducer/detector is amplified and manipulated or processed as desired, *e.g.* convert the signal from dc to ac, change the phase of the signal, perform mathematical operations on the signal, *etc.* Readouts of modern fluorescence instruments are mostly in digital form.

1.2.6 Instrument Design

Fluorescence instruments may be grouped according to the performance characteristics, sophistication of design, and costs. *Fluorimeters* employ filters to restrict the wavelengths of excitation and emission radiation. Those fluorescence instruments equipped with monochromators are referred to as *Spectrofluorimeters*. Commercial spectrofluorimeters often employ a filter to limit the excitation radiation and a grating or prism to isolate the peak of fluorescence spectrum.

A true spectrofluorimeter is equipped with two monochromators, one of which restricts the excitation radiation to a narrow band; the other isolates particular fluorescent wavelengths. Wavelength variation in such instruments permits spectrum measurement of excitation or absorption, and fluorescence. An excitation spectrum is obtained by measuring the emitted fluorescence at a fixed emission wavelength while the excitation wavelength is varied. On the other hand, a fluorescence spectrum involves a fixed excitation wavelength while the emission wavelength is scanned.

2. Synchronous Scanning Fluorescence Spectrophotometry

Synchronous scanning fluorescence (SSF) is a spectrofluorimetric technique first proposed by Lloyd in 1971. The fluorescence measurement is carried out by synchronously (simultaneously) varying both the excitation and emission wavelengths while keeping a constant wavelength interval between them. Because the excitation is varied continuously, thus the emission spectrum cannot be monitored in a usual manner. The feature of synchronous scanning is, however, a distinctive advantage.

2.1 Basic Principle of SSF

The intensity of a fluorescence signal recorded at emission wavelength λ, $I(\lambda)$, is proportional to the spectral radiant power (F) emitted by the fluorescent species excited at λ', $F_{\lambda'}$. It is also dependent on the distribution pattern of the emission at λ, *i.e.* an emission spectrum, $E_m(\lambda)$. The recorded intensity, then, can be expressed:

$$I(\lambda) = kF_{\lambda'}E_m(\lambda) \qquad (7)$$

where k is a constant factor.

Since the emitted fluorescence depends principally on the excitation wavelength λ', the equation (5) may be written specifically as a function of λ' :

$$F_{\lambda'} = k'\phi(\lambda')P_0(\lambda')\varepsilon(\lambda')\,bc \quad (8)$$

where k' is an experimental constant factor.

The absorption of fluorescent species is an excitation function. Thus, the distribution pattern of the absorption at λ' (that is an absorption or excitation spectrum), $E_x(\lambda')$ can be presented as follows:

$$E_x(\lambda') = k''\phi(\lambda')P_0(\lambda')\varepsilon(\lambda') \quad (9)$$

where k'' is a constant factor.

The synchronous fluorescence intensity, I_s , can be obtained as a function of λ' and λ by relating equations (7), (8), and (9).

$$I_s(\lambda',\lambda) = Kbc\,E_x(\lambda')E_m(\lambda) \quad (10)$$

with $K = k\cdot k'\cdot k''^{-1}$.

The SSF is measured under one specific condition, that is a constant interval between the scanning excitation and emission wavelengths ($\Delta\lambda$).

$$\lambda - \lambda' = \Delta\lambda = \text{constant}$$

or

$$\lambda = \lambda' + \Delta\lambda \quad (11)$$

Therefore, the I_s in equation (10) can be explicitly expressed by introducing the parameter $\Delta\lambda$.

$$I_s(\lambda',\lambda) = Kbc\,E_x(\lambda - \Delta\lambda)E_m(\lambda) \quad (12)$$

In conventional fluorescence (CF), the intensity of emission spectrum is restricted solely to the intensity factor of the spectrum, as shown in equation (7), but the spectral features remain generally unchanged. The excitation wavelength λ' acts only as a multiplicative parameter in the emission expressions of CF. On the other hand, the fluorescence intensity expression in the SSF, is an explicit function of emission wavelength as well as excitation wavelength. The relation in equation (12) signifies the basic principle of SSF. The sensitivity of the technique is improved through the involvement of two functions instead of only one as in the CF. A new degree of selectivity can also be achieved via the experimental parameter $\Delta\lambda$.

The fluorescence signal obtained by SSF is normally referred to as *synchronously-excited emission spectrum*, or simply as a 'synchronous signal' or 'synchronous spectrum'. Nevertheless, the synchronous spectrum can be considered either as an emission or as an excitation spectrum. It is noticeable that equation (10) does not give priority to the emission wavelength λ or to the excitation wavelength λ'. The equation (12) may be re-written categorically in the function of λ', and the synchronous signal may be considered as an excitation spectrum with synchronously-scanned emission wavelength.

$$I_s(\lambda',\lambda) = Kbc\, E_x(\lambda')E_m(\lambda' + \Delta\lambda) \qquad (13)$$

2.2 Advantageous Characteristics of Synchronous Scanning Technique

2.2.1 Spectral Simplification

Complex fluorescence spectra of multi-component mixtures can be greatly simplified by using the synchronous scanning technique. Two graphical examples are given in Figure 3. A signal can be observed only when the particular $\Delta\lambda$ matches the interval between a pair of excitation and emission bands. In Figure 3a, only one single peak is obtained at λ_1 when the $\Delta\lambda = \lambda_1 - \lambda'_0$ is selected for a pair of excitation peak at λ'_0 and emission peak at λ_1 .

In cases that more than one pair of excitation and emission bands display identical intervals (δλ), the Δλ may be selected to match one unique pair. As illustrated in Figure 3b, the Δλ is chosen to match the two strong peaks at λ'_0 and λ_1. The intense peak at λ_1 is enhanced more strongly than the weak one at λ_0. It clearly demonstrates that the selectivity can be improved when SSF is properly applied. The characteristic intense peaks are enhanced whilst the interfering weak bands can be reduced.

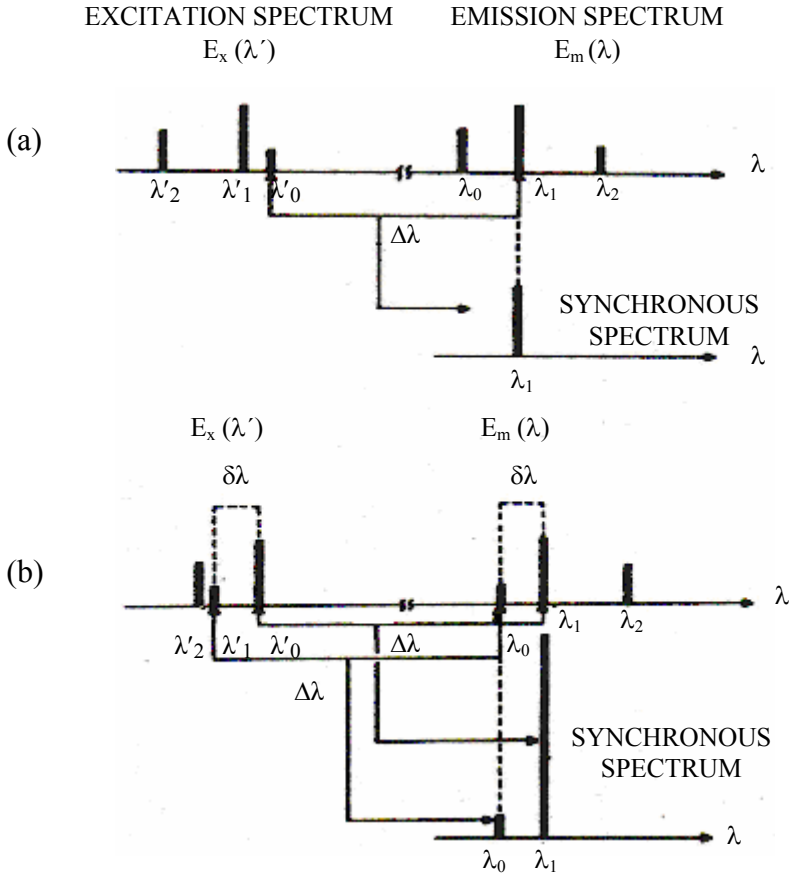

Figure 3 Simplification of synchronous scanning spectrum.

Source: Vo-Dinh (1978)

2.2.2 Spectral Band Narrowing

A spectrum can exhibit a resolved feature only when it consists of narrow bands. For multi-component mixtures, superimposition and overlap of the component spectra are the causes of diffusion in fluorescence spectra. The example in Figure 4 illustrates the band-narrowing effect produced by the synchronous scanning technique. In Figure 4a, $E_x(\lambda')$ and $E_m(\lambda)$ represent two hypothetical bands of excitation and emission spectra, respectively. When the sample is excited mono-chromatically at λ'_1, λ'_2, and λ'_3, the intensity of the observed emission spectrum (labeled as I_{L1}, I_{L2}, and I_{L3}, respectively) increases proportionally with the excitation intensity as shown in Figure 4b. The bandwidth of the observed spectrum, however, remains unchanged.

In synchronous scanning mode, the emission spectrum is observed while varying the excitation wavelength. The chosen $\Delta\lambda$, as seen in Figure 4c, is the match of wavelength interval between the maxima of the excitation and emission peaks. The synchronous peak obtained shows a narrower width than the one of the same intensity — the maximum value I_{L1} in Figure 4b. This band-narrowing effect is essentially a consequence of the multiplication of two functions increasing and/or decreasing simultaneously.

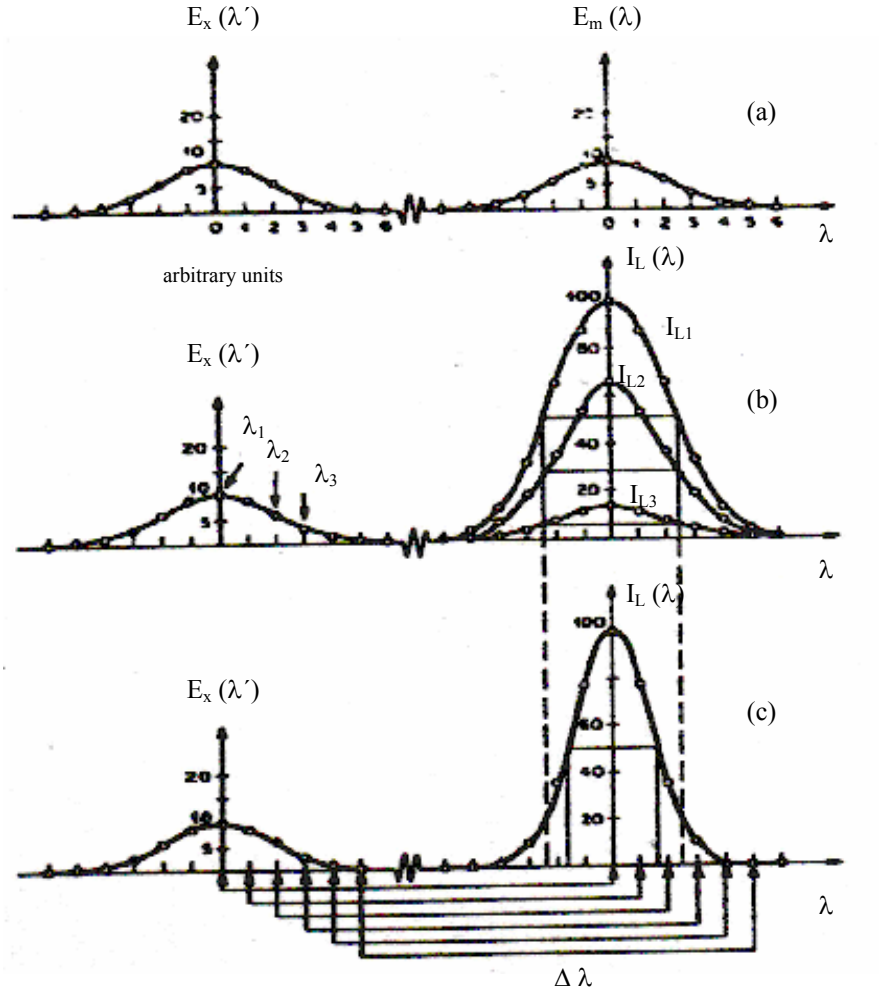

Figure 4 Schematic diagram depicting the band-narrowing effect.

Source: Vo-Dinh (1978)

2.2.3 Spectral Range Shortening

Three examples of spectral overlap are schematically shown in Figure 5. The shortest wavelength of the emission spectrum $E_m(\lambda)$ is denoted as λ_0 — it is the wavelength where the emission starts. As for the excitation spectrum $E_x(\lambda)$, the longest wavelength where the fluorescent species no longer absorbs the excitation radiation is denoted λ'_0. When $\lambda'_0 = \lambda_0$, as in Figure 5a, the value of spectral overlap between $E_m(\lambda)$ and $E_x(\lambda)$ is assumed to be zero. Using a wavelength interval $\Delta\lambda$ the synchronous signal exhibits a band of $\Delta\lambda$ wide, extending from λ_0 where the emission starts up to $[\lambda_0 + \Delta\lambda]$ — a range corresponds to the variation of excitation wavelengths from $[\lambda'_0 - \Delta\lambda]$ to λ'_0.

Figure 5b illustrates a spectral overlap between the emission and the excitation spectra. For the overlap $\delta\lambda_s = \lambda'_0 - \lambda_0$ where $\lambda_0 < \lambda'_0$, the synchronous spectrum then ranges from λ_0 to $[\lambda_0 + \Delta\lambda] + \delta\lambda_s$ with the excitation wavelengths varied from $[\lambda'_0 - \Delta\lambda] - \delta\lambda_s$ to λ'_0. The band width is, thus, $\Delta\lambda + \delta\lambda_s$.

Some cases may involve a *Stokes shift* of $\delta\lambda_s$ (a shift in emission to longer wavelengths). As depicted in Figure 5c where $\lambda_0 > \lambda'_0$, the synchronous signal is recorded from λ_0 to $[\lambda_0 + \Delta\lambda] - \delta\lambda_s$ while the excitation wavelength is varied from $[\lambda'_0 - \Delta\lambda] + \delta\lambda_s$ to λ'_0. The result is a spectral band width of $\Delta\lambda - \delta\lambda_s$.

The emission spectral range of a fluorescent species is thus reduced when synchronous scanning technique is applied. The width of synchronous spectrum can be directly compressed or expanded just by decreasing or increasing the experimental parameter $\Delta\lambda$. The decrease in the width of a synchronous band would be advantageous since spectral overlap could be greatly reduced. Furthermore, a synchronous signal can be modified by varying the $\delta\lambda_s$ through a change in the solvent system. This possibility of modifying the emission spectrum of each individual component in a mixture is the most outstanding feature offered by the synchronous scanning technique.

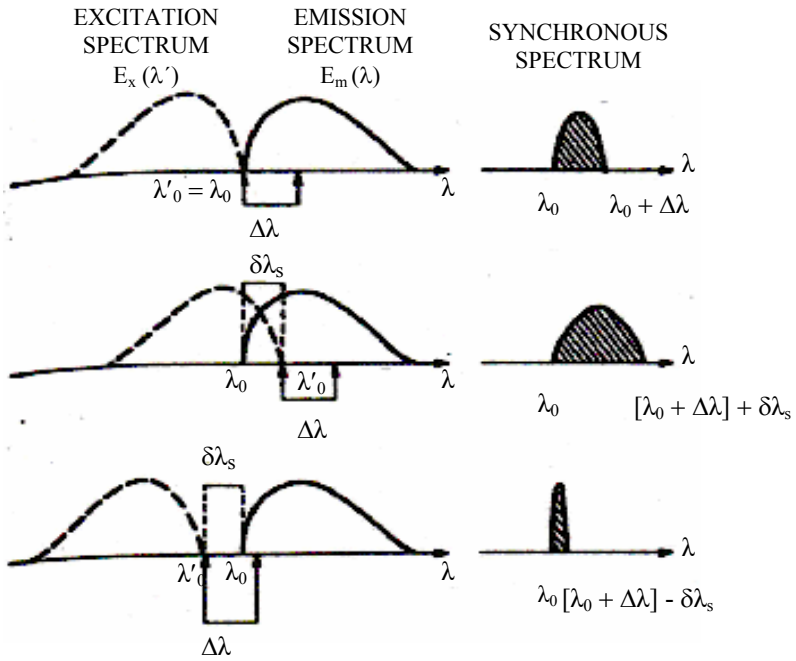

Figure 5 Modification of emission spectrum by synchronous scanning technique.

Source: Vo-Dinh (1978)

3. Derivative Fluorescence Spectrophotometry

Derivative methods in spectrophotometry had been proposed for many years. In the early 1920s, Lord Rutherford suggested the first-derivative technique for the detection of discontinuities in mass-spectrometric studies of gas-excitation potentials. Singleton and Collier built the earliest derivative spectrophotometer in 1953. An IR spectrophotometer was modified using an analog device to generate second-order derivative spectra. In 1955, Giese and French adapted the *principle of wavelength modulation*, proposed by Hammond and Price in 1953, to study first-order derivative visible spectra of photosynthetic systems (Talsky, 1994). The method was, however, accepted hesitantly because the initial lack of reasonably-priced instruments and the original limitation to the first derivative. Only recently that derivative spectrophotometry has become a generally applied analytical method. The rapid progress in microcomputer technology made it possible to directly present the first, the second and higher order derivative spectra (Poppović *et al.*, 2000).

Derivative spectrophotometry (DS) is defined as a spectral measurement technique in which the slope of the spectrum, *i.e.* the rate of change in absorbance with wavelength, is measured as a function of the wavelength. Thus, the first-derivative spectrum is a plot of spectral slope against the wavelength; whereas the second derivative spectrum is itself the derivative of the first-derivative spectrum; and so on. The shapes of the derivative spectra are different as shown in Figure 6 — the first four derivatives of an unperturbed Gaussian maximum. The first- and the odd-numbered derivatives display the highest change in the slope through the zero-crossing at the wavelengths of maximum or minimum absorption. Figure 7 shows an absorption spectrum with some details in the first-derivative calculation.

$$dA/d\lambda = (A_2 - A_1)/(\lambda_2 - \lambda_1) = \Delta A/\Delta\lambda = \text{slope} \qquad (14)$$

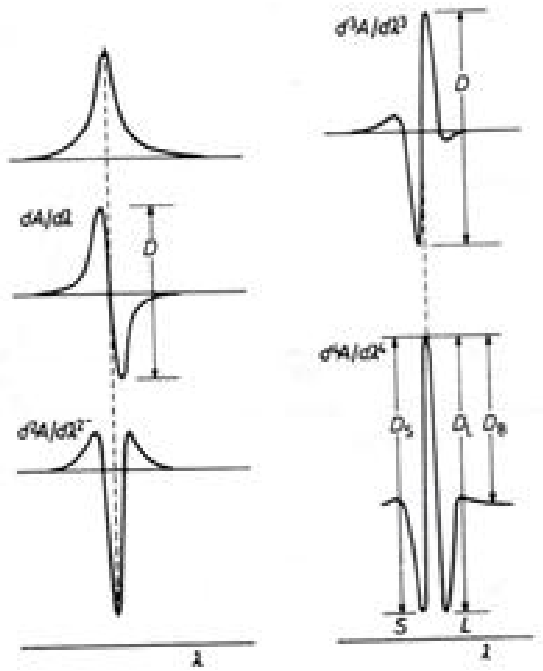

Figure 6 Characteristic profiles of derivative orders of an ideal Gaussian peak. A: zero order; B: first order; C: second order; D: third order; and E: forth order.

Source: Sommer (1989)

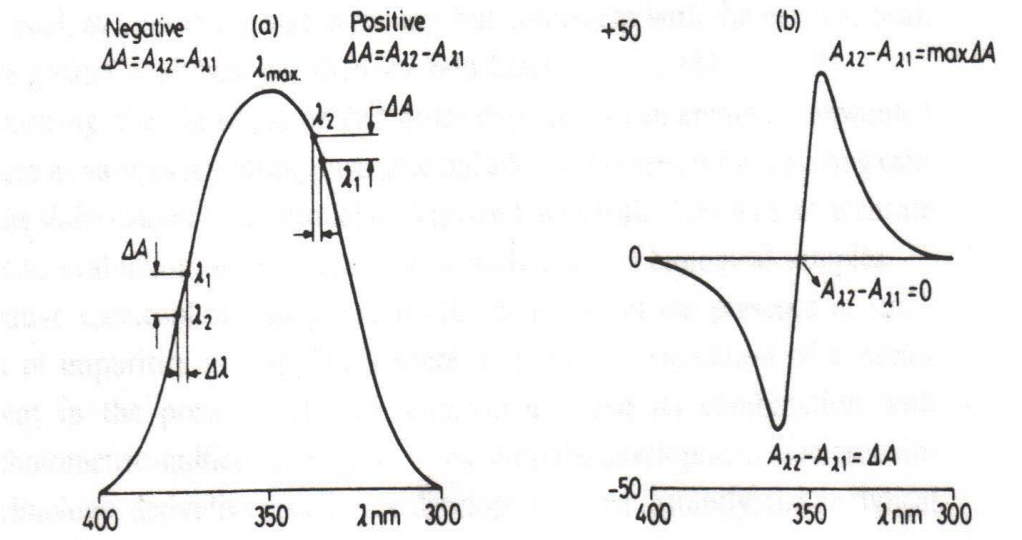

Figure 7 Details in first-derivative calculation of an absorption spectrum.
a: zero order; b: first order.

Source: Sommer (1989)

3.1 Advantageous Characteristics of Derivative Spectrophotometry

3.1.1 Enhancement of Spectral Resolution

The resolution of overlapping spectral bands is enhanced as a consequence of differentiation that discriminates against broad bands in favour of a sharp peak. The extent of resolution increases, *i.e.* the decrease in bandwidth, with the increasing order of derivative. The decrease in the bandwidth also depends on the shape, the relative bandwidth, and the height of the overlapping peaks, as can be seen in Figure 6.

For bands of simple shape, *e.g.* a Gaussian absorption band, the amplitude in the *n*-th derivative order (^{n}D) is inversely related to the *n*-th power of the bandwidth (W) of the original spectrum.

$$ {}^{n}D \propto {}^{1}/_{W^n} \tag{15} $$

For two emission bands of same intensity but different width, the derivative amplitude of the narrower band is, thus, greater than that of the broader one. The relative increase in amplitude of the narrower band in higher derivative orders presents the most important factor for the increase of sensitivity and selectivity in DS.

3.1.2. Elimination of Baseline Shifts and Matrix Interferences

Qualitative and quantitative investigations of broad spectra are often difficult, especially when the low signals are measured, since the baseline shift and matrix interferences are uncontrollable. The general equation used for describing interferences is a polynomial function.

$$ P = a_0 + a_1\lambda + a_2\lambda^2 + \ldots + a_n\lambda^n \tag{16} $$

If n represents the highest degree of the polynomial equation, the interference is then reduced to a constant by using the n-th order derivative and is completely eliminated in the (n+1)-th derivative.

$$ {\mathrm{d}^n P}/{\mathrm{d}\lambda^n} = n!a_n \tag{17} $$

$$ {\mathrm{d}^{(n+1)} P}/{\mathrm{d}\lambda^{(n+1)}} = 0 \tag{18} $$

The order of derivatisation for eliminating the interference signal, hence, depends upon the order of the polynomial equation. In many cases, matrix interference can be approximated by a linear or quadratic function. When the interference is described by a linear function, that is $P = a\lambda + b$, the first derivative yields a function which reduces the interference to a constant a ; from equation (17) $\mathrm{d}^1P/\mathrm{d}\lambda^1 = 1!a$. In the second derivative transformation the interference is completely eliminated, $\mathrm{d}^2P/\mathrm{d}\lambda^2 = 0$.

Figures 8 and 9 illustrate the reducing effect of derivatisation on baseline shift. Three scans of normal spectrum of a chromophore in Figure 8a display the different baseline shifts and tilts but identical absorption. In Figure 8b, the second derivatives of these three scans superimpose exactly. Figure 9 depicts the absorption spectrum of a chromophore (A), a curved baseline (----), and the observed spectrum superimposed on the baseline (B). The second-derivative plot shows the spectra A and B are almost identical.

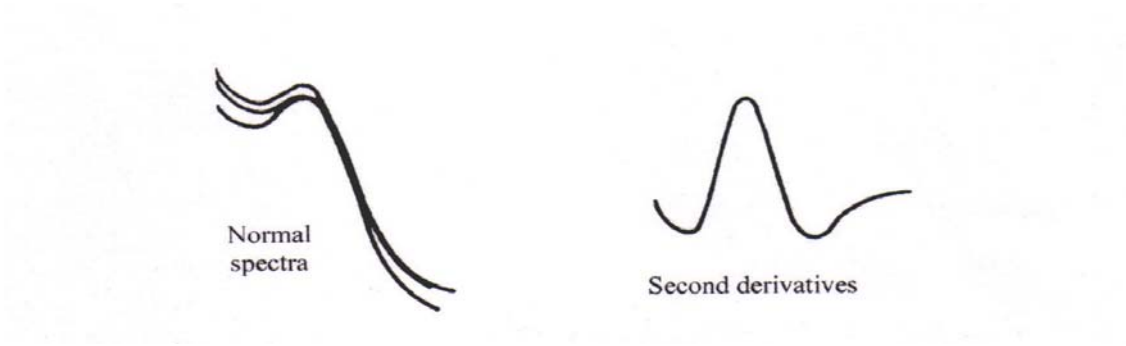

(a) (b)

Figure 8 Reduction of baseline shift and tilt by the derivative technique.

Source: Poppović *et al.* (2000)

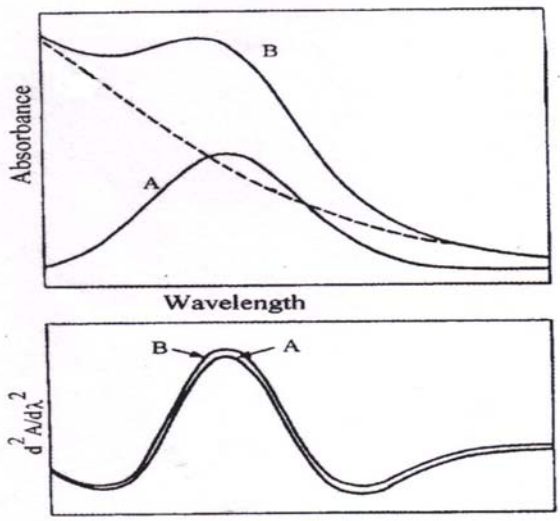

Figure 9 Reducing effect of derivatisation on a curved baseline.

Source: Poppović *et al.* (2000)

3.1.3 Enhancement of Detectability

Derivatisation of broad spectra increases both the possibility of detection and measurement of minor spectral features, and discrimination against interference. However, the derivative transformation does not increase the number of intrinsic data (some can even be lost as a constant factor) but visually enhances subtle changes in those spectra. Besides qualitative information, the transformation provides better possibility for quantitative analysis in cases where the main peak is obscured by intensive interfering peak (Figures 8 and 9), and for the multi-component analysis. Although a great number of theoretical and practical investigations have been developed, a general approach to the application of DS in quantitative analysis is still impossible, because each combination of bands and the degree of their overlapping tends to be an individual case.

3.1.4 Precise Position of Peak Maximum

When main feature of a single-peak spectrum is broad banded, the position of the absorption maximum can be determined only approximately. The characteristic profiles of the first and higher odd-numbered derivatives (in Figure 6) shows the zero-crossing at the peak maximum. Thus, the peak position can be accurately located.

As for the second and higher even-numbered derivatives ($d^2A/d\lambda^2$, $d^4A/d\lambda^4$, ...), the characteristic peak contains a changeable sign (negative in the second order, positive in the fourth order, *etc.*) which locates at the same position as the peak maximum in a normal spectrum. The width of the characteristic peak progressively decreases with increasing order of the even derivatives, resulting in a sharpen peak of exact feature. However, every even-derivative peak is accompanied by symmetrical satellites of the opposite sign, the number of which is equal to the derivative order. In higher order derivatives ($n \geq 6$), the satellites of adjacent bands may interfere, thus limiting the observed resolution. Moreover, during differentiation of synthesized spectral profiles, peaks of certain components might be shifted, compared to their original positions.

3.2 Quantitative Analysis

The application of derivative synchronous technique for quantitative analyses is based on the validity of Beer's law. The derivative amplitude of the *n*-th order (^nD), at a wavelength λ, can be expressed according to Beer's law as follows:

$$^nD = {d^nA}/{d\lambda^n} = (d^n\varepsilon/d\lambda^n)\, bc \qquad (19)$$

In multi-component spectra, total derivative amplitude at the *n*-th order, $^nD(\mathrm{T})$, is equal to the algebraic sum of each absorbing component X, Y, *etc.*.

$$^nD(\mathrm{T}) = {}^nD(\mathrm{X}) + {}^nD(\mathrm{Y}) + \ldots \qquad (20)$$

A successful application of DS in quantitative analysis depends on a previous choice of optimal conditions including the selection of appropriate analytical bands, the suitable derivative order, the method of measurement and optimization of all significant instrument parameters. The measurement of derivative peak amplitude for the construction of a calibration curve can be done by different methods as shown in Figure 10: peak-to-peak method, D_L and D_S ; peak-to-baseline method, D_Z ; peak-to-tangent method, D_B , and in Figure 11 the zero-crossing method for measurement of overlapping peaks of chromophores X and Y.

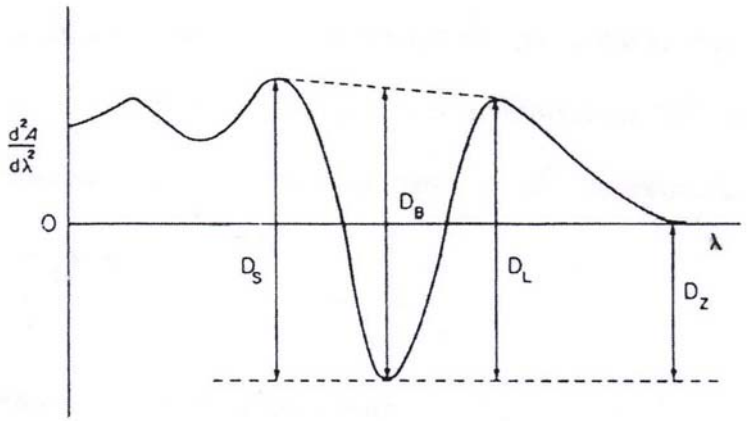

Figure 10 Measurements of derivative-peak amplitudes.

Source: Sommer (1989)

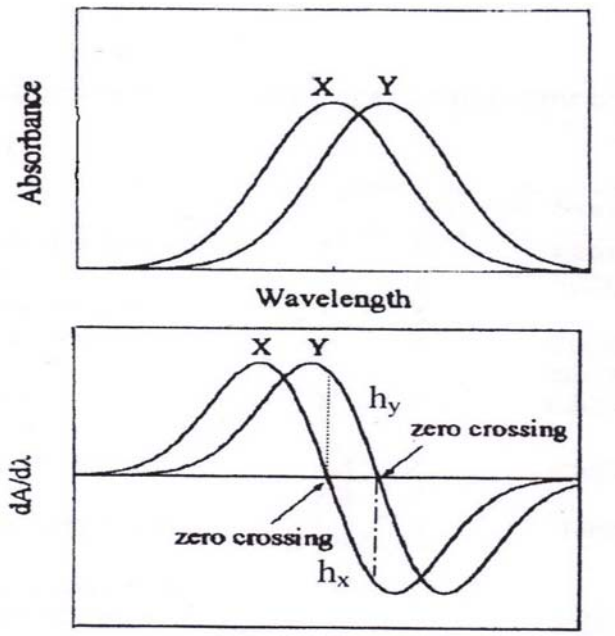

Figure 11 Zero-crossing method for derivative peak measurement.

Source: Poppović *et al.* (2000)

LITERATURE REVIEW

8-Hydroxyquinoline and its derivatives have been widely used as fluorogenic reagent for fluorimetric determination of various metal species. Aluminium, calcium, magnesium, cadmium, and zinc were determined by capillary electrophoresis (CE) with fluorescence detection based on the post-column complexation with HQS (Zhu and Kok, 1998). The optimal pH for complexation of aluminium and zinc was 3-4, whilst for calcium and magnesium was 8-9.

The fluorescence enhancement of Al(III)-HQS complex in reverse micelles of low-water-content systems were studied in comparison to those in aqueous media (Devol and Bardez, 1998). Two surfactants were used: the cationic cetyltrimethyl-ammonium chloride (CTAC), and the anionic sodium bis(2-ethylexyl)sulfosuccinate (AOT). Three reverse micellar systems were used, *i.e.* CTAC/dichloromethane, AOT/heptane, and AOT/dichloromethane. No micellar effect was obtained from the CTAC/CH_2Cl_2. Formation of Al(III)-HQS took place very slowly in CH_2Cl_2 with the fluorescence being enhanced by a factor of 35 — the same order of magnitude usually achieved in organic media relative to water. On the contrary, specific micellar effects were observed in the presence of AOT, particularly in AOT/heptane with fluorescence enhancement factor of 120. The positively charged AlQ^{2+} and AlQ^{2+} complexes were stabilised by the interaction with the negative polar heads of the surfactant.

In the presence of surfactant Triton X-114, aluminium(III) and zinc(II) were extracted by 8-hydroxyquinoline as hydrophobic complexes entrapping in surfactant micelles (Tabrizi, 2007). This cloud-point extraction was used for the determination of trace amounts of Al(III) and Zn(II) in foodstuffs and water samples. The limit of detection was found to be 0.79 μg l^{-1} for aluminium, and 1.2 μg l^{-1} for zinc.

8-Hydroxyquinoline was used for the determination of aluminium in human biological fluids, dialysis concentrates, and tap water (Buratti *et al.*, 2006). Being excited at λ_{ex} 380 nm, the fluorescence intensity of the toluene-extracted aluminium

trioxinate chelate was measured at λ_{em} 504 nm. The calibration graph was linear for Al(III)concentration over a range of 2-1,000 μg l^{-1} with detection limit of 0.7-2 μg l^{-1}.

Using octadecylsilica column, cadmium(II) in environmental water samples was separated by on-column complexation with HQS (Paull *et al.*, 2000). Cadmium-to-HQS ratio in the complex was 1:2. The complex was excited at λ_{ex} 360 nm and the fluorescence intensity was detected at the wavelength of 500 nm.

The complex formations of oxovanadium(IV) with 8-hydroxyquinoline and four quinoline derivatives, *i.e.* 8-hydroxyquinoline-5-sulphonic acid (HQS), 2-methyl-8-hydroxyquinoline (8-HQD), 8-hydroxyquinoline-N-oxide (8-HQNO), and 8-quinolinecarboxylic acid (8-QC), in aqueous solution were studied using combined techniques of potentiometry and spectrometry, *i.e.* electronic absorption and EPR (Garribba *et al.*, 2003). The results showed that all the ligands form mono- and bis-chelate complexes with VO(IV) ion. The bis-chelate complexes are neutral and poorly soluble. Four five-coordinated complexes were isolated in solid form: [VO(8-HQ)$_2$]; [VO(8-HQD)$_2$]; [VO(8-HQNO)$_2$]; and [VO(8-QC)$_2$]. 8-HQ and 8-HQS form two cis-isomers in solution, bearing a water molecule in the equatorial plane.

The complex of zirconium(IV) and 8-hydroxyquinoline was used for fluoride ion detection in aqueous media by simple fluorescence technique (Sathish *et al.*, 2006). The determination is based on the exchange of HQ coordinated to Zr(IV) by fluoride ion without interference from other common anions. In the presence of EDTA, oxine forms a ternary complex with [Zr(H_2O)$_2$EDTA]·2H_2O by replacing two water molecules in the aqueous solution. The intensity of the green fluorescence (λ_{em} 532 nm), emitted by the complex upon the excitation at 247 nm, decreases with the addition of fluoride. The system is sensitive for the detection of fluoride over a concentration range from 6×10^{-7} M to 8×10^{-4} M, with a detection limit of 12-ppb F. The stoichiometric composition of the chelate, Zr:HQ, in aqueous media, determined by the continuous variation (Job's) and the molar-ratio methods, is 1:1.

Being excited at λ_{ex} 338-415 nm, the polymeric complexes of Cu(II), Zn(II), and Al(III) with the functionalized polybenzimidazole containing 8-hydroxyquinoline side group (PBI-8Q) emit blue light of ~415 nm in solution, and blue-green light of 483-552 nm in solid state (Zhong *et al.*, 2008). The polymeric ligand was synthesized by the reaction of polybenzimidazole (PBI) with 5-chloro-8-hydroxyquinoline (5-Cl-8Q) in DMSO using NaH as deprotonation reagent. The luminescence properties of the complexes were studied at ambient temperature. The results from thermal analysis show that these complexes are thermally stable.

8-Hydroxyquinoline benzoates with diverse azo substituents were reported to be selective to mercury(II) (Cheng *et al.*, 2008). The dyes were synthesized by diazo-reaction of 2-methyl-8-hydroxyquinoline with arylamines, followed by esterification with benzoyl chloride. Different changes in the UV-Vis absorption spectra were observed among these azo dyes depend on the azo substituents: bathochromic shift by electron-donating substituents, and hypsochromic shift by electron-withdrawing substituents. In the presence of Hg^{2+}, a notable color change was found in 5-(4-dimethylaminophenylazo)-2-methylquinolin-8-yl benzoate enabling it to distinguish Hg(II) from other metal species by naked eye.

First proposed by Lloyd in 1971, the synchronous scanning fluorescence (SSF) technique was employed in an empirical manner in the field of forensic science (Lloyd, 1974, 1975, 1980; Lloyd and Evett, 1977). Owing to its several advantages, the technique had been developed and widely used for simultaneous determination of multi-component samples without prior separation (Patra and Mishra, 2002). Ten different polycyclic aromatic hydrocarbons (PAHs) in liquid-coal (solvent-refined coal) product were identified and quantified by SSF without a pre-separation step, a feat almost impossible by conventional fluorimetry (Vo-Dinh and Martinez, 1981).

Benzo[*a*]pyrene, perylene, and chrysene in non-ionic micellar media were determined simultaneously using an SSF method (Rodriguez *et al.*, 1992). The SSF characteristics of chrysene, perylene, dibenz[*a*,*c*]anthracene, and coronene in the presence of surfactants were also studied (Rodriguez *et al.*, 1993). The fluorescence

of PAHs was found greatly enhanced in hexadecyltrimethylammonium bromide (CTAB). Consequently, two SSF methods based upon micellization were developed for the analysis of binary and ternary mixtures of these PAHs in sea water. Dibenz-[*a*,*c*]anthracene and coronene were determined simultaneously using a wavelength interval ($\Delta\lambda$) of 89 nm. For chrysene, coronene, and perylene, three $\Delta\lambda$ values were used: 41.3 nm, 89 nm, and 140 nm, respectively.

Trace amounts of benzo[*a*]pyrene, benzo[*a*]anthracene, and pyrene, which exhibited native fluorescence in solution, were determined by solid-phase SSF (Vilchez *et al.*, 1994). The relative fluorescence intensity of the fluorophores fixed on Sephadex G-25 gel was measured after packing the gel beads into a 1-mm silica cell. Using the synchronous-scanning spectra obtained from different wavelength intervals, the residue of PAHs in water can be estimated simultaneously.

An SSF method was developed for simultaneous analysis of multi-component PAHs in water samples using mixture of micellar solution (Patra and Mishra, 2001). The method is fairly effective for analysis of 6, 7, and 10 components in a mixture solution. Another SSF method was also developed for determination of sodium dodecylbenzenesulphonate (SDBS) and pyrene in environtmental samples such as river water and mucus of fish gills (Liu *et al.*, 2006). The results showed the simultaneous analyses of pyrene and SDBS in these samples were feasible. The $\Delta\lambda$ used for SDBS and pyrene were 46-55 and 38 nm, respectively.

Benzo[*a*]pyrene in complex solvent extract of soil was confirmed and quantified using SSF method (Hua *et al.*, 2006). Solvent extracts from five contrasting soils spiked with four different PAHs were rapidly analysed. The optimal $\Delta\lambda$ for the quantification of benzo[*a*]pyrene was found to be 20 nm. A narrowed single spectrum with maximised selectivity for benzo[*a*]pyrene and minimised interference of other three PAHs was obtained.

An SSF method was used for qualitative analysis of the aromatic fraction of low-temperature tar from hard coal (Matuszewska and Czaja, 2000). Each particular

component the mixture could be identified by the respective value of Δλ. The spectrum recorded at a value Δλ of 53 nm presented a rather simple shape with a wavelength maximum at 346 nm, and was attributed to phenanthrene. The developed method was used for investigating aromatic fraction containing phenanthrene among other compounds, and also for estimating the degree of condensation of aromatic compounds.

Apart from applications in multi-component PAH samples, the SSF has been used in the studies of various matters, *e.g.* determination of aloe-emodin and rhein (Jiang and He, 2002), serum albumin (Cui *et al.*, 2006).

Using triphenylmethane acid dyes as fluorescence probe, the human serum albumin (HSA) was determined by SSF (Huo *et al.*, 2006). With a Δλ of 140 nm, the SSF peak of methyl blue is located at wavelength of 323 nm. The fluorescence intensity of methyl blue is significantly enhanced by the presence of trace HSA due to the complex formation at pH 4.1.

The SSF was also used for characterizing the algae *Chlorella vulgaris* solution with and without a quencher (Liu *et al.*, 2005). Fe(III) and humic acid (HA) were found to be effective quencher. The Δλ used for the characterization was 90 nm.

An SSF was used to investigate the binding-site interactions of soil fulvic acid (fua) and Al(III) in acidic pH of 2.5-5.0 (Esteves da Silva *et al.*, 1997). The SSF spectral data were pre-processed and analysed. The information obtained from self-modeling mixture analysis showed that the complexes were quite less stable at pH < 4 than those at a higher pH. A release of Al(III)-bound to fua is, therefore, expected when the pH is decreased to below 4.5 upon acidification.

The binding-site interactions of caffeic acid with Al(III) in aqueous low-acidic medium was also investigated by both UV-Vis absorption and SSF techniques combined with chemometric method (Cornard *et al.*, 2006). The results confirmed the competition of catechol and carboxylic groups in complex formation with Al(III).

The complexing capacity of catechol site was found higher than that of carboxylic group, and increased with pH. At pH 5, Al(III) coordinates only with the catecholate group to form a 1:1 complex that largely predominates in the solution of low amount of metal (*i.e.* molar ratios of Al(III) to caffeic acid less than 0.1). At higher concentration of Al(III), the carboxylic function involves rather rapidly in the chelation of a 2:1 Al(III)-to-caffeic acid complex. At pH 6.5, only the catechol site involves in the simultaneous formation of 1:2 and 1:3 complexes.

A constant-energy SSF method was developed for the determination of PAHs with rich spectral features (Inman and Winefordner, 1982). The method implemented a constant-energy difference between the excitation and emission monochromators when each was scanned through the spectral region of interest. The method provides considerable improvement over the constant-$\Delta\lambda$ SSF with the applications to multi-component samples.

An excitation-resolved synchronous fluorescence (ERSF) technique was proposed and used for the analysis of aromatic compounds and fuel oil (Taylor and Patterson, 1987). Both excitation and emission monochromators were scanned synchronously as in SSF but using different width of the excitation and emission slits. The resulting ERSF spectra were plotted as a function of excitation wavelength. By using different bandwidths, a narrow excitation band and a broad emission band, the resolution was improved without compromising too much of the sensitivity. With a typical bandwidth at half-height of 3-8 nm, the detection limit was found between parts per million (ppm) and parts per billion (ppb).

Solvents, such as ethanol and water, often cause light scattering and the fluctuation of which affects the SSF remarkably. Polarization was found to suppress the scattered light appreciably; and its fluctuation could be reduced by applying a magnetic field. With simultaneous application of polarization and magnetic field, a new SSF technique named magnetic-polarization-resonance-synchronous fluorimetry (MPRSF) was developed (Chen *et al.*, 1998). The technique was applied for simultaneous determination of PAHs in mixed samples with better sensitivity.

Combined techniques of synchronous-scanning fluorescence and derivative spectrometry have been reported during the last two decades, particularly in pharmaceutical analysis. The combination provides direct resolution of mixtures, enhances minor spectral features, and allows more reliable identification of chemical species.

A first derivative linear variable-angle synchronous fluorescence spectrometric method was developed for mixture analysis of three similar-structured drug compounds, *i.e. p*-aminobenzoic acid, salicylic acid, and gentisic acid (Pulgarín and Molina, 1996). In the variable-angle mode, the wavelength separation between the monochromators is continuously varied. This continuous variation can be achieved either mechanically by varying the relative scanning speeds of each monochromator, or digitally by processing the stored spectral data via microcomputer. The analysis was carried out in aqueous medium of pH 7 using phosphate buffer. The variable angle was obtained from the data stored in the contour plot by means of a developed programme in BASIC. Passing through and around the excitation and emission maxima of all components, the variable angle of 65.8° was optimised for minimum spectral interference caused by each component in the mixture without lossing the sensitivity. The optimal $\lambda_{ex}/\lambda_{em}$ values of 264.4/325.2, 319.6/447.8, and 337.6/478.8 nm were selected for simultaneous determination of *p*-aminobenzoic acid, salicylic acid and gentisic acid, respectively. The proposed method demonstrated a great potential in developing an efficient, fast, and straightforward method for simultaneous analysis of mixtures. Two years later, another first-derivative non-linear variable-angle SSF was developed for simultaneous determination of salicylamide, salsalate, and naproxen in serum and urine using a single spectrum from one single scan (Pulgarín and Bermejo, 1998).

A simple second-derivative SSF method was developed for simultaneous determination of naproxen and salicylic acid in human serum by (Konstantianos and Ioannou, 1996). The method was based on the intrinsic fluorescence of naproxen and salicylic acid in chloroform-1% acetic acid solution. A $\Delta\lambda$ of 130 nm was used for the direct measurement of salicylic acid in the binary mixture, whilst the measurement

of naproxen, using Δλ 60 nm, was to be corrected by an equation which incorporated the concentration of salicylic acid. The method was sensitive and rapid.

Propanolol (PRO) and pindolol (PIN) were determined simultaneously by a first-derivative SSF method (Ruiz *et al.*, 1998). The natural fluorescence of these two drugs in a 50% v/v ethanol-water medium was measured. The SSF spectra of PRO, PIN, and that of the mixture were taken at the Δλ of 18 nm. The first-derivative SSF peaks at the wavelengths of 305 nm and 323 nm corresponded to PIN and PRO, respectively. The zero-crossing method was used to measure the amplitude of the peak profile (*i.e.* the vertical distance to the zero line). The ^{1}D-peak amplitudes at zero-crossing 291 and 341 nm were found to be proportional to the concentration of PIN and PRO, respectively. The resolution of the peaks was accurate.

The coupled techniques of SSF and derivative spectrometry are also applied for determination of metal chelates which are characterized by the broad and poorly structured excitation and/or emission spectra. The derivative SSF method was used to determine cadmium based on the formation of a fluorescent chelate with benzyl-2-pyridylketone-2-quinolylhydrazone (BPKQH) (Sánchez *et al.*, 1985). The measurement was carried out in 80% v/v ethanol at pH 11. The best results were obtained from a Δλ of 80 nm, a scan speed of 240 nm min^{-1}, and a time constant of 0.3 s. A 10-nm increment was employed for recording both first- and second-derivative spectra. Better signal-to-noise ratio was achieved but not for the resolution. The first- and second-derivative SSF provide better detection limits and sensitivity than those obtained from normal spectrofluorimetry.

The binary and ternary mixtures of titanium, zirconium and hafnium were determined by derivative SSF based on the formation of fluorescent complexes with biacetylmonooximenicotinylhydrazone in acidic medium (Rubio *et al.*, 1985). The second-derivative SSF method enables the determination of binary and ternary mixtures of these ions, and improves the ratio in which an individual can be determined in the presence of the another.

Conventional fluorimetry and derivative SSF were applied for the simultaneous determination of gallium and aluminium in biological samples based on the formation of fluorescent complexes with salicylaldehyde carbohydrazone (SACH) (Pavon *et al.*, 1990). In conventional fluorimetric method, the samples were analysed under different analytical conditions, and the results were evaluated by solving a system of two simultaneous equations. The SSF method was carried out in an ethanol-water medium containing 72% of ethanol at pH 2.6. The instrumental parameters used were: a constant $\Delta\lambda$ of 20 nm, a time constant of 1.5 s, a scan speed of 120 nm min^{-1}, and a derivative wavelength difference of 10 nm. Under the working conditions, gallium can be determined over the range of 7-38 ng ml^{-1}, and aluminium 6-45 ng ml^{-1}.

A method of first-derivative synchronous solid-phase spectrofluorimetry was developed for determination of aluminium and beryllium, based on the reaction with morin (Capitán *et al.*, 1992). The fluorescent complexes, of which the spectra were fairly broad and overlapped, were fixed on dextran-type resin packed in a 1-mm silica cell. The fluorescence was measured directly with a solid-surface attachment. A $\Delta\lambda$ of 75 nm was used. The range of application was 0.5-5.0 ng ml^{-1} for both aluminium and beryllium. The method was successfully applied for the was determination of aluminium and beryllium in natural waters and synthetic mixtures.

By using second-derivative SSF, a simple resolution of the anti-coagulant rodenticides, warfarin and bromadiolone, in the presence of *b*-cyclodextrin was accomplished through a differential effect on the fluorescence intensity of these compounds (Panadero *et al.*, 1993). Mixtures of warfarin and bromadiolone at the ratios of 4:1 and 1:10 were satisfactorily resolved. A similar method was applied for determining samarium, europium and terbium with quinaldic acid and phenanthroline in aqueous solution (Du *et al.*, 1994).

A derivative SSF method was proposed for simultaneous determination of molybdenum and boron in plant leaves based on the highly-sensitive fluorescence reaction with alizarin red S (Blanco *et al.*, 1993). The $\Delta\lambda$ of 25 nm was used for the

first- and second-derivative calculations. The concentration was determined from the amplitude of derivative peaks. For boron, the ^{1}D-peak is at 477 nm and the ^{2}D-peak at 447 nm; whereas for molybdenum the ^{1}D-peak is at 447 nm and ^{2}D-peak at 475 nm. The proposed method provided a sensitive and rapid procedure for field work and could be extended to other metal ions in different samples. Two years later, a similar method was developed for determination of molybdenum and tungsten in complex mixture of steels (Blanco *et al.*, 1995). The fluorescence intensity of both molybdenum and tungsten complexes with alizarin red S were enhanced by the presence of cationic surfactant hexadecyltrimethylammonium bromide. The method was found sensitive for simultaneous analysis of both ions over the ranges of 30-4,000 ng ml^{-1} for molybdenum, and of 49-2,500 ng ml^{-1} for tungsten.

MATERIALS AND METHODS

Materials

1. Instruments and Apparatus

1.1 Luminescence spectrometer (Perkin-Elmer™, model LS-55) was used for the fluorescence measurement.

1.2 pH Meter (WTW, inoLab level 1) was used for the pH measurement.

1.3 Automatic pipette (Transferpette®, BRAND™ ; 10-100 µl, 100-1,000 µl)

2. Reagents

The chemicals used are listed in Table 1. All the reagents are of analytical reagent grade, unless stated otherwise. Doubly deionised water was used throughout.

2.1 Aluminium(III) stock standard solution, 500 ppm (1.85×10^{-2} M)

Dissolve 6.9520 g of $Al(NO_3)_3\cdot9H_2O$ with deionised water and make up to volume in a 1000-ml volumetric flask.

2.2 Cadmium(II) stock standard solution, 500 ppm (4.45×10^{-3} M)

Dissolve 1.3722 g of $Cd(NO_3)_2\cdot4H_2O$ with deionised water and make up to volume in a 1000-ml volumetric flask.

2.3 8-Hydroxyquinoline-5-sulphonic acid solution, 0.1 M

Dissolve 2.4820 g of 8-hydroxyquinoline-5-sulphonic acid monohydrate in 50 ml of 0.25-M $NaHCO_3$, and make up to volume in a 100-ml volumetric flask with deionised water.

Table 1 List of chemicals.

Chemicals	Formula	M.W.	Manufacturer
Acetic acid	CH_3COOH	60.05	BDH
Aluminium(III) nitrate nonahydrate	$Al(NO_3)_3{\cdot}9H_2O$	375.13	BDH
Ammonium chloride	NH_4Cl	53.49	Ajax
Ammonium hydroxide	NH_4OH	35.05	J.T. Baker
Cadmium(II) nitrate tetrahydrate	$Cd(NO_3)_2{\cdot}4H_2O$	308.48	Sigma-Aldrich
Cobalt(II) nitrate hexahydrate	$Co(NO_3)_2{\cdot}6H_2O$	291.03	Fisher
Copper(II) nitrate trihydrate	$Cu(NO_3)_2{\cdot}3H_2O$	241.60	Carlo Erba
Chromium(III) nitrate nonahydrate	$Cr(NO_3)_3{\cdot}9H_2O$	400.17	Fluka
Iron(III) nitrate nonahydrate	$Fe(NO_3)_3{\cdot}9H_2O$	404.00	Carlo Erba
Iron(II) sulphate heptahydrate	$FeSO_4{\cdot}7H_2O$	278.01	May&Baker
8-Hydroxyquinoline-5-sulphonic acid - monohydrate (HQS), 98%	$C_9H_7NO_4S{\cdot}H_2O$	243.24	ACROS
Lead(II) nitrate	$Pb(NO_3)_2$	331.20	Fluka
Magnesium(II) sulphate heptahydrate	$MgSO_4{\cdot}7H_2O$	246.48	MERCK
Sodium acetate trihydrate	$CH_3COONa{\cdot}3H_2O$	136.08	Carlo Erba
Zinc(II) nitrate tetrahydrate	$Zn(NO_3)_2{\cdot}4H_2O$	261.44	MERCK

2.4 Buffer solutions, pH 2.0-12.0

Buffer solutions of various pHs ranging from 2.0 to 12.0 were prepared by mixing the reagents as shown in Table 2 and finely adjusting to the required pH with appropriate reagent(s).

Table 2 Reagents used for preparing a 300-ml buffer solution of various pHs.

Reagents	Volumes used (ml) for buffer preparation of various pHs										
	2.0	**3.0**	**4.0**	**5.0**	**6.0**	**7.0**	**8.0**	**9.0**	**10.0**	**11.0**	**12.0**
0.2-M CH_3COOH	299.5	294.8	255.3	109.1	16.2	1.7	–	–	–	–	–
0.2-M CH_3COONa	0.5	5.2	44.7	190.9	283.8	298.3	–	–	–	–	–
0.2-M NH_3	–	–	–	–	–	–	16.1	108.7	255.1	294.8	299.5
0.2-M NH_4NO_3	–	–	–	–	–	–	283.9	191.3	44.9	5.2	0.5

Methods

1. Conventional Fluorescence Spectrometry

The complex formation of cadmium(II) and aluminium(III) with 8-hydroxy-quinoline-5-sulphonic acid (HQS) were studied by means of conventional fluorescence spectrometry. The fluorescence behaviors of the complexes were examined, and the experimental conditions were optimised. The compositions of the complexes were also determined.

1.1 Fluorescence spectra of Cd(II)-HQS and Al(III)-HQS complexes

The excitation and emission spectra of sulphoxinate complexes of 10-ppm Cd(II) and 10-ppm Al(III) (buffered to pH 8.4 and 5.4, respectively) were recorded, respectively, over a range of 200-900 nm by a fluorescence spectrometer — using excitation and emission slit widths of 5 nm and a scan speed of 1,000 nm min^{-1}. The spectral characteristics were observed from the fluorescence spectra, as shown in Figure 12 and Figure 13. The excitation and emission wavelengths of maximum fluorescence intensity, determined as λ_{ex} and λ_{em}, were used subsequently.

1.2 Instrumental parameters

1.2.1 Spectrum scanning speed

The speed for spectrum scanning was examined by comparing the emission spectra of aluminium(III) sulphoxinate scanned at various speeds, from 10 to 1,500 nm min^{-1}. The sulphoxinate complex solution of 1-ppm Al(III) was excited at λ_{ex} 404 nm and the emission spectra were recorded over a range of 350-650 nm using the excitation and emission slit widths of 10 nm. The spectral signals recorded at various speeds were compared. The speed chosen for the subsequent works was the one that generated a considerably low fluctuation in the signal. The fluctuation of signal at different scanning speeds is shown in Figure 14, with details in Appendix A.

1.2.2 Slit widths

The slit widths of excitation and emission monochromators were optimized in an univariate manner. The sulphoxinate complexes of 1-ppm Al(III) and 1-ppm Cd(II) were excited and the fluorescence intensity was measured using the λ_{ex} and λ_{em} corresponding to each individual complex. The excitation slit was varied over a width of 3-10 nm with an 1-nm increment. For each fixed excitation slit width, the emission slit was then varied over a width of 3-15 nm with an 1-nm increment. The slit widths that yielded the highest fluorescence intensity were selected for the following works. The results are shown in Figures 15 and 16, with detailed data in Appendix B.

1.3 Formation of sulphoxinate complexes

1.3.1 Optimization of sulphoxinate-complex formation

1.3.1.1 pH of complexation systems

The optimal pH for the formation of Cd(II)-HQS and Al(III)-HQS complexes were separately investigated. Series of HQS-complex solutions of 1-ppm Cd(II) and 1-ppm Al(III) were prepared and buffered to various pHs ranging from 2.0 to 12.0 (see the preparation of buffer solutions in Table 2). The fluorescence intensity of each complex solution was measured using the excitation and emission wavelengths corresponding to the individual metal complex. The pHs that yielded the maximum intensity were selected for the complexation of Cd(II) and Al(III) in the subsequent works. The results plotted as a function of pH are shown in Figure 17.

The appropriate volumes of buffer solution used for the complex systems were also examined in order to minimise the consumption of reagents. Sulphoxinate complexes of 1-ppm Cd(II) and 1-ppm Al(III) were prepared in a series of 25-ml volumetric flasks and buffered to the optimal pH for complexation

of individual metal with various volumes of buffer, *i.e.* 1, 2, 4, 6, 8, 10, 12, 14, 16, and 19 ml. The minimum volume that was capable to maintain the required pH was used thereafter. The results are shown in Figures 18 and 19.

1.3.1.2 Amount of HQS in complex formation

Various amounts of HQS were examined for the complex formation of 1-ppm Cd(II), and 1-ppm Al(III). Aliquot of 1×10^{-2} M HQS (0-500 µl) was added to a fixed 25-µg of metal ion of interest in a 25-ml volumetric flask, buffered to the pH, and made up to volume with deionised water. The fluorescence intensity of each complex solution was measured, using the λ_{ex} and λ_{em} corresponding to the individual metal complex. The amount of HQS that yielded the maximum fluorescence, plotted in Figure 20, was selected for the complexation in the subsequent works.

1.3.1.3 Standing period for complexation

The standing period for the complete formation of sulphoxinate complexes was determined by repeating the fluorimetric measurement after the reagent mixing for 3 hours — every 15 minutes within the first hour, then every 30 minutes for the next two hours. The fluorescence of sulphoxinate complexes of 1-ppm Cd(II), 1-ppm Al(III), and a mixture of 1-ppm Cd(II) and 1-ppm Al(III) were inspected separately using the λ_{ex} and λ_{em} corresponding to the individual metal complex. Developments of the complexes with time are shown in Figure 21.

1.3.2 Stability of sulphoxinate complexes

The stability of each complex was also observed by repeating the measurement every an hour over a period of 10 hours as shown in Figure 21.

1.4 Compositions of Cd(II)-HQS and Al(III)-HQS complexes

The compositions of Cd(II)-HQS and Al(III)-HQS complexes were determined by continuous variation method (Job's method). Two series of metal complexes were prepared by mixing 1.0×10^{-4} M metal-ion solution with 1.0×10^{-4} M HQS solution at various volume ratios as shown in Table 3 and making to volume with buffer solution corresponding to each metal used. The fluorescence intensity of Cd(II)-HQS and Al(III)-HQS complex solutions were measured using λ_{ex} and λ_{em} corresponding to the individual metal complex. The fluorescence intensities obtained were plotted versus the mole fractions of HQS or/and metal ion. The composition of Cd(II)-HQS and Al(III)-HQS were determined from abrupt change in the slope of the Job's plot as shown in Figures 22 and 23, respectively. The postulated structures of the complexes are shown in Figure 24. The stability constant, K_s , of the two complexes were also calculated, as shown in Appendix C.

Table 3 Variable amounts of reagents used in the continuous variation method.

Volume of reagents, ml		**Mole fraction in the system**	
Metal ion[a]	**HQS**[a]	**Metal ion**	**HQS**
0.00	10.00	0.0	1.0
1.00	9.00	0.1	0.9
2.00	8.00	0.2	0.8
3.00	7.00	0.3	0.7
4.00	6.00	0.4	0.6
5.00	5.00	0.5	0.5
6.00	4.00	0.6	0.4
7.00	3.00	0.7	0.3
8.00	2.00	0.8	0.2
9.00	1.00	0.9	0.1
10.00	0.00	1.0	0.0

[a]A concentration of 1.0×10^{-4} M.

2. Synchronous-scanning Fluorescence Spectrometry

The sulphoxinate complexes of cadmium(II) and aluminium(III) were also studied by synchronous-scanning fluorescence (SSF) method. Under the SSF mode, the excitation and emission monochromators are locked together and simultaneously scanned with a constant wavelength interval between them, $\Delta\lambda = \lambda_{em} - \lambda_{ex}$. Previous conditions were used for the formation of sulphoxinate complexes.

2.1 SSF spectra of Cd(II)-HQS and Al(III)-HQS complexes

The synchronous-scanning fluorescence spectra of HQS complexes of 1-ppm Cd(II) and 1-ppm Al(III) solutions were recorded, respectively, over a range of 200-700 nm using a wavelength interval of 150 nm together with the excitation and emission slit widths and scanning speed obtained from the previous CF studies. The synchronous spectra, recorded in the function of excitation wavelength, were shown in Figure 25. The spectral characteristics were observed, and the wavelengths of maximum fluorescence intensity, determined as λ_{ss}, were used subsequently.

2.2 Wavelength interval parameter

The wavelength interval for SSF of individual metal-complex and the binary mixture were examined. The synchronous spectra of sulphoxinate complexes of 1-ppm Cd(II), 1-ppm Al(III), and a mixture of 1-ppm Cd(II) and 1-ppm Al(III) were recorded under two separate complexation conditions: that of Cd(II)-HQS, and of Al(III)-HQS. The value of $\Delta\lambda$ was varied over a range of 100-170 nm with a 5-nm increment, *i.e.* 100, 105, 110, 115, 120, ... , 170 nm. The difference in λ_{ss} between the complex of interest in the binary mixture and in pure solution was compared to that between the complex of interest in the binary mixture and its counterpart in pure solution. The $\Delta\lambda$ that generated the most appreciable resolution of the spectral peaks was selected for later use. The effects of $\Delta\lambda$ on peak resolution are shown in Figures 26 and 27. The SSF spectra recorded at different $\Delta\lambda$s are shown in Appendix D.

3. Derivative Synchronous-scanning Fluorescence Spectrometry

Derivative calculations were applied to synchronous-scanning fluorescence spectra in order to enhance the spectral resolution and to locate the precise positions of the overlapping peaks. The derivative SSF spectra were acquired from the FL-WinLab programme (see Appendix E). The derivative calculations were also aimed to eliminate the matrix interference.

3.1 Number of point for derivative-spectral calculation

The number of point used for calculating the derivatives of SSF spectra was optimised. The first derivative of SSF (D1SSF) spectra of HQS complexes of 1-ppm Cd(II) and 1-ppm Al(III) were calculated using various numbers of point over a range of 5-95 points with a 10-point increment. Fluctuation in the amplitude of the resulted spectra, shown in Figures 28 and 29, were compared. The numbers of point that yielded the minimum fluctuation without losing the amplitude of the peak (^1D) were selected for subsequent derivative calculations.

3.2 Zero-crossing wavelengths of derivative spectra

The λ_D , at which the amplitude of derivative peaks was to be measured, was determined by the zero-crossing method (Figure 11). Four series of sulphoxinate complexes of the metal of interest were prepared under two separate complexation conditions: that of its own, and of its counterpart, as shown in the table below.

	Concentrations in the system under complexation conditions:	
	of Cd(II) sulphoxinate	**of Al(III) sulphoxinate**
Series of Cd(II)	0, 0.2, 0.4, 0.6, 0.8, 1.0 ppm	0, 70, 75, 80, 85, 90, 95, 100 ppm
Series of Al(III)	0, 1.2, 2.4, 3.6, 4.8 ppm	0, 0.2, 0.4, 0.6, 0.8, 1.0 ppm
HQS	4.0×10^{-5} molar	8.0×10^{-5} molar

The SSF spectrum of each complex solution was recorded over a range of 200-700 nm. The D1SSF and D2SSF of all SSF spectra were acquired from the FL-WinLab programme using the number of point obtained previously. The wavelengths in the derivative spectra of each complex series at which no contribution of signal was found were determined as zero-crossing wavelengths, λ_Z. The D1SSF and D2SSF spectra of Cd(II)-HQS complex with zero-crossing wavelengths are shown in Figures 30 and 31, respectively; and those of Al(III)-HQS in Figures 32 and 33. The wavelengths λ_{ex} and λ_{em} obtained in CF, λ_{ss} in SSF, and λ_{Z1} and λ_{Z2} in derivative SSFs, are summarised in Table 4.

3.3 Independence of signal measurements

The suitable zero-crossing wavelengths used for determination of the metal sulphoxinate complexes were investigated. Series of HQS-complex solutions were prepared in which a fixed concentration of metal of interest containing its counterpart with various molar-concentration ratios were mixed under the conditions for complexation of the metal of interest. The D1SSF and D2SSF spectra were acquired. The amplitudes ^1D and ^2D of the complex at different zero-crossing wavelengths of its counterpart were compared. The wavelength at which the presence of counterpart did not affect the peak amplitudes was chosen for the determination of metal complex. The effects of Al(III) on the peak amplitudes of Cd(II)-HQS measured at different zero-crossing wavelengths of Al(III)-HQS, $\lambda_{Z,Al(III)}$, are shown in Figures 34 and 35. Figures 36 and 37 display the effects of Cd(II) on the peak amplitudes of Al(III)-HQS measured at different zero-crossing wavelengths of Cd(II)-HQS, $\lambda_{Z,Cd(II)}$.

The independence of signal measurements in each method between those of Cd(II)-HQS and Al(III)-HQS was also tested. Series of binary complex solutions were prepared at various molar-concentration ratios of Cd(II) to Al(III). Calibration graphs of the complex of interest obtained from CF, SSF, D1SSF, and D2SSF methods using were compared. The working wavelength which produced a calibration graph with good correlation coefficient (r^2) for the metal of interest was

considered to be an independent position — free from the influence of its counterpart. The results are shown in Table 5.

4. Effect of Foreign Species

Potentially interfering species in the complexation of Cd(II) and Al(III) with HQS were investigated. Series of complex solutions were prepared by mixing the individual metal ion of interest and HQS in the presence of interfering species at various molar concentration ratios to the metal ion of interest, *i.e*. 0:1, 0.25:1, 0.5:1, 1:1, 1:5, and 1:10 respectively. Each solution was prepared under the complexation conditions of the metal of interest. Nine foreign species were studied, namely Cr(III), Fe(II), Fe(III), Co(II), Ni(II), Cu(II), Zn(II), Pb(II), and Mg(II). The SSF spectrum of each complex solution was recorded over a range of 200-700 nm, and the D1SSF and D2SSF of all SSF spectra were acquired from the FL-WinLab programme using all the parameters obtained previously. The peak amplitudes ^{1}D and ^{2}D of D1SSF and D2SSF spectra were measured and compared. The presence of foreign species that caused change in amplitude less than 5% was accepted in this work as non-significant interfering effect — *i.e.* the tolerance limit. The degree of interference of the foreign species in the complexation of Cd(II) and Al(III) with HQS are summarised in Tables 6 and 7, and Tables 8 and 9, respectively.

5. Determination of Cd(II) and Al(III) as Sulphoxinate Complexes

The determination of Cd(II) and Al(III) as sulphoxinate complexes in binary mixture were examined by means of CF, SSF, D1SSF, and D2SSF methods using external standard calibration graphs. The results were compared. Previously optimised conditions and instrumental parameters were used for the formation of sulphoxinate complexes and for the fluorescence measurements.

5.1 Standard calibration graphs for Cd(II)

Two series of Cd(II)-HQS solutions: Cd(II) and Cd(II) in binary mixture of Cd(II)-Al(III), were prepared over a concentration range of 0-1,000 ppb of Cd(II). Aliquots of standard solutions, as shown in the following Table, were mixed and buffered to pH 8.8, then made up to volume with de-ionised water in a 25-ml volumetric flask. The fluorescence intensity of Cd(II)-HQS in each solution was measured by CF method. The SSF spectra of Cd(II)-HQS in the solutions were recorded over a range of 200-700 nm, and the D1SSF and D2SSF of all SSF spectra were acquired. The signals and peak amplitudes obtained from each method were plot as a function of concentration of Cd(II).

Concentration series	**Volume, μl, of reagents used in preparation of calibration graphs**		
	50-ppm Cd(II) solution	**100-ppm Al(III) solution**	**0.01-M HQS**
Cd(II)	0, 100, 200, 300, 400, and 500	—	100
Mixture 1	0, 100, 200, 300, 400, and 500	0, 360, 720, 1080, 1440, and 1800	100

Standard calibration graphs for Cd(II) obtained from the two series were compared in Figure 38. The mutual independence of the measured signals of Cd(II)-HQS and Al(III)-HQS was observed.

5.2 Standard calibration graphs for Al(III)

Two series of Al(III)-HQS solutions: Al(III) and Al(III) in binary mixture of Al(III)-Cd(II), were prepared over a concentration range of 0-1,000 ppb of Al(III). Aliquots of standard solutions, as shown in the following Table, were mixed and buffered to pH 4.0, then made up to volume with de-ionised water in a 25-ml volumetric flask. The fluorescence intensity of Al(III)-HQS in each solution was measured by CF method. The SSF spectra of Al(III)-HQS in the solutions were recorded over a range of 200-700 nm, and the D1SSF and D2SSF of all SSF spectra were acquired. The signals and peak amplitudes obtained from each method were plot as a function of concentration of Al(III).

Concentration series	Volume, μl, of reagents used in preparation of calibration graphs		
	50-ppm Al(III) solution	500-ppm Cd(II) solution	0.01-M HQS
Al(III)	0, 100, 200, 300, 400, and 500	—	200
Mixture 2	0, 100, 200, 300, 400, and 500	0, 1028, 2055, 3083, 4111, and 5139	200

Standard calibration graphs for Al(III) obtained from the two series were compared in Figure 39. The mutual independence of the measured signals of Al(III)-HQS and Cd(II)-HQS was observed.

5.3 Analysis of samples

5.3.1 Determination of Cd(II) in the presence of Al(III)

Synthetic mixture solutions of Al(III) and Cd(II) were used for examining the spectrofluorimetric determination of Cd(II) in the presence of Al(III). A series of Cd(II)-HQS complex solutions were prepared from the synthetic solutions — a mixture of 500 μl of 50-ppm-Cd(II)standard solution with 100-ppm-Al(III) standard solution at molar concentration ratios of Cd(II) to Al(III) of 1:0, 1:7.5, 1:15, 1:22.5, and 1:30. The fluorescence intensity of Cd(II)-HQS in each synthetic sample was measured by CF method. The SSF spectra of Cd(II)-HQS were recorded, and the D1SSF and D2SSF of SSF spectra were acquired. The concentrations of Cd(II) in the samples were evaluated from the corresponding calibration graphs. The results are shown in Table 10.

5.3.2 Determination of Al(III) in the presence of Cd(II)

Synthetic mixture solutions of Al(III) and Cd(II) were used for examining the spectrofluorimetric determination of Al(III) in the presence of Cd(II). A series of Al(III)-HQS complex solutions were prepared from the synthetic solutions — a mixture of 500 μl of 50-ppm-Al(III) standard solution with 500-ppm-Cd(II) standard solution at molar concentration ratios of Al(III) to Cd(II) of 1:0, 1:6.25, 1:12.5, 1:18.75, and 1:25. The fluorescence intensity of Al(III)-HQS in each

synthetic sample was measured by CF method. The SSF spectra of Al(III)-HQS were recorded, and the D1SSF and D2SSF of SSF spectra were acquired. The concentrations of Al(III) in the samples were evaluated from the corresponding calibration graphs. The results are shown in Table 11.

RESULTS AND DISCUSSIONS

1. Conventional Fluorescence Spectrometry

1.1 Fluorescence spectra of Cd(II)-HQS and Al(III)-HQS complexes

The excitation and emission spectra of sulphoxinate complexes of 10-ppm Cd(II) and 10-ppm Al(III), obtained from a Perkin-Elmer^{TM} LS55 luminescence spectrometer, are shown in Figures 12 and 13, respectively. Both complexes possess spectra that look much alike. The spectra are board-banded with the peak maximum covering a wavelength range of approximately 5-10 nm. The λ_{ex} of cadmium(II) sulphoxinate complex, Cd(II)-HQS, is found over the wavelength of 373.0 ± 5.0 nm, whilst that of aluminium(III) sulphoxinate is 394.0 ± 2.5 nm. The maximum fluorescence of Cd(II)-HQS was located over the λ_{em} of 519.0 ± 5.0 nm, and that of Al(III)-HQS over the range of 497.0 ± 2.0 nm. The overlap of those spectra, however, renders a serious spectral interference between Cd(II)-HQS and Al(III)-HQS.

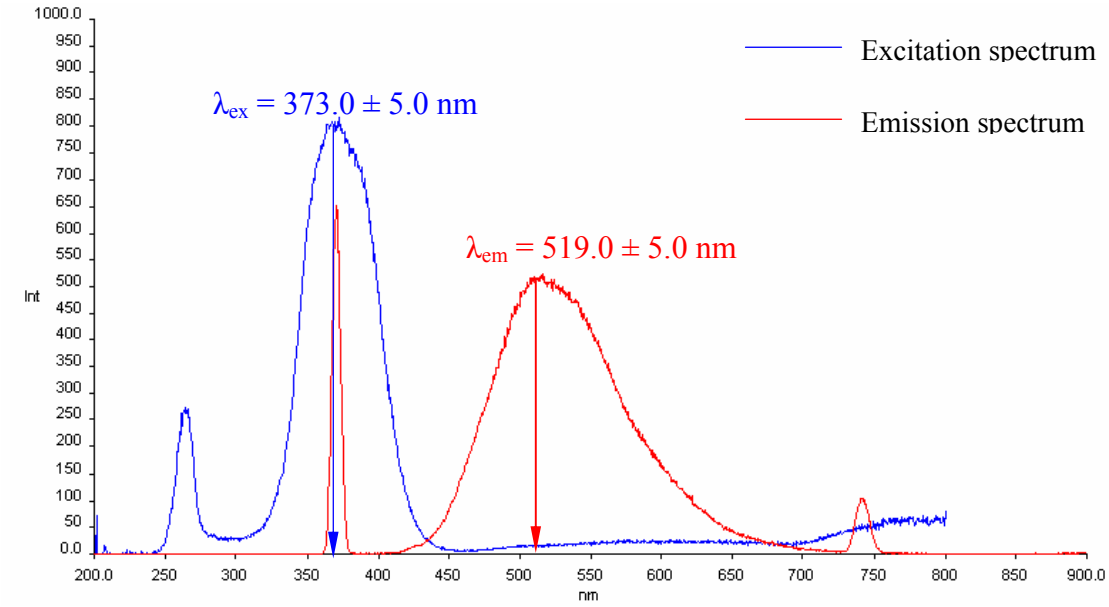

Figure 12 Excitation and emission spectra of cadmium(II) sulphoxinate.

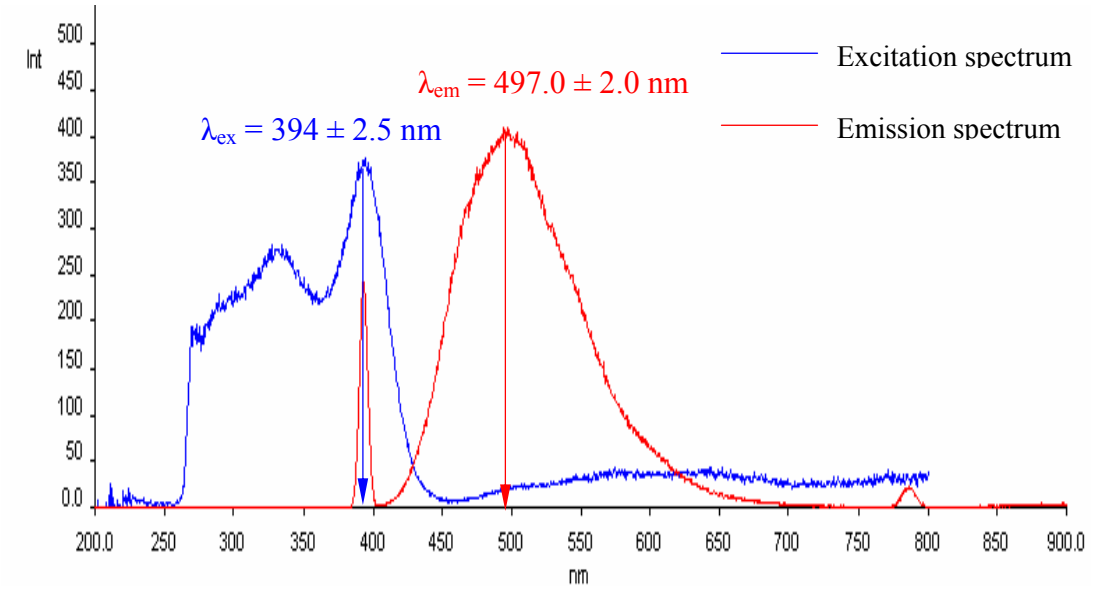

Figure 13 Excitation and emission spectra of aluminium(III) sulphoxinate.

1.2 Instrumental parameters

1.2.1 Spectrum scanning speed

The times used for spectrum scanning of Al(III)-HQS complex were calculated from scanning speeds — the data shown in Appendix A; the faster the scanning speed, the shorter the scanning time. It was found that fluctuation in the signal tended to increase with the scanning speed. The fluctuation of signal at peak maxima (over a range of 494-501 nm) at different scanning speeds is shown in Figure 14. The plot shows a periodic pattern in the fluctuation. However, the speeds over the ranges of 10-100 and 400-500 nm min^{-1} were found to generate a rather constant and considerably low fluctuation in the signal. The scanning speed of 450 nm min^{-1} was chosen for the subsequent use as the scanning time of 0.67 min was acceptable in this work.

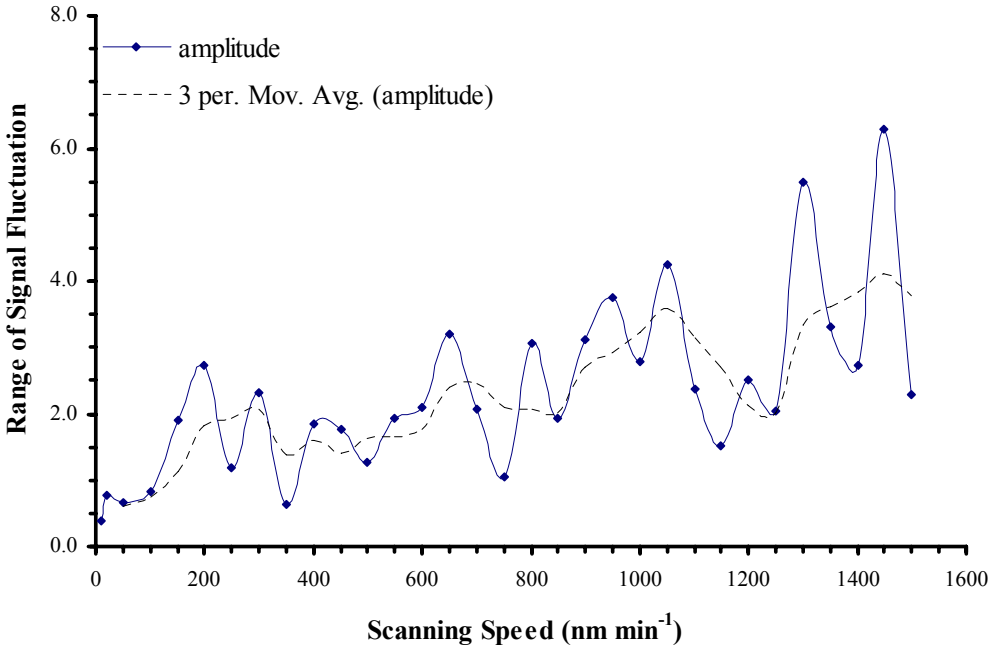

Figure 14 Fluctuation of fluorescence signals at different scanning speeds.

1.2.2 Slit widths

The effect of slit widths on the measured fluorescence intensity of Al(III)-HQS complex is shown in Figure 15. The fluorescence intensity increases slightly over the excitation slit widths from 3-5 nm, then drops instantaneously at the width of 6 nm and remains almost so up to 10-nm width. The fluorescence intensity was found to be increase with the width of the emission slit.

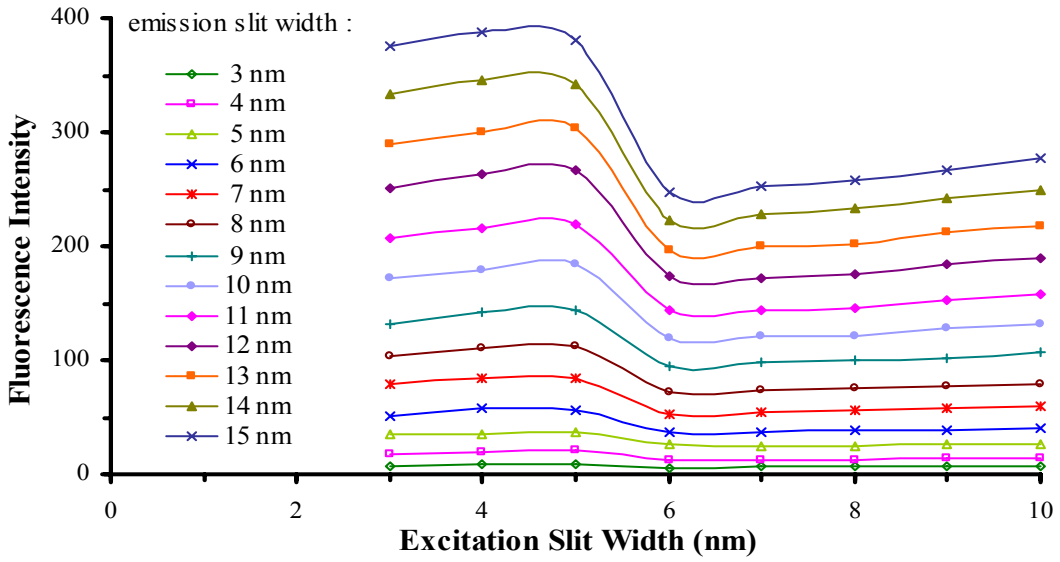

Figure 15 Effect of slit widths on the measured fluorescence of Al(III)-HQS.

The effect of slit widths on the measured fluorescence intensity of Cd(II)-HQS complex, shown in Figure 16, was found to be similar to that of Al(III)-HQS. However, the intensity of Cd(II)-HQS could not be measured when the width of emission slit was >5 nm, as the detailed data shown in Appendix B. The full-scale of intensity measurement, set up by the manufacturer, is 1,000.

Consequently, the slit widths of excitation and emission mono-chromators were optimized at 5 nm for both Al(III)-HQS and Cd(II)-HQS, as to accommodate the fluorescence measurement of Cd(II)-HQS.

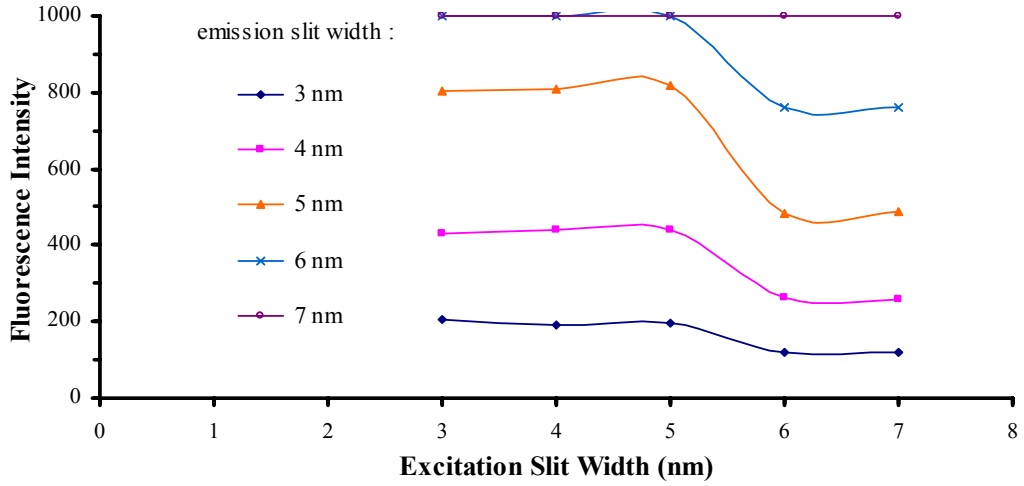

Figure 16 Effect of slit widths on the measured fluorescence of Cd(II)-HQS.

1.3 Formation of HQS complexes

1.3.1 Optimization of HQS-complex formation

1.3.1.1 pH of complexation systems

The effect of pH upon the formation of Cd(II)-HQS and Al(III)-HQS complexes is shown in Figure 17. The fluorescence of Cd(II)-HQS at λ_{em} 519 nm rapidly increase with the pH from 5.0 to 7.0, and becomes constant up to pH 8.8. The Al(III)-HQS yielded maximum fluorescence intensity (λ_{em} 497 nm) at pH 4.0 where the fluorescence intensity of Cd(II)-HQS was found to be insignificant and could be neglected. The pH 4.0 was, therefore, selected for Al(III)-HQS complexation in the subsequent experiments. For the formation of Cd(II)-HQS, the pH 8.8 was chosen as to avoid the fluorescence of Al(III)-HQS.

The buffering capacity of the buffer reagents used for the HQS-complexation of Cd(II) and Al(III) are shown in Figure 18 and 19, respectively. The complexation of Cd(II)-HQS was buffered to pH 8.8 by basic buffer NH_3-NH_4Cl, and Al(III)-HQS to pH 4.0 by acidic buffer CH_3COOH-CH_3COONa. It was found that each complex system attained the desired pH by adding the appropriate buffer

solution from 8 to 19 ml. Since the buffer volume of 8 ml was sufficient, it was, therefore, chosen for the subsequent use as to minimise the consumption of buffer reagents.

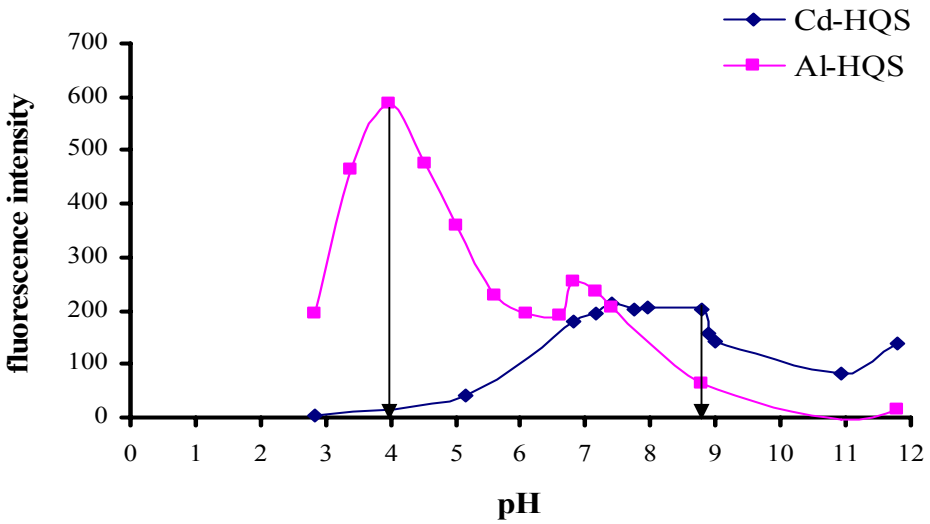

Figure 17 Effect of pH on formation of Cd(II)-HQS and Al-HQS complexes.

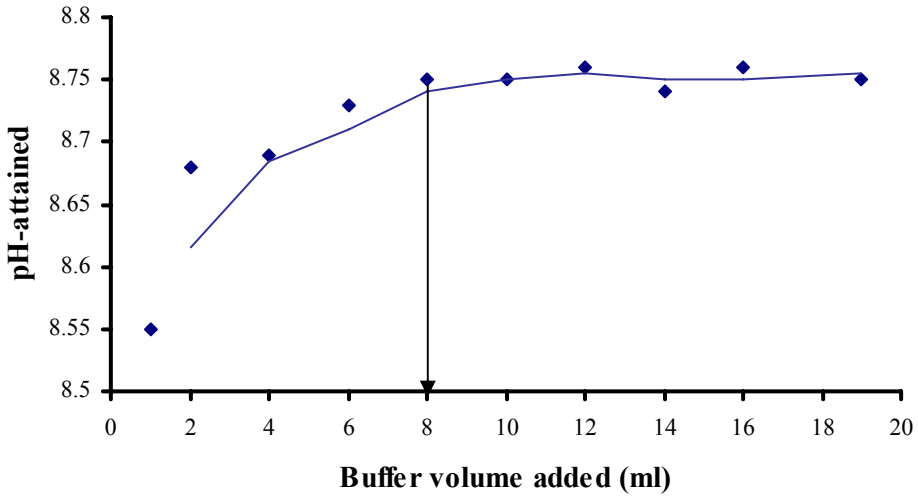

Figure 18 Buffering capacity of NH_3-NH_4Cl on complexation of Cd(II)-HQS.

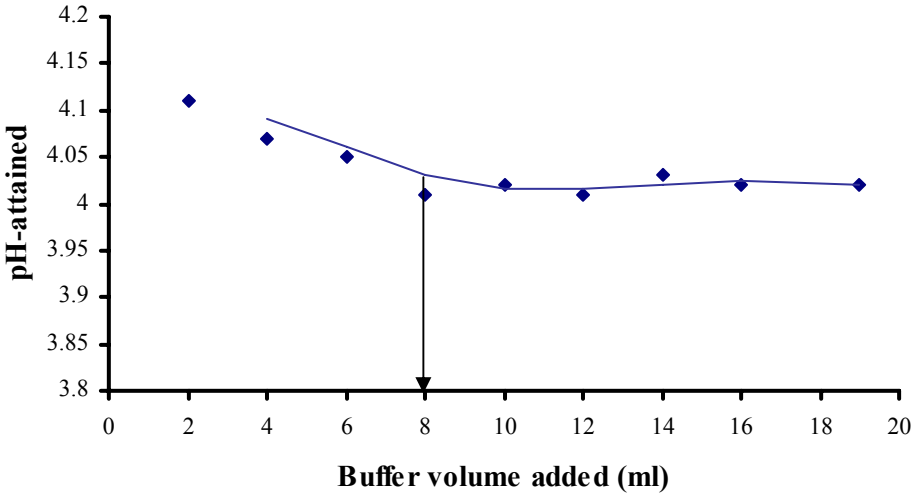

Figure 19 Buffering capacity of AcOH-AcONa on complexation of Al(III)-HQS.

1.3.1.2 Amount of HQS in complex formation

Figure 20 illustrates that the fluorescence intensity initially increases with the amount of HQS added for complexation, and becomes constant over a range of HQS added; then decreases slowly with further addition of HQS. In the complexation of 1-ppm Cd(II) 25.00 ml, HQS of 2.0×10^{-5} to 5.0×10^{-5} M (*i.e.* 50-125 μl of 0.01-M HQS) was found forming Cd(II)-HQS of maximum fluorescence. The volume of 100 μl (4.0×10^{-5} M HQS) was then used in later Cd(II)-HQS formation. As for 25.00 ml of 1-ppm Al(III), it was found that HQS of 6.8×10^{-5} to 1.1×10^{-4} M (*i.e.* 170-275 μl of 0.01-M HQS) formed Al(III)-HQS complex with maximum fluorescence. The volume of 200 μl (8.0×10^{-5} M HQS) was used consequently for Al(III)-HQS formation.

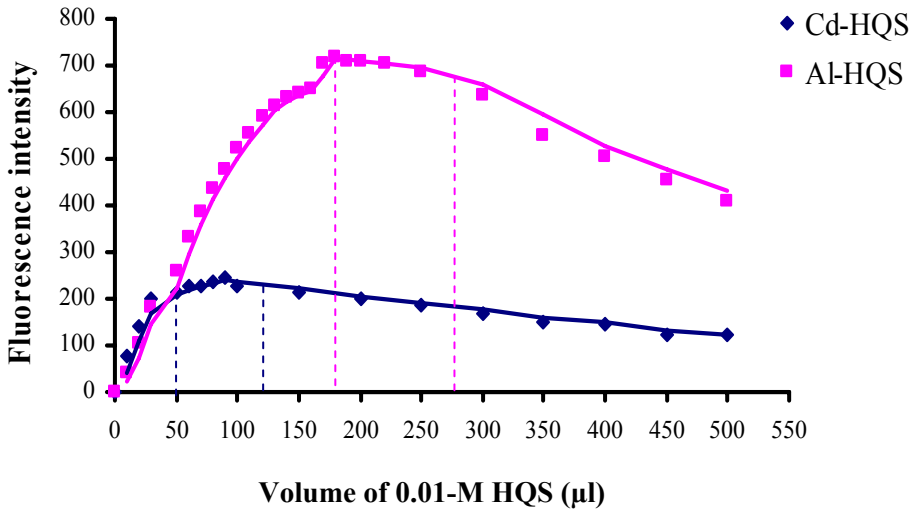

Figure 20 Amounts of HQS for complexation of 1-ppm Cd(II) and 1-ppm Al(III).

1.3.1.3 Standing period for complexation

The plots in Figure 21 display the development of fluorescence intensity with respect to the standing time after the reagent mixing. The high intensity obtained from the first measurement suggested that the complexes were formed almost instantly after the mixing but the reaction was not yet complete. The fluorescence intensity of cadmium(II) sulphoxinate (Figure 21-a) gradually increases with the standing time and reaches the maximum after 2.5 hours, from which the intensity remains constant. The formation of aluminium(III) sulphoxinate was complete after 3.0 hours (Figure 21-b).

1.3.2 Stability of sulphoxinate complexes

Both sulphoxinate complexes are stable up to at least 10 hours, Figure 21. In the subsequent measurements, the complexation of Cd(II) and Al(III) were to be stood for 2.5 hours and 3.0 hours, respectively.

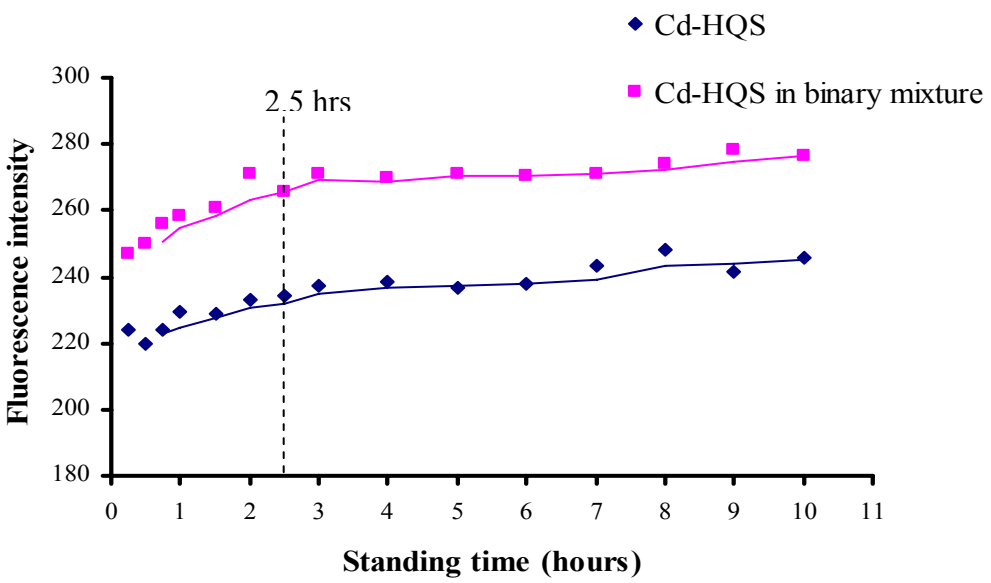

(a)

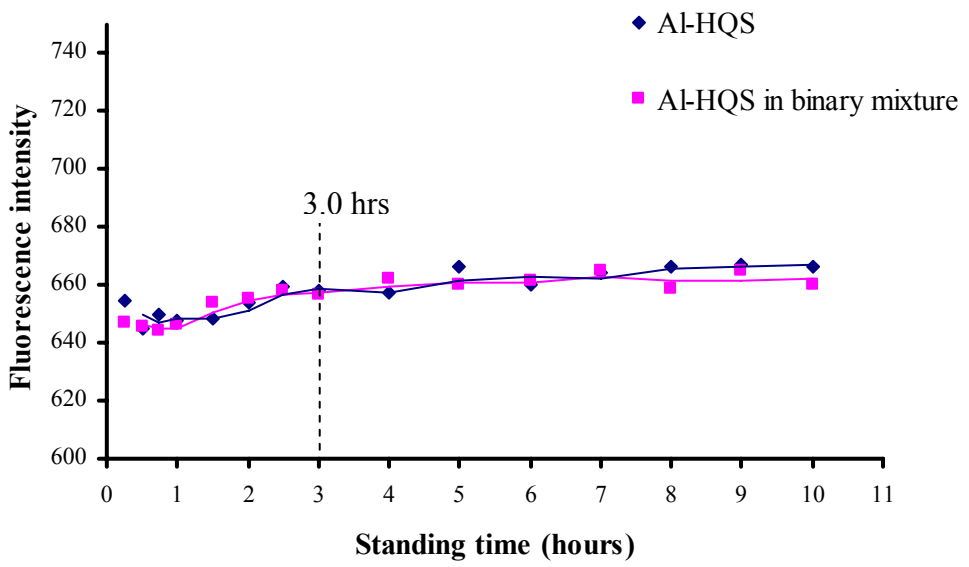

(b)

Figure 21 Standing times for development of fluorescence intensity:
a) cadmium(II) sulphoxinate, b) aluminium(III) sulphoxinate.

1.4 Compositions of Cd(II)-HQS and Al(III)-HQS complexes

The continuous variation plot of Cd(II)-HQS in Figure 22 shows that the maximum fluorescence is obtained at mole fractions of 0.525 Cd(II) and 0.475 HQS. The composition of Cd(II)-HQS was then established at 1:1 of Cd(II) to HQS. The composition of Al(III)-HQS was also found to be 1:1 of Al(III) to HQS. Figure 23 shows the maximum fluorescence is obtained at mole fractions of 0.462 Al(III) and 0.538 HQS. The structures of the complexes are postulated as shown in Figure 24.

The stability constant, K_s , of Cd(II)-HQS and Al(III)-HQS complexes are found to be 2.3143×10^3 and 2.0761×10^3, respectively (see Appendix C). It may be concluded from the stability constants that HQS forms a complex with Cd(II) that is more slightly stable than with Al(III).

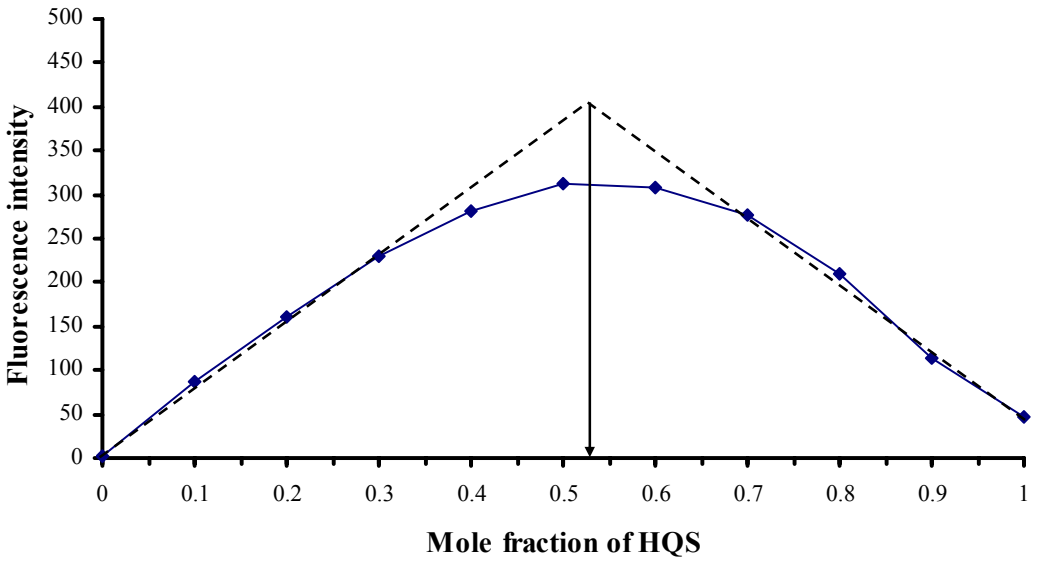

Figure 22 Continuous variation plot of Cd(II)-HQS complex at λ_{em} 519 nm.

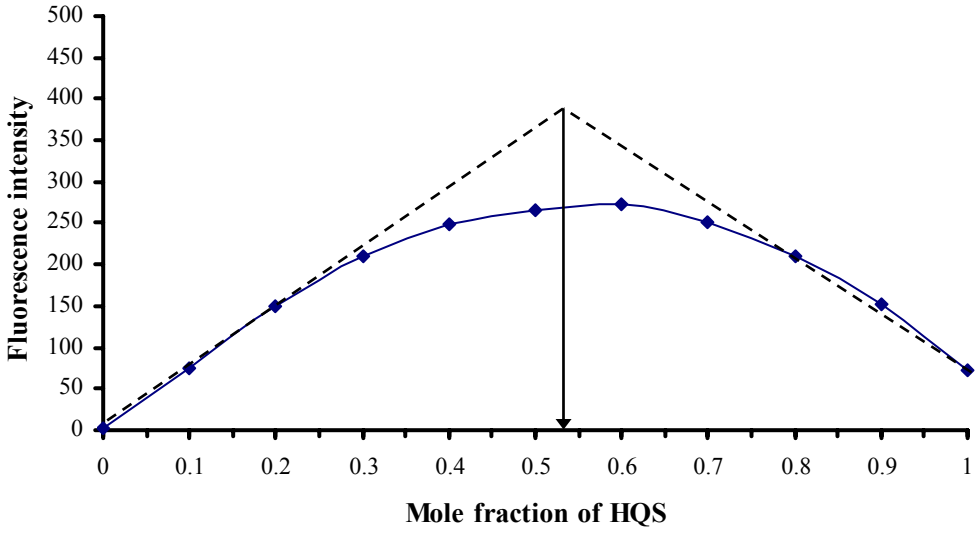

Figure 23 Continuous variation plot of Al(III)-HQS complex at λ_{em} 497 nm.

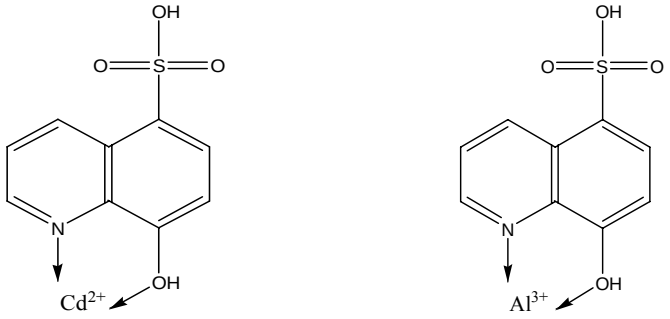

(a) (b)

Figure 24 Postulated structures of HQS complexes:
a) cadmium(II) sulphoxinate, b) aluminium(III) sulphoxinate.

2. Synchronous-scanning Fluorescence Spectrometry

2.1 SSF spectra of Cd(II)-HQS and Al(III)-HQS complexes

Figure 25 shows, the synchronous spectra of HQS complexes of 1-ppm Cd(II) and 1-ppm Al(III) solution, obtained from a Perkin-Elmer^{TM} LS55 fluorescence spectrometer in the mode of synchronous scanning. The SSF spectra, recorded in the function of excitation wavelength, display the sharp and narrow characteristics of the peaks compared to those of conventional fluorescence spectra. The SSF peak width at half height was reduced to about two-third of the CF peak in both Cd(II)-HQS and Al(III)-HQS spectra. Nonetheless, the overlap of spectral bands is still found and the spectral interference between Cd(II)-HQS and Al(III)-HQS still exists. The maximum intensity of Cd(II)-HQS was found over the λ_{ss} of 370.0 ± 5.0 nm. As for Al(III)-HQS, the maximum fluorescence was found over the range of 363.0 ± 5.0 nm.

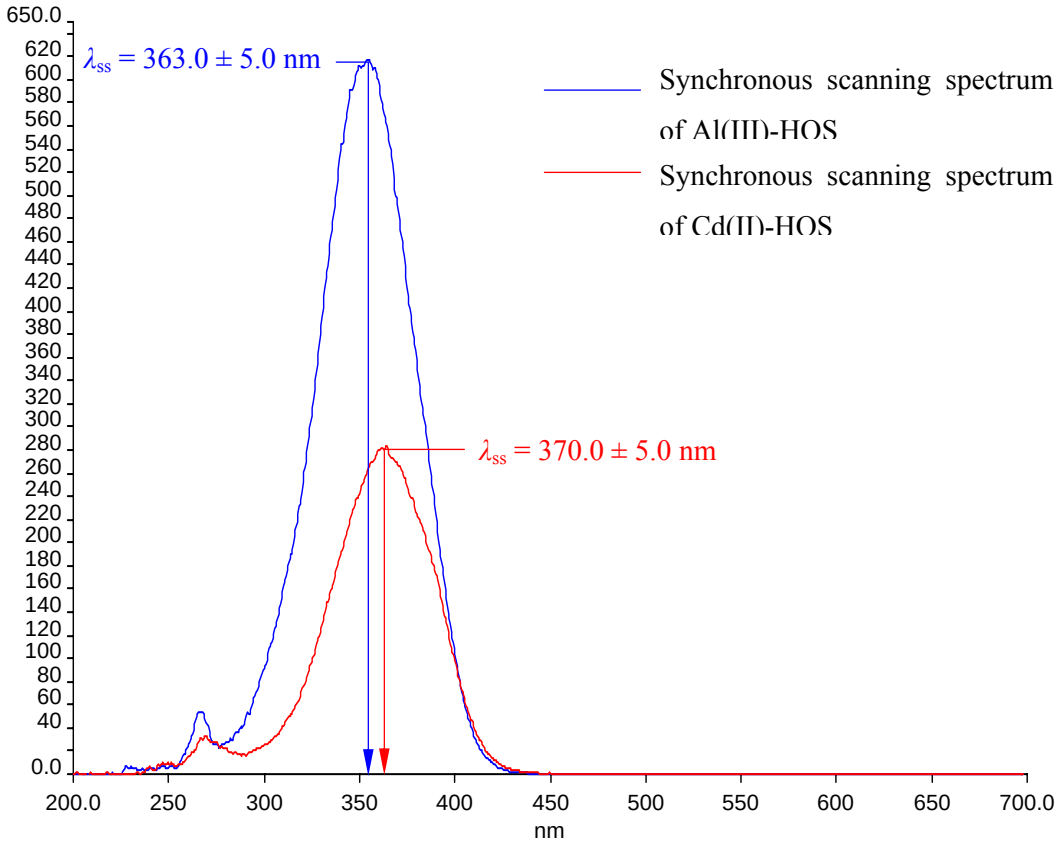

Figure 25 Synchronous-scanning fluorescence spectra of Cd(II)-HQS and Al(III)-HQS using Δλ of 150 nm.

2.2 Wavelength interval parameter

The SSF spectra of Cd(II)-HQS, Al(III)-HQS, and binary mixture of both ions, in buffer solutions of pH 8.8 and 4.0, recorded at different Δλs (100-170 nm) are shown in Appendix D. Figure 26 shows the difference in λ_{ss} between that of Cd(II)-HQS complex in the binary mixture and in pure solution (Figure 26-a) compared to that between Cd(II)-HQS in the binary mixture and Al(III)-HQS in pure solution (Figure 26-b). At Δλ of 120 nm, the division between (a) and (b) is of maximum, that is the most appreciable resolution of the spectral peaks. Hence, the Δλ of 120 nm was selected for later SSF measurements of Cd(II)-HQS. From figure 27, a Δλ of 115 nm was used for SSF measurements of Al(III)-HQS thereafter.

It was found upon the optimisation of Δλ values that the band-narrowing effect had improved. However, it was still not possible to resolve the overlapping peaks of Cd(II)-HQS and Al(III)-HQS by SSF method.

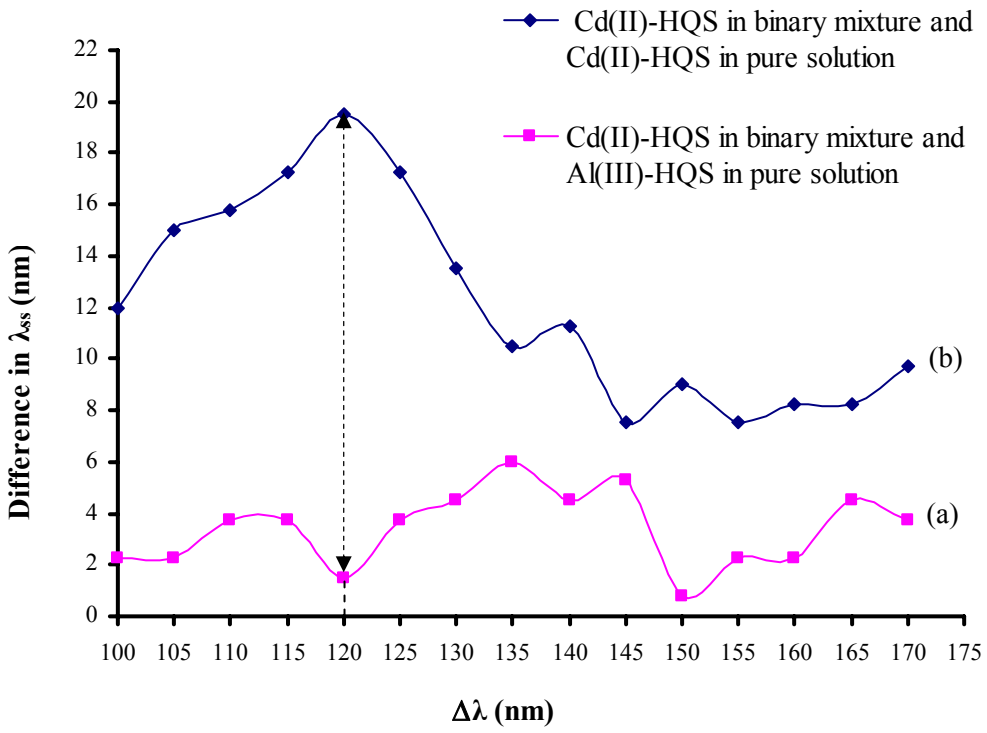

Figure 26 Effect of Δλ on spectral resolution of Cd(II)-HQS in binary mixture at the pH 8.8 of Cd(II)-HQS formation.

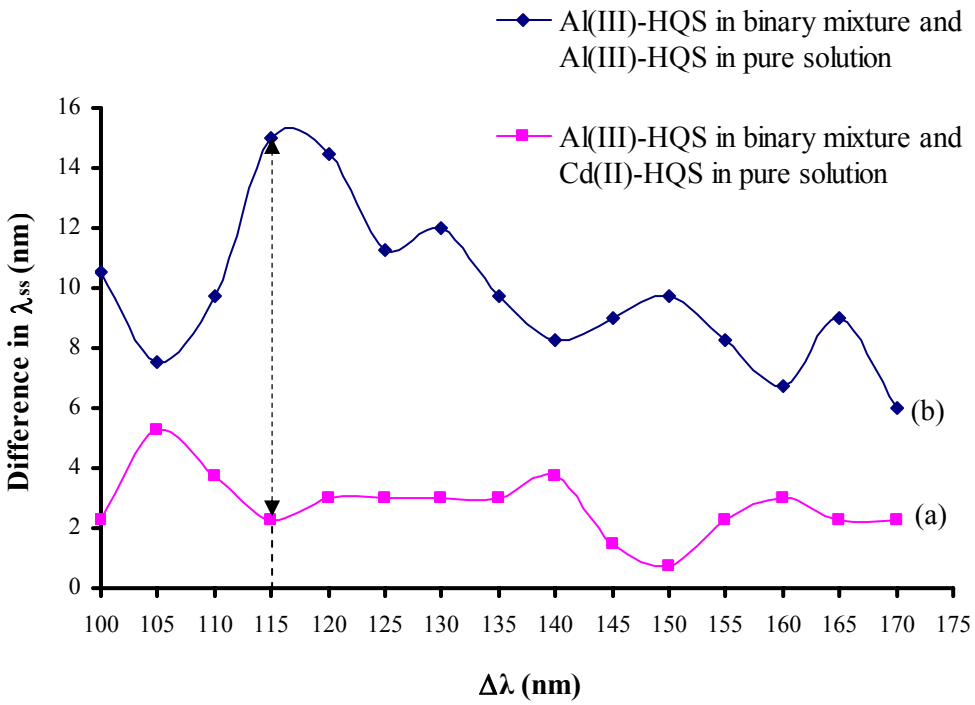

Figure 27 Effect of Δλ on spectral resolution of Al(III)-HQS in binary mixture at the pH 4.0 of Al(III)-HQS formation.

3. Derivative Synchronous-scanning Fluorescence Spectrometry

3.1 Number of point for derivative-spectral calculation

Derivative spectra of SSF were acquired from FL-WinLab programme shown in Appendix E. Figures 28 and 29 display the D1SSF spectra of Cd(II)-HQS and Al(III)-HQS complexes calculated from various numbers of point. Fluctuation in the amplitude of the resulted spectra, together with the peak amplitudes, was found to decrease with the increasing number of point. The number of 25 points was chosen for subsequent derivative calculations as the decrease in peak amplitude (^1D) was accepted in this work as insignificant.

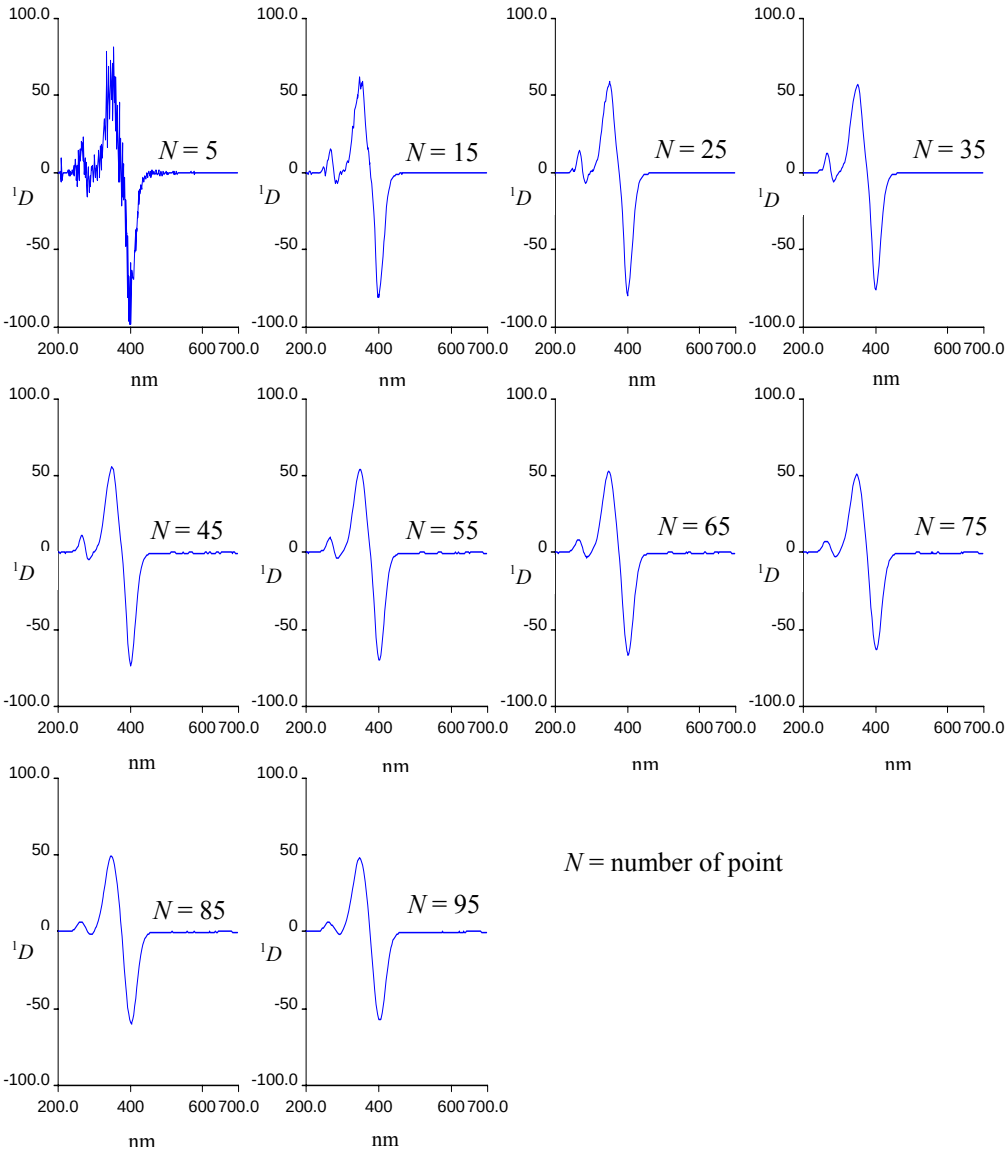

Figure 28 D1SSF spectra of Cd(II)-HQS complex, at pH 8.8, calculated from different numbers of point.

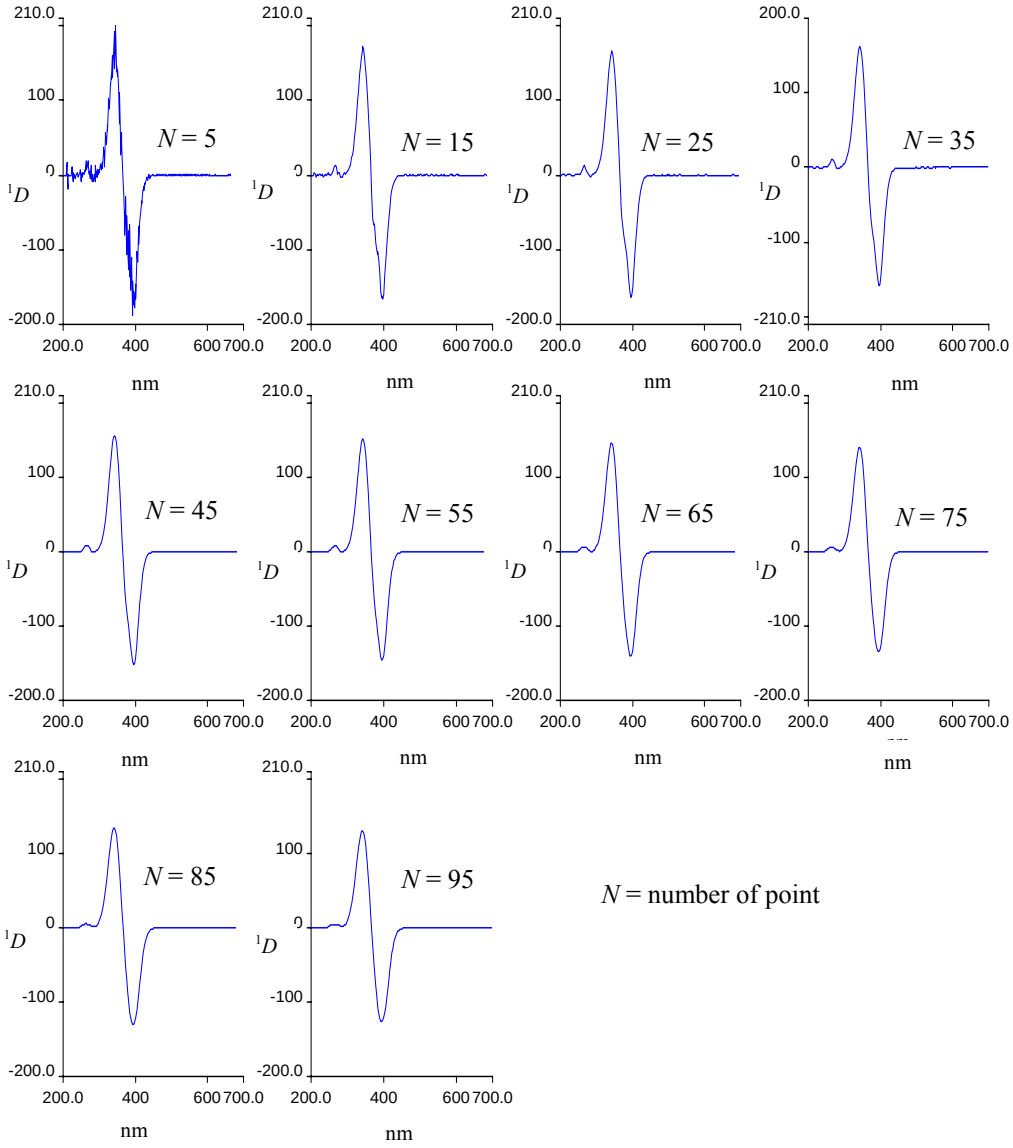

Figure 29 D1SSF spectra of Al(III)-HQS complex, at pH 4.0, calculated from different numbers of point.

3.2 Zero-crossing wavelengths of derivative spectra

The zero-crossing wavelength in derivative spectra, λ_Z ,is defined as the wavelength at which no contribution of signal is found. Figures 30 and 31 display the D1SSF and D2SSF spectra of Cd(II)-HQS complex with the wavelengths at zero-crossing. Those of Al(III)-HQS are shown in Figures 32 and 33. Comparing each Figures (a) and (b), it was found that the values of λ_Z remained the same under either complexation conditions. The optimised wavelengths λ_{ex} and λ_{em} obtained under final complexation conditions in CF, λ_{ss} in SSF, and λ_{Z1} and λ_{Z2} in derivative SSFs, are summarised in Table 4.

Table 4 Optimised wavelengths of Cd(II)-HQS and Al(III)-HQS complex in various spectrofluorimetric methods.

	Optimised wavelengths, nm, **in various spectrofluorimetric methods**				
	CF		**SSF**	**D1SSF**	**D2SSF**
	λ_{ex}	λ_{em}	λ_{ss}	λ_{Z1}	λ_{Z2}
Cd(II)	364	519	385	302, 386, 450	298, 358, 400, 453
Al(III)	356	497	363	284, 362, 438	279, 340, 395, 443

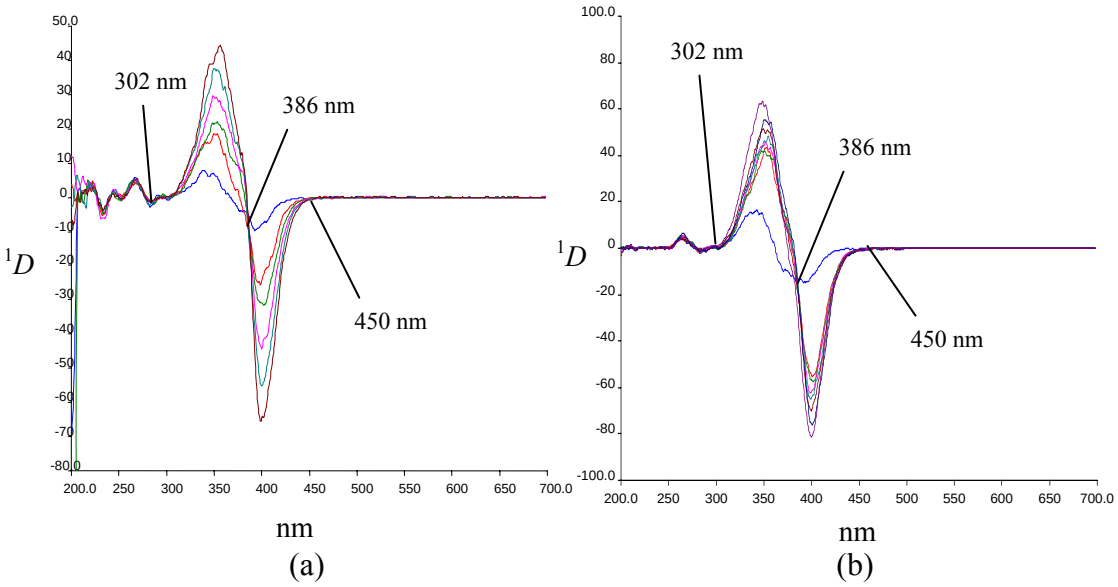

Figure 30 D1SSF spectra of Cd(II)-HQS complex showing λ_{Z1} at zero crossing: a) 0-1 ppm Cd(II) at pH 8.8, b) 0-100 ppm Cd(II) at pH 4.0.

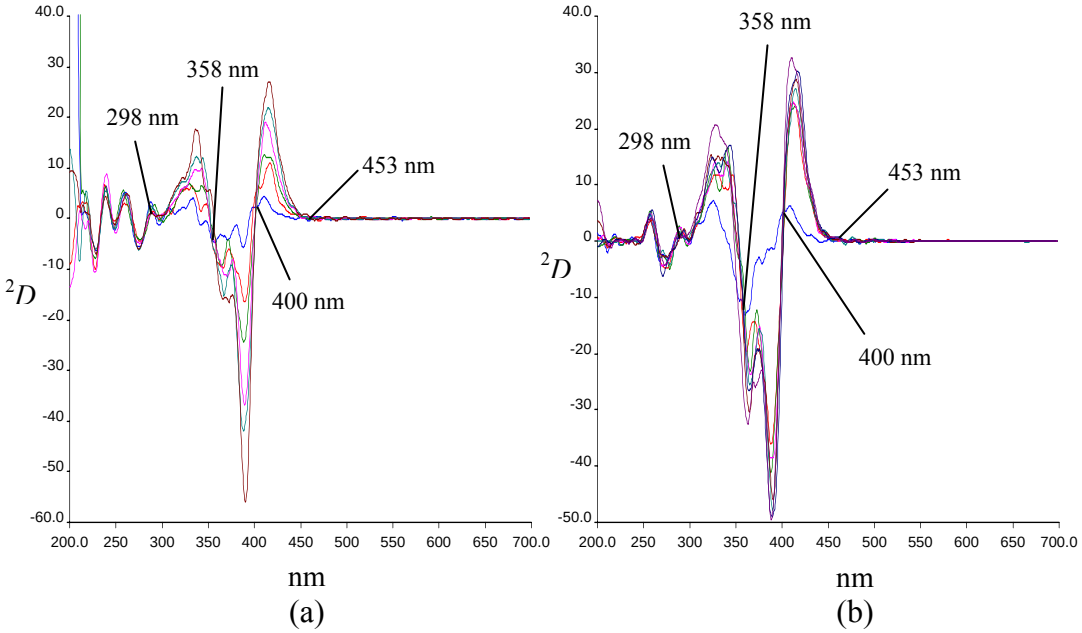

Figure 31 D2SSF spectra of Cd(II)-HQS complex showing λ_{Z2} at zero crossing: a) 0-1 ppm Cd(II) at pH 8.8, b) 0-100 ppm Cd(II) at pH 4.0.

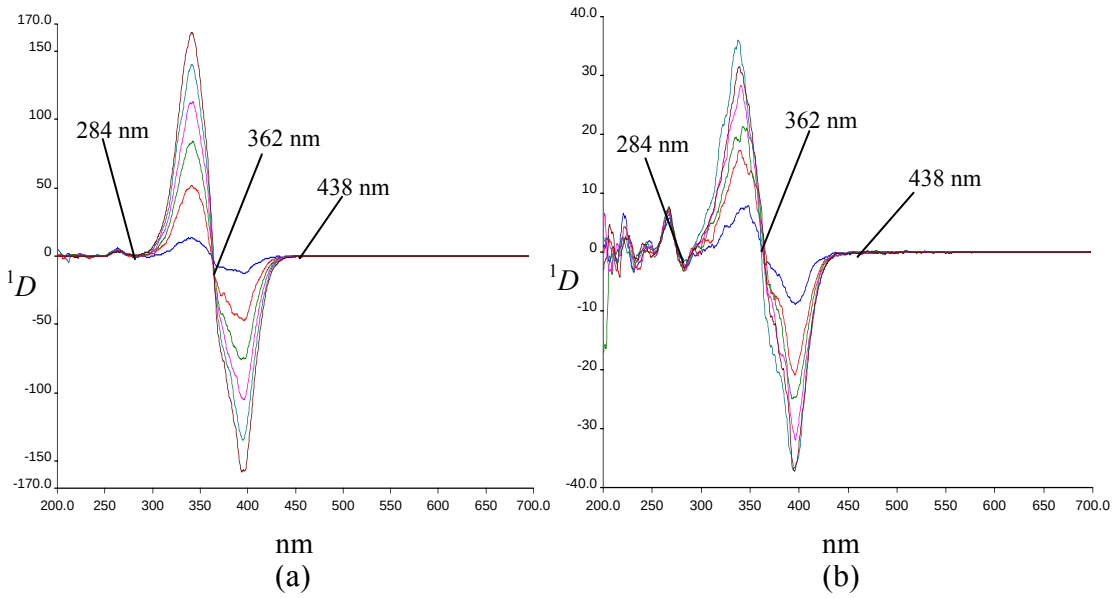

Figure 32 D1SSF spectra of Al(III)-HQS complex showing λ_{Z1} at zero crossing: a) 0-1 ppm Al(III) at pH 4.0, b) 0-4.8 ppm Al(III) at pH 8.8.

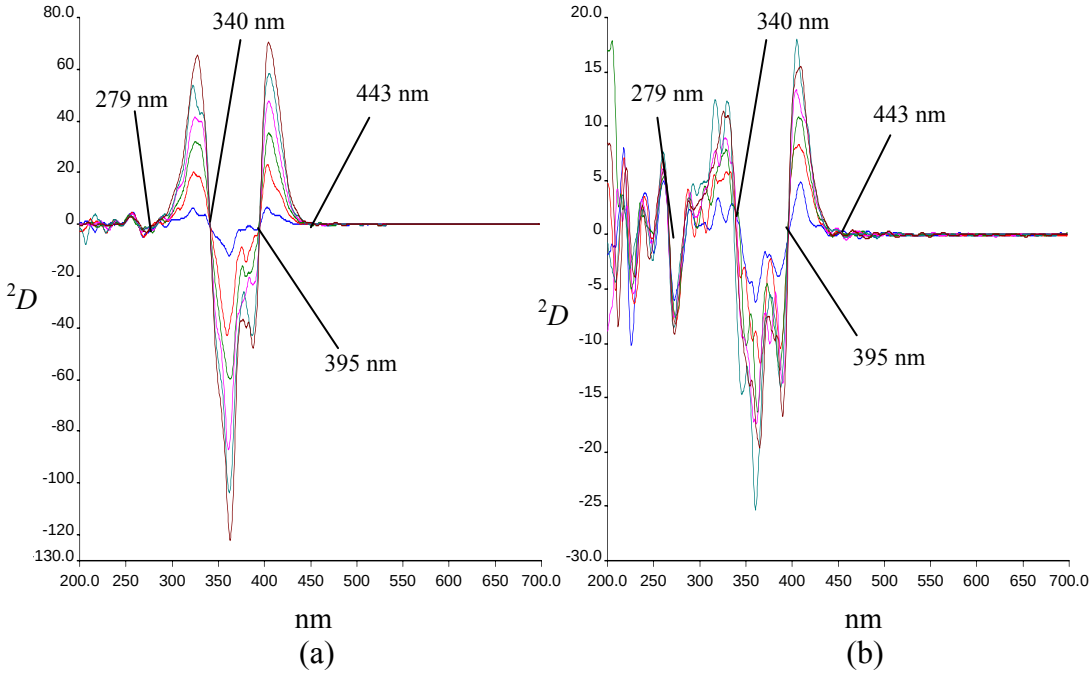

Figure 33 D2SSF spectra of Al(III)-HQS complex showing λ_{Z2} at zero crossing: a) 0-1 ppm Al(III) at pH 4.0, b) 0-4.8 ppm Al(III) at pH 8.8.

3.3 Independence of signal measurements

The suitable wavelength used for signal measurements of Cd(II)-HQS in the presence of Al(III) was investigated at the wavelengths of zero crossing of Al(III)-HQS, $\lambda_{Z,Al(III)}$, and vice versa. Figures 34 and 35 display the effects of Al(III) on the peak amplitudes of Cd(II)-HQS measured at different $\lambda_{Z,Al(III)}$. At $\lambda_{Z1,Al(III)}$ of 438 nm, the measured ^1D of Cd(II)-HQS was not affected by the presence of Al(III) up to the molar-concentration ratio Al(III)-to-Cd(II) of 30:1 (Figure 34). Similar result was for the measured ^2D of Cd(II)-HQS at $\lambda_{Z2,Al(III)}$ of 443 nm (Figure 35).

The effects of Cd(II) on the peak amplitudes of Al(III)-HQS measured at different $\lambda_{Z,Cd(II)}$ are shown in Figures 36 and 37. It was found that the ^1D and ^2D amplitudes of Al(III)-HQS were not interfered by the presence of Cd(II) up to the molar-concentration ratio Cd(II)-to-Al(III) of 25:1 at $\lambda_{Z1,Cd(II)}$ of 302 nm (Figure 36), and at $\lambda_{Z2,Cd(II)}$ of 400 nm (Figure 37), respectively.

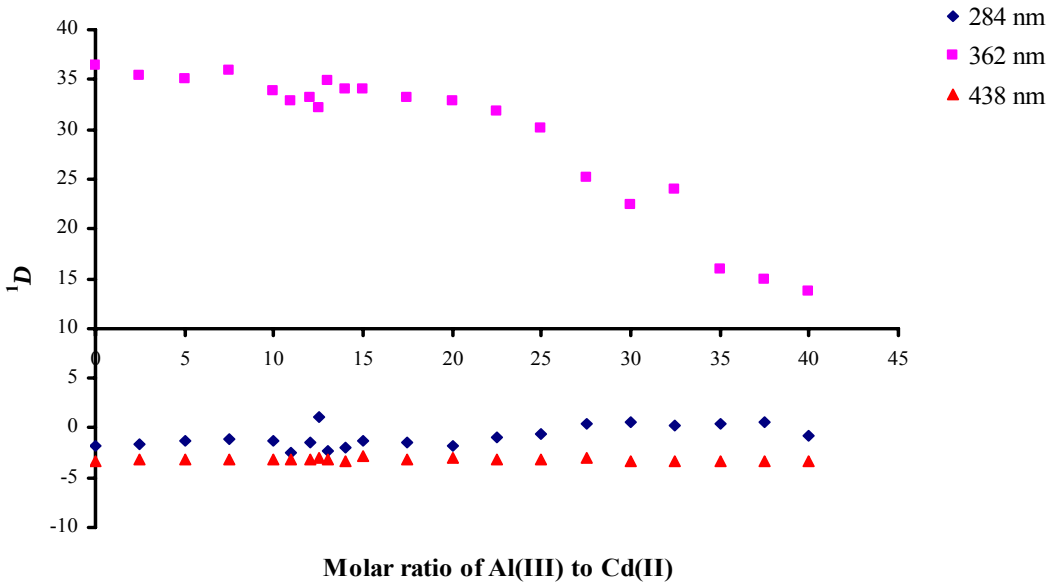

Figure 34 Effect of Al(III) on ^1D amplitudes of Cd(II)-HQS at various molar ratios of Al(III) to Cd(II), measured at $\lambda_{Z1,Al(III)}$ 284, 362, and 438 nm.

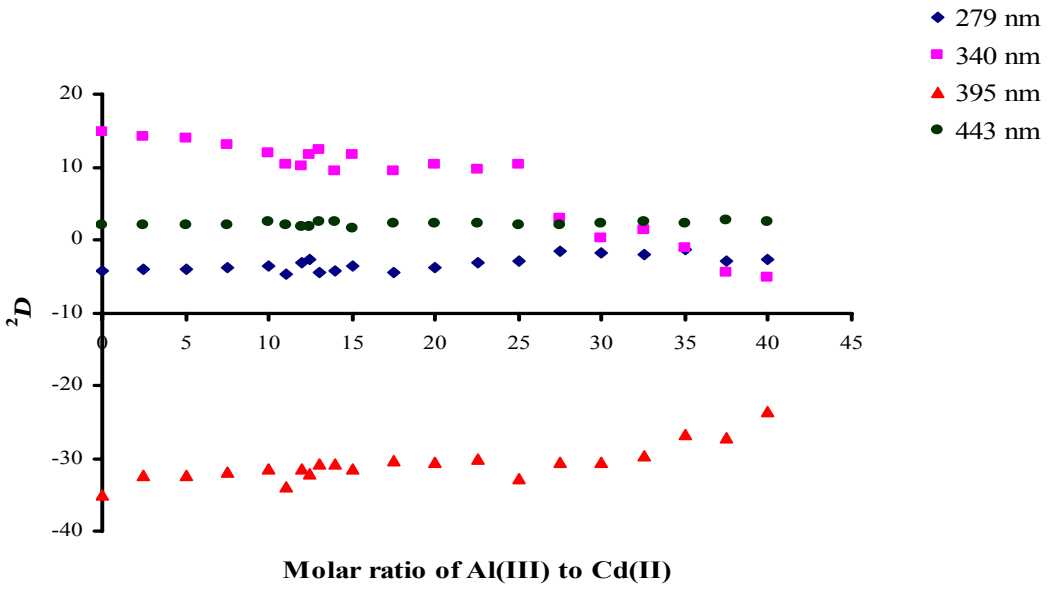

Figure 35 Effect of Al(III) on ^2D amplitudes of Cd(II)-HQS at various molar ratios of Al(III) to Cd(II), measured at $\lambda_{Z2,Al(III)}$ 279, 340, 395, and 443 nm.

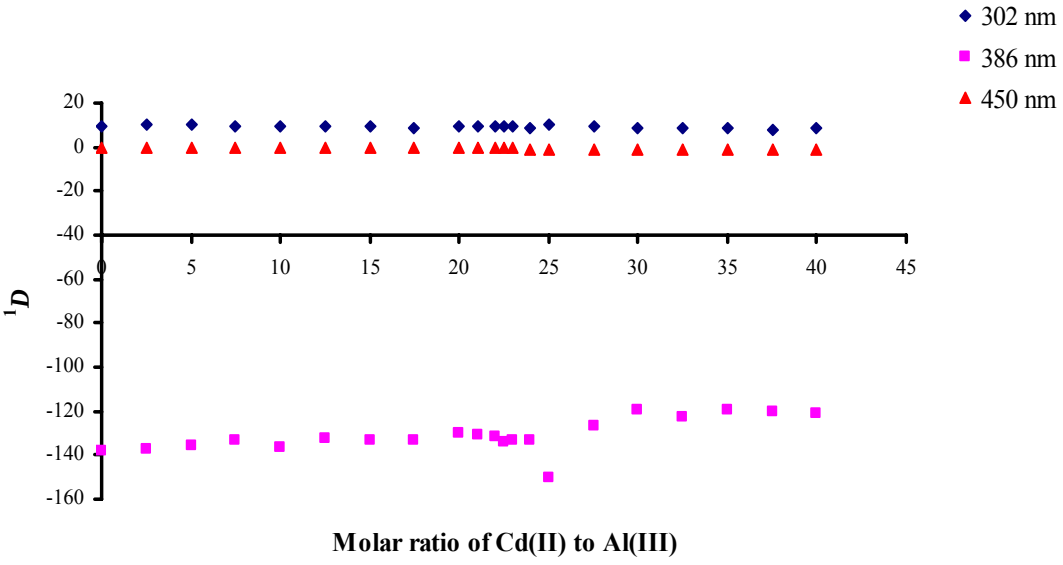

Figure 36 Effect of Cd(II) on ^1D amplitudes of Al(III)-HQS at various molar ratios of Cd(II) to Al(III), measured at $\lambda_{Z1,Cd(II)}$ 302, 386, and 450 nm.

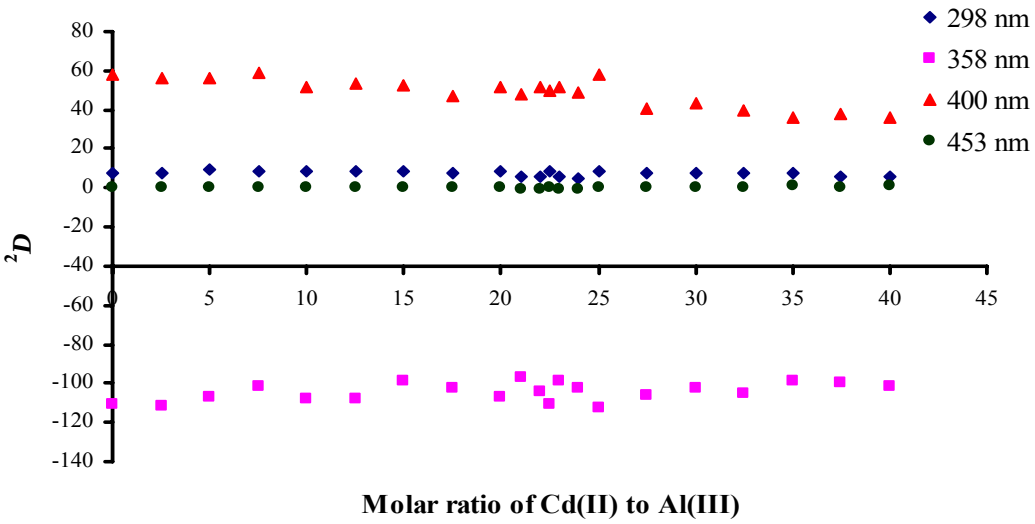

Figure 37 Effect of Cd(II) on ^2D amplitudes of Al(III)-HQS at various molar ratios of Cd(II) to Al(III), measured at $\lambda_{Z2,Cd(II)}$ 298, 358, 400 and 453 nm.

The independence of signal measurements between those of Cd(II)-HQS and Al(III)-HQS was also tested by comparing the calibration graphs of the complex of interest in binary complex solutions. The working wavelength which produced a calibration graph with good correlation coefficient (r^2) for the metal of interest was considered to be location free from the influence of its counterpart. The results were in good agreement with the previous finding. The calibration graphs of Cd(II)-HQS, obtained at $\lambda_{Z1,Al(III)}$ 438 nm and $\lambda_{Z2,Al(III)}$ 443 nm, were found to be linear with the r^2 of 0.9768 and 0.9486, respectively. Using the $\lambda_{Z1,Cd(II)}$ 302 nm and $\lambda_{Z2,Cd(II)}$ 400 nm, the correlation coefficient of Al(III)-HQS calibration graphs were found to be 0.9903 and 0.9919, respectively. The results are summarised in Table 5.

Table 5 Calibration test of Cd(II)-HQS and Al(III)-HQS by CF, SSF, D1SSF, and D2SSF methods, showing linear regression of the graphs.

Metal*	**Method**	**Measuring wavelength**, nm	**Molar ratio♣**	**Slope**	**Intercept**	r^2
Cd(II)	CF	519	1:10	0.1993	41.695	0.9947
	SSF	385	1:10	0.1692	34.888	0.9950
	D1SSF	284	1:0	–0.0016	0.4790	0.6683
		362	1:7.5	0.0335	2.9200	0.9870
		438	1:30	–0.0033	–0.2548	0.9768
	D2SSF	279	1:0	–0.0025	–1.1429	0.8580
		340	1:2.5	0.0159	0.5714	0.9558
		395	1:11	–0.0339	0.0762	0.9780
		443	1:30	–0.0027	2.5571	0.9486
Al(III)	CF	497	1:22.5	0.5399	121.93	0.9942
	SSF	363	1:22.5	0.4914	163.99	0.9954
	D1SSF	302	1:25	0.0086	0.2281	0.9903
		386	1:10	–0.1142	–0.3257	0.9867
		450	1:22.5	–0.0001	–15.1540	0.0954
	D2SSF	298	1:25	0.0062	0.7690	0.8891
		358	1:12.5	–0.0929	–15.2490	0.9823
		400	1:25	0.0490	6.0393	0.9919
		453	1:25	0.0001	0.0679	0.0117

* Concentration series of 0-1,000 ppb.

♣ Molar ratio of metal to its counterpart at which no interfering effect was found.

4. Effect of Foreign Species

Nine potentially interfering species, *i.e.* Cr(III), Fe(II), Fe(III), Co(II), Ni(II), Cu(II), Zn(II), Pb(II), and Mg(II), in the formation of Cd(II)-HQS and Al(III)-HQS were investigated. The degree of interference in the formation of Cd(II)-HQS are summarised in Tables 6 and 7. The metal ions that caused change in amplitude more than 5% were considered herein as interfering ions. In general, a 95% confidence level is a realistic basis for deciding whether the change in signal is a response arises from the presence of the interfering species (Fifield and Kealy, 1995). This means

there is only 5% risk in considering a peak amplitude obtained as the sole response from Cd(II)-HQS complex and Al(III)-HQS complex without interference from other species present. The degree of interference in the formation of Al(III)-HQS are shown in Tables 8 and 9.

It was found that most of the metal species strongly interfered in the formation of Cd(II)-HQS and Al(III)-HQS. Cr(III) and Pb(II) interfere slightly. Although the data obtained from D1SSF and D2SSF of individual metal are varied, but the overall results are found to be insignificantly different. The application of D2SSF, herein, shows no advantage over D1SSF in the aspect of elimination of interfering effects.

The metal ions involved in the investigation may be categorised according to Pearson's hard-soft acid-base (HSAB) concept (Miessler and Tarr, 2004): Cd(II) and Pb(II) as soft acids; Fe(III), Cr(III), Mg(II), and Al(III) as hard acids; and Fe(II), Co(II), Ni(II), Cu(II), and Zn(II) are borderline acids. The complexing agent HQS is considered as a borderline base since its molecule is quite large and polarizable.

Being borderline acids, the complexations of Fe(II), Co(II), Ni(II), Cu(II), and Zn(II) with HQS are favorable. Hence, these species strongly interfere in the complex formation of a soft acid such as Cd(II), as seen in Tables 6 and 7. However, although being hard acid, Fe(III) is considered a softer acid than is Cr(III). Having d^5-electron configuration, Fe(III) is much readily available for π-back bonding than Cr(III) with a d^3-electron configuration. Consequently, Fe(III) moderately interferes in the complex formation of Cd(II) whilst Cr(III) interferes at a lesser degree. The soft acid Pb(II) interfered slightly.

As a hard acid, the complexation of Al(III) with HQS is less favorable than those of soft- and borderline-acid species. Therefore, Cr(III), Fe(II), Fe(III), Co(II), Ni(II), Cu(II), Zn(II), and Pb(II), strongly interfere in the formation of Al(III)-HQS, as seen in Tables 8 and 9. The complex formation of Mg(II) with HQS is also not favored since it is a hard-borderline reaction; thus, Mg(II) interferes rather slightly.

Table 6 Effect of diverse metal ions upon complexation of Cd(II)-HQS using the first derivative synchronous spectrometry.

Cation [a]	% Change in fluorescence intensity [b] at different Metal : Cd ratios				
	0.25:1	**0.5:1**	**1:1**	**5:1**	**10:1**
Cr(III)	1.11	–6.39	6.11	–0.56	–18.33
Fe(II)	–9.84	–15.28	–17.62	–34.46	–52.33
Fe(III)	–13.95	–7.63	3.95	–10.00	–18.95
Co(II)	–25.26	–27.72	–37.78	–92.20	–97.13
Ni(II)	–10.10	–14.77	–27.20	–97.15	–100.00
Cu(II)	–17.45	–33.47	–37.58	–98.97	–96.51
Zn(II)	20.28	29.17	36.94	57.78	29.17
Pb(II)	3.89	9.17	–6.39	–16.39	–10.28
Mg(II)	10.28	11.67	19.17	43.06	43.89

[a] Cations added as nitrate or sulphate.

[b] Change in amplitude >5% was considered as being interfered.

Table 7 Effect of diverse metal ions upon complexation of Cd(II)-HQS using the second derivative synchronous spectrometry.

Cation [a]	% Change in fluorescence intensity [b] at different Metal : Cd ratios				
	0.25:1	**0.5:1**	**1:1**	**5:1**	**10:1**
Cr(III)	4.61	5.07	21.66	12.44	–8.29
Fe(II)	–26.32	–34.39	–31.93	–39.30	–66.32
Fe(III)	–13.06	–13.47	7.35	–13.88	–21.22
Co(II)	–29.09	–23.33	–45.45	–89.09	–99.39
Ni(II)	1.75	–27.02	–31.93	–100.70	–110.53
Cu(II)	–12.73	–42.42	–49.39	–97.27	–99.39
Zn(II)	26.27	56.22	48.39	74.65	37.79
Pb(II)	10.60	35.48	10.14	–5.07	–9.68
Mg(II)	23.04	32.26	35.94	59.45	63.13

[a] Cations added as nitrate or sulphate.

[b] Change in amplitude >5% was considered as being interfered.

Table 8 Effect of diverse metal ions upon complexation of Al(III)-HQS using the first derivative synchronous spectrometry.

Cation [a]	% Change in fluorescence intensity [b] at different Metal : Al ratios				
	0.25:1	**0.5:1**	**1:1**	**5:1**	**10:1**
Cr(III)	–28.48	6.62	–15.56	–39.40	–55.30
Fe(II)	–5.17	28.04	10.70	–22.51	–55.35
Fe(III)	–49.08	2.58	–11.44	–69.37	–83.76
Co(II)	–23.08	–12.82	–5.41	–34.76	–24.50
Ni(II)	–5.17	–2.95	20.66	–52.77	–47.97
Cu(II)	19.84	17.81	–47.37	–88.66	–92.71
Zn(II)	–17.87	0.94	–6.27	–15.36	–11.91
Pb(II)	9.72	30.77	18.22	4.45	–18.62
Mg(II)	3.99	–1.14	–36.75	–4.56	–9.69

[a] Cations added as nitrate or sulphate.

[b] Change in amplitude >5% was considered as being interfered.

Table 9 Effect of diverse metal ions upon complexation of Al(III)-HQS using the second derivative synchronous spectrometry.

Cation [a]	% Change in fluorescence intensity [b] at different Metal : Al ratios				
	0.25:1	**0.5:1**	**1:1**	**5:1**	**10:1**
Cr(III)	7.53	6.34	–2.33	–17.18	–30.50
Fe(II)	–7.45	–9.28	–17.38	–32.17	–38.14
Fe(III)	–8.90	–15.69	–26.22	–64.22	–87.54
Co(II)	–16.58	–2.64	–8.42	–26.31	–50.41
Ni(II)	–16.07	–19.79	–46.25	–76.27	–88.13
Cu(II)	–27.98	–55.77	–80.07	–99.06	–100.22
Zn(II)	–68.57	–2.10	–4.53	–45.52	–1.66
Pb(II)	–1.68	–9.03	–11.78	–11.52	–70.67
Mg(II)	6.87	1.93	–7.31	–6.30	–13.33

[a] Cations added as nitrate or sulphate.

[b] Change in amplitude >5% was considered as being interfered.

5. Determination of Cd(II) and Al(III) as Sulphoxinate Complexes

5.1 Standard calibration graphs for Cd(II)

The calibration graphs of single component Cd(II)-HQS complex and those of Cd(II)-HQS in the presence of Al(III) by CF, SSF, D1SSF, and D2SSF methods were compared as shown in Figure 38. The calibration graphs are linear over the range of 0-1,000 ppb of Cd(II). Deviation of the calibration graphs in Figures 38-a and 38-b indicate the strong interference of Al(III) in CF and SSF methods. The applications of D1SSF and D2SSF clearly eliminate the interference of Al(III) as illustrate in Figures 38-c and 38-d. The calibration graphs of Cd(II)-HQS in a pure solution and in the presence of Al(III) almost superimpose — having the same slope and insignificant difference in the intercept.

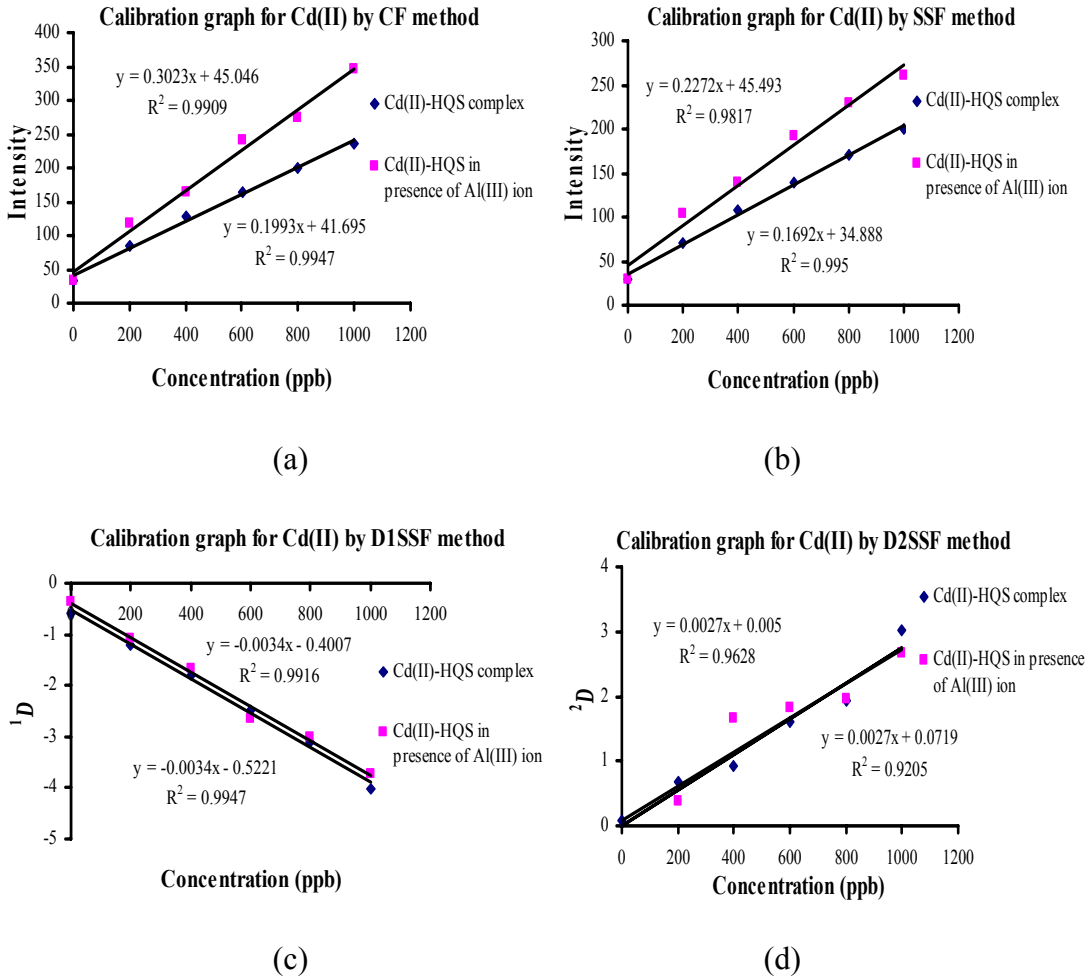

Figure 38 Calibration graphs for Cd(II) as HQS complex in pure solution compared to that in the presence of Al(III):
(a) CF, (b) SSF, (c) D1SSF, and (d) D2SSF methods.

5.2 Standard calibration graphs for Al(III)

The calibration graphs of single component Al(III)-HQS complex and those of Al(III)-HQS in the presence of Cd(II) by CF, SSF, D1SSF, and D2SSF methods were compared as shown in Figure 39. The calibration graphs are linear over the range of 0-1,000 ppb of Al(III). Unlike the calibration graphs of Cd(II)-HQS, great deviation was found in D2SSF method (Figure 39-d); whilst similar slope of the graphs were found in CF, SSF, and D1SSF (Figures 39-a, 39-b, and 39-c). The

parallel calibration graphs indicate some bias in the systems. Under the conditions of Al(III)-HQS complexation at pH 4.0, the formation Cd(II)-HQS is insignificant and does not interfere with Al(III), Figure 17. This suggests that SSF, D1SSF, and D2SSF methods are not quite necessary for the determination of Al(III) in the presence of Cd(II) if proper determination of the bias can be achieved.

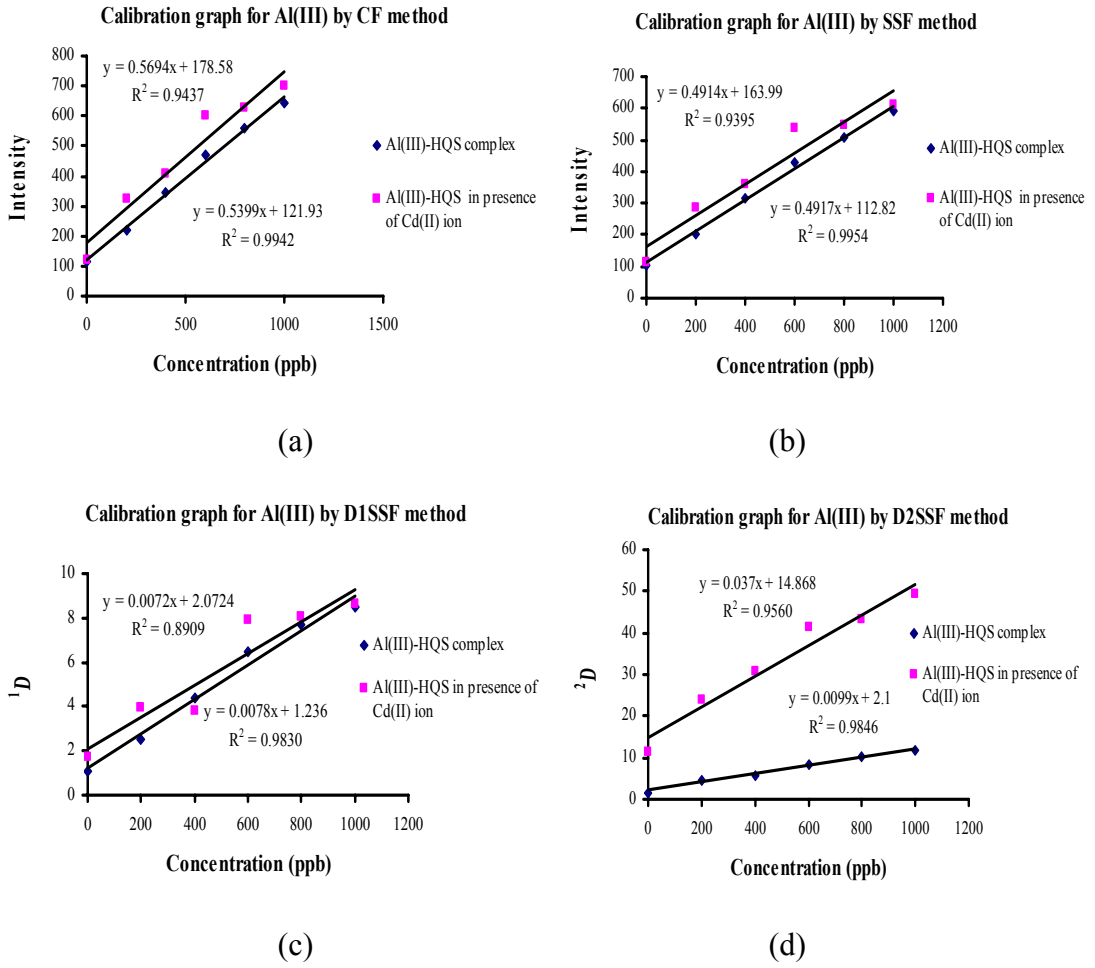

Figure 39 Calibration graphs for Al(III) as HQS complex in pure solution compared to that in the presence of Cd(II):
(a) CF, (b) SSF, (c) D1SSF, and (d) D2SSF methods.

5.3 Analysis of samples

5.3.1 Determination of Cd(II) in the presence of Al(III)

Determinations of Cd(II) in synthetic solutions, a series of binary mixtures of Cd(II) and Al(III) at various molar ratios of Cd(II)-to-Al(III) up to 1:30, were carried out by CF, SSF, D1SSF, and D2SSF methods. The amounts of Cd(II) were evaluated from calibration graphs of Cd(II)-HQS in pure solution and from those of Cd(II)-HQS in the presence of Al(III). The results are summarised in Tables 10 and 11.

Table 10 Analysis of Cd(II), evaluated from pure-Cd(II) calibration graphs.

Cd(II) in sample		**Concentration of Cd(II): Found**, ppb**; Recovery**, %							
Cd:Al	**Conc$^{n.}$**	**CF**		**SSF**		**D1SSF**		**D2SSF**	
Molar	**ppb**	**ppb**	**%**	**ppb**	**%**	**ppb**	**%**	**ppb**	**%**
1:0	500	449.35	89.87	458.46	91.96	452.32	90.46	477.78	95.56
1:7.5	500	559.73	111.95	578.07	115.61	488.60	97.72	503.09	100.62
1:15	500	642.01	128.40	648.91	129.78	798.40	99.68	599.38	119.88
1:22.5	500	702.42	140.48	697.14	139.43	517.03	103.41	594.44	118.89
1:30	500	765.82	153.16	752.79	150.56	462.13	92.43	538.89	107.78

Table 11 Analysis of Cd(II), evaluated from Cd(II)-Al(III) calibration graphs.

Cd(II) in sample		**Concentration of Cd(II): Found**, ppb**; Recovery**, %							
Cd:Al	**Conc$^{n.}$**	**CF**		**SSF**		**D1SSF**		**D2SSF**	
Molar	**ppb**	**ppb**	**%**	**ppb**	**%**	**ppb**	**%**	**ppb**	**%**
1:0	500	285.16	57.03	294.75	58.95	488.03	97.61	453.00	90.60
1:7.5	500	357.94	71.59	383.82	76.76	524.30	104.86	478.31	95.66
1:15	500	412.18	82.44	436.58	87.32	534.11	106.82	574.60	114.92
1:22.5	500	452.00	90.40	472.49	94.50	552.74	110.55	569.67	113.93
1:30	500	493.10	98.62	513.94	102.79	497.83	99.57	514.11	102.82

The interference of Al(III) rendered great errors in the analytical results obtained from CF and SSF methods. The extent of error in SSF method was reduced, though not to a satisfactory level, compared to that in CF. The applications

of D1SSF and D2SSF methods greatly eliminated the error imposed by Al(III). The recoveries of 97.61-110.55% were obtained from D1SSF, whilst 90.60-113.93% were obtained from D2SSF. The results from D1SSF were found to be much satisfactory.

5.3.2 Determination of Al(III) in the presence of Cd(II)

Determinations of Al(III) in synthetic solutions, a series of binary mixtures of Al(III) and Cd(II) at various molar ratios of Cd(II)-to-Al(III) up to 1:25, were carried out by CF, SSF, D1SSF, and D2SSF methods. The amounts of Al(III) were evaluated from calibration graphs of Al(III)-HQS in pure solution and from those of Al(III)-HQS in the presence of Cd(II). The results are summarised in Tables 12 and 13.

Table 12 Analysis of Al(III), evaluated from pure-Al(III) calibration graphs.

Al(III) in sample		**Concentration of Al(III): Found**, ppb**; Recovery**, %							
Al:Cd	**Conc$^{n.}$**	**CF**		**SSF**		**D1SSF**		**D2SSF**	
Molar	**ppb**	**ppb**	**%**	**ppb**	**%**	**ppb**	**%**	**ppb**	**%**
1:0	500	561.40	112.28	561.75	112.35	619.32	123.86	3307.58	661.52
1:6.25	500	522.70	104.54	513.36	102.67	470.17	94.03	3124.24	624.85
1:12.5	500	528.97	105.79	516.17	103.23	561.41	112.28	2891.41	578.28
1:18.75	500	584.76	116.95	562.67	112.53	505.64	101.13	2814.48	562.90
1:25	500	591.71	118.34	562.22	112.44	465.26	93.05	2894.95	578.99

Table 13 Analysis of Al(III), evaluated from Al(III)-Cd(II) calibration graphs.

Al(III) in sample		**Concentration of Al(III): Found**, ppb**; Recovery**, %							
Al:Cd	**Conc$^{n.}$**	**CF**		**SSF**		**D1SSF**		**D2SSF**	
Molar	**ppb**	**ppb**	**%**	**ppb**	**%**	**ppb**	**%**	**ppb**	**%**
1:0	500	432.82	86.56	457.96	91.59	554.76	110.95	540.19	108.04
1:6.25	500	396.12	79.22	409.54	81.91	512.86	102.57	491.14	98.23
1:12.5	500	402.07	80.41	412.35	82.47	560.31	112.06	428.84	85.77
1:18.75	500	454.97	90.99	458.88	91.78	431.61	86.32	408.25	81.65
1:25	500	461.56	92.31	458.44	91.69	480.22	96.04	429.78	85.96

The analytical results obtained from CF and SSF methods revealed a quite constant bias, positive bias from the pure solution of Al(III)-HQS and negative bias from the binary mixture. This constant bias corresponds to the calibration graphs with similar slope in Figures 39-a and 39-b. The bias suggests some systematic errors in the complex system. The analytical results from CF and SSF can be corrected if proper determination of the bias can be achieved. The applications of D1SSF and D2SSF slightly improved the %recoveries of Al(III) when calibration graphs of binary mixture were used. However, drastic errors were found in D2SSF results when calibration graph of pure Al(III)-HQS was applied. The error was corresponded to the great deviation shown in Figures 39-d. Thus, not much advantages were gained from D1SSF and D2SSF methods for determination of Al(III) in the presence of Cd(II). Under the conditions of Al(III)-HQS complexation at pH 4.0, the formation Cd(II)-HQS is insignificant and does not interfere with Al(III).

CONCLUSION

Four spectrofluorimetric methods were investigated and developed for simple determination of Cd(II) and Al(III). The methods are based upon the formation of fluorescent complexes of Cd(II) and Al(III) with 8-hydroxyquinoline-5-sulphonic acid. Conditions of complex formation were examined and optimised, using conventional spectrofluorimetry, CF. Instrumental parameters were also optimised. Complex Al(III)-HQS was best formed in solutions of pH 4.0, whereas Cd(II)-HQS formed in rather basic solutions. Under those different conditions, it was presumed that the interference between the two complexes should be least expected. However, the emission wavelengths of Cd(II)-HQS and Al(III)-HQS were found at 519 nm and 497 nm, respectively. With a difference of 22 nm, the spectral interference between the two complexes was found in a great extent.

In order to eliminate the spectral interference, synchronous spectrofluorimetric methods was then examined. The wavelength interval for synchronous-scanning of the excitation and emission monochromators was optimised. A $\Delta\lambda$ of 120 nm was used for the study of Cd(II)-HQS, while 115 nm was used for Al(III)-HQS. The synchronous spectra wavelengths of Cd(II)-HQS and Al(III)-HQS were found at 385 nm and 363 nm, respectively; a difference of 22 nm still, but narrower peak-width. The resolution of spectral peaks was improved but inadequate for use in binary mixture.

Further developments were attempted on derivative synchronous-scanning spectrofluorimetric methods. The first and second derivative spectra were acquired from a FL-WinLab programme. Zero-crossing method was used to determine the wavelengths at which interfering signals were not appreciable. The zero-crossing wavelengths in derivative spectra of Cd(II)-HQS were used for signal measurement of Al(III)-HQS, and vice versa. The D1SFF zero-crossing wavelengths of Cd(II)-HQS and Al(III)-HQS were 302 nm and 438 nm, respectively. With a difference of 136 nm, the resolution of spectral peaks and the independence of signals were improved tremendously. As a consequence, elimination of interference was achieved at a

satisfactory level. The D2SFF zero-crossing wavelengths of Cd(II)-HQS and Al(III)-HQS were 400 nm and 443 nm, respectively. At a difference of 43 nm, the resolution of spectral peaks and the independence of signals were also improved although not as much as in D1SSF method. The tolerance limit for measurement of Cd(II)-HQS was found at molar-concentration ratio Al(III)-to-Cd(II) of 30:1; and Cd(II)-to-Al(III) molar ratio of 25:1 for the measurement of Al(III)-HQS.

Under optimised conditions and instrumental parameters, Cd(II) and Al(III) in synthetic samples were determined by means of external standard calibration graphs. The calibration graphs were linear over a range of 0-1,000 μg l^{-1} of Cd(II) and Al(III) with good correlation coefficient, *e.g.* the r^2 of D1SSF calibration graphs for Cd(II) and Al(III) were 0.9916 and 0.8909, respectively; 0.9628 and 0.9560 in D2SSF calibration graphs for Cd(II) and Al(III), respectively. The analytical results were in good agreement with the synthetic values, *e.g.* recoveries of 97.61-110.55% in D1SSF of Cd(II).

The developed derivative synchronous-scanning spectrofluorometric methods offer advantages over the conventional spectrofluorimetry. The overlapping spectra can be resolved for multi-component analysis without prior separation step, thus less reagent consumption. Simple, rapid, and cost-effective procedures are also achieved. The proposed methods are applicable to water samples with simple matrices.

CONCLUSION

Four spectrofluorimetric methods were investigated and developed for simple determination of Cd(II) and Al(III). The methods are based upon the formation of fluorescent complexes of Cd(II) and Al(III) with 8-hydroxyquinoline-5-sulphonic acid. Conditions of complex formation were examined and optimised, using conventional spectrofluorimetry, CF. Instrumental parameters were also optimised. Complex Al(III)-HQS was best formed in solutions of pH 4.0, whereas Cd(II)-HQS formed in rather basic solutions. Under those different conditions, it was presumed that the interference between the two complexes should be least expected. However, the emission wavelengths of Cd(II)-HQS and Al(III)-HQS were found at 519 nm and 497 nm, respectively. With a difference of 22 nm, the spectral interference between the two complexes was found in a great extent.

In order to eliminate the spectral interference, synchronous spectrofluorimetric methods was then examined. The wavelength interval for synchronous-scanning of the excitation and emission monochromators was optimised. A $\Delta\lambda$ of 120 nm was used for the study of Cd(II)-HQS, while 115 nm was used for Al(III)-HQS. The synchronous spectra wavelengths of Cd(II)-HQS and Al(III)-HQS were found at 385 nm and 363 nm, respectively; a difference of 22 nm still, but narrower peak-width. The resolution of spectral peaks was improved but inadequate for use in binary mixture.

Further developments were attempted on derivative synchronous-scanning spectrofluorimetric methods. The first and second derivative spectra were acquired from a FL-WinLab programme. Zero-crossing method was used to determine the wavelengths at which interfering signals were not appreciable. The zero-crossing wavelengths in derivative spectra of Cd(II)-HQS were used for signal measurement of Al(III)-HQS, and vice versa. The D1SFF zero-crossing wavelengths of Cd(II)-HQS and Al(III)-HQS were 302 nm and 438 nm, respectively. With a difference of 136 nm, the resolution of spectral peaks and the independence of signals were improved tremendously. As a consequence, elimination of interference was achieved at a

satisfactory level. The D2SFF zero-crossing wavelengths of Cd(II)-HQS and Al(III)-HQS were 400 nm and 443 nm, respectively. At a difference of 43 nm, the resolution of spectral peaks and the independence of signals were also improved although not as much as in D1SSF method. The tolerance limit for measurement of Cd(II)-HQS was found at molar-concentration ratio Al(III)-to-Cd(II) of 30:1; and Cd(II)-to-Al(III) molar ratio of 25:1 for the measurement of Al(III)-HQS.

Under optimised conditions and instrumental parameters, Cd(II) and Al(III) in synthetic samples were determined by means of external standard calibration graphs. The calibration graphs were linear over a range of 0-1,000 μg l^{-1} of Cd(II) and Al(III) with good correlation coefficient, *e.g.* the r^2 of D1SSF calibration graphs for Cd(II) and Al(III) were 0.9916 and 0.8909, respectively; 0.9628 and 0.9560 in D2SSF calibration graphs for Cd(II) and Al(III), respectively. The analytical results were in good agreement with the synthetic values, *e.g.* recoveries of 97.61-110.55% in D1SSF of Cd(II).

The developed derivative synchronous-scanning spectrofluorometric methods offer advantages over the conventional spectrofluorimetry. The overlapping spectra can be resolved for multi-component analysis without prior separation step, thus less reagent consumption. Simple, rapid, and cost-effective procedures are also achieved. The proposed methods are applicable to water samples with simple matrices.

LITERATURE CITED

Berman, E. 1980. **Toxic Metals and Their Analysis**. Cambridge University Press, London.

Blanco, C.C., A.M.G. Campaña, F.A. Barrero and M.R. Ceba. 1993. Simultaneous spectrofluorimetric determination of traces of molybdenum and boron in plant leaves. **Anal. Chim. Acta** 283: 213-223.

_____, _____, _____ and _____. 1995. Micellar medium for the analysis of complex mixtures of molybdenum and tungsten by derivative synchronous spectrofluorimetry in steels. **Talanta** 42: 1037-1044.

Buratti, M., C. Valla, O. Pellegrino, F.M. Rubino and A. Colombi. 2006. Aluminium determination in biological fluids and dialysis concentrates via chelation with 8-hydroxyquinoline and solvent extraction/fluorimetry. **J. Anal. Biochem.** 353: 63-68.

Capitán, F., E. Manzano, A. Navalón, J.L. Vilchez and L.F. Capitán-Vallvey. 1992. Simultaneous determination of aluminium and beryllium by first-derivative synchronous solid-phase spectrofluorimetry. **Talanta** 39: 21-27.

Chen, Z., M. Ying, T. Chen, X. Qiu and Z. Li. 1998. Study on the magnetic-polarization-resonance-synchronous-fluorimetry and its application to simultaneous determination of polycyclic aromatic hydrocarbons. **Anal. Chim. Acta** 367: 11-15.

Cheng, Y., M. Zhang, H. Yang, F. Li, T. Yi and C. Huang. 2008. Azo dye based on 8-hydroxyquinoline benzoate: synthesis and application as chromogenic Hg^{2+}-selective chemosensor. **Dyes and Pigments** 76: 775-783.

Clyne, P.W. and P.J. Withers. 1993. **An Introduction to Metal Matrix Composite**. Cambridge University Press, London.

Cornard, J.-P., A. Caudron and J.-C. Merlin. 2006. UV-visible and synchronous fluorescence spectroscopic investigations of the complexation of Al(III) with caffeic acid, in aqueous low acidic medium. **Polyhedron** 25: 2215-2222.

Cui, F.L., J.L. Wang, Y.R. Cui and J.P. Li. 2006. Fluorescence investigation of the interactions between *N*-(*p*-chlorophenyl)-*N*'-(1-naphthyl) thiourea and serum albumin: Synchronous fluorescence determination of serum albumin. **Anal. Chim. Acta** 571: 175-183.

Daintith, J. (editor). 1996. **A Dictionary of Chemistry**, 3rd ed. Oxford University Press, Oxford.

Devol, I. and E. Bardez. 1998. Complexation of Al(III) by 8-hydroxyquinoline and drastic fluorescence enhancement in reverse micelles. **J. Colloid Interface Sci.** 200: 241-248.

Du, X., J. Gao, Q. Xie and J. Kang. 1994. Simultaneous determination of samarium, europium and terbium with quinaldic acid and phenanthroline by synchronous derivative fluorimetry. **Talanta** 41: 201-204.

Esteves da Silva, J.C.G., A.A.S.C. Machado and C.J.S. Oliviera. 1997. Study of the interaction of Al(III) with a soil fulvic acid in the acid pH range by self-modeling mixture analysis of synchronous fluorescence spectral data. **Anal. Chim. Acta** 349: 23-31.

Fifield, F.W. and D. Kealy. 1995. **Principles and Practice of Analytical Chemistry**, 4th ed. Blackie Academic & Professional, Glasgow.

Garribba, E., G. Micera, D. Sanna and E. Lodyga-Chruscinska. 2003. Oxovanadium(IV) complexes of quinoline derivatives. **Inorg. Chim. Acta** 348: 97-106.

Greenwood, N.N. and A. Earnshaw. 1995. **Chemistry of the Elements**. Butterworth-Heinemann, Oxford.

Hollingshead, R.G.W. 1954-56. **Oxine and Its Derivatives**, **Vol. I-IV**. Butterworths, London.

Hua, G., K. Killham and I. Singleton. 2006. Potential application of synchronous fluorescence spectroscopy to determine benzo[*a*]pyrene in soil extracts. **Environmental Pollution** 139: 272-278.

Huo, X., X. Tong, W. Dong, C. Dong and S. Shuang. 2006. Synchronous fluorescence determination of human serum albumin with methyl blue as a fluorescence probe. **Spectrochim. Acta Part A** 66: 552–556.

Inman, Jr., E.L., and J.D. Winefordner. 1982. Low-temperature constant energy synchronous luminescence spectroscopy. **Anal. Chim. Acta** 141: 241-254.

Jiang, C. and J. He. 2002. Simultaneous determination of aloe-emodin and rhein by synchronous fluorescence spectroscopy. **J. Pharm. Biomed. Anal.** 29: 737-742.

Konstantianos, D.G. and P.C. Ioannou. 1996. Second-derivative synchronous fluorescence spectroscopy for the simultaneous determination of naproxen and salicylic acid in human serum. **Analyst** 121: 909-912.

Lee, J.D. 1991. **Concise Inorganic Chemistry**, 4th ed. Chapman & Hall, London.

Liu, X., S. Tao and N. Deng. 2005. Synchronous-scan fluorescence spectra of *Chlorella vulgaris* solution. **Chemosphere** 60: 1550-1554.

_____, _____, _____, Y. Liu, B. Meng, B.Xue and G. Liu. 2006. Synchronous-scan fluorescence as a selective detection method for sodium dodecylbenzene-sulfonate and pyrene in environmental samples. **Anal. Chim. Acta** 572: 134-139.

Lloyd, J.B.F. 1974. Partly quenched, synchronously excited fluorescence emission spectra in the characterization of complex mixtures. **Analyst** 99: 729-738.

_____. 1975. Characterisation of rubbers, rubber contact traces and tyre prints by fluorescence spectroscopy. **Analyst** 100: 82-95.

_____. 1980. Examination of petroleum products of high relative molecular mass for forensic purposes by synchronous fluorescence spectroscopy. Part I. Appraisal of experimental factors. **Analyst** 105: 97-109.

_____ and I.W. Evett. 1977. Prediction of peak wavelengths and intensities in synchronously excited fluorescence emission spectra. **Anal. Chem.** 49: 1710-1715.

Marczenko, Z. 1986. **Separation and Spectrophotometric Determination of Elements**, 2nd ed. Ellis Horwood, Chichester.

Matuszewska, A. and M. Czaja. 2000. The use of synchronous luminescence spectroscopy in qualitative analysis of aromatic fraction of hard coal thermolysis products. **Talanta** 52: 457-464.

Miessler, G.L. and D.A. Tarr. 2004. **Inorganic Chemistry**, 3rd ed. Pearson-Prentice Hall, Northfield.

Panadero, S., A. Gómez-Hens and D. Pérez-Bendito. 1993. Simultaneous determination of warfarin and bromadiolone by derivative synchronous fluorescence spectrometry. **Talanta** 40: 225-230.

Patra, D. and A.K. Mishra. 2001. Investigation on simultaneous analysis of multi-component polycyclic aromatic hydrocarbon mixtures in water samples: a simple synchronous fluorimetric method. **Talanta** 55: 143-153.

_____ and _____. 2002. Recent developments in multi-component synchronous fluorescence scan analysis. **Trends in Anal. Chem.** 21: 787-798.

Paull, B., E. Twohill and W. Bashir. 2000. Determination of trace cadmium in environmental water samples using ion-interaction reversed-phase liquid chromatography with fluorescence detection. **J. Chromatogr. A** 877: 123-132.

Pavon, J.M.C., A.G. de Torres and M.E.U. Pozo. 1990. Simultaneous determination of gallium and aluminium in biological samples by conventional luminescence and derivative synchronous fluorescence spectrometry. **Talanta** 37: 385-391.

Poppović, G.V., L.B. Pfendt and V.M. Stefanović. 2000. Analytical application of derivative spectrophotometry. **J. Serb. Chem. Soc.** 65: 457-472.

Pulgarín, J.A.M. and L.F.G. Bermejo. 1998. First-derivative non-linear variable-angle synchronous fluorescence spectroscopy for the simultaneous determination of salicylamide, salsalate and naproxen in serum and urine. **Anal. Chim. Acta** 373: 119-129.

_____, and A.A. Molina. 1996. Derivative linear variable-angle scanning fluorescence spectrometry for the determination of closely overlapping drug. **Anal. Chim. Acta** 319: 361-368.

Rubio, S., A. Gómez-Hens and M. Valcárcel. 1985. Analysis of binary and ternary mixtures of titanium, zirconium, and hafnium by derivative synchronous fluorescence spectrometry. **Anal. Chem.** 57: 1101-1106.

Ruiz, T.P., C. Martínez-Lozano, V. Tomás and J. Carpena. 1998. Simultaneous determination of propranolol and pindolol by synchronous spectrofluorimetry. **Talanta** 45: 969-976.

Rodriguez, J.J.S., Z.S. Ferrera, A.A. Perera and V.G. Diaz. 1992. Sensitive simultaneous determination of benzo(*a*)pyrene, perylene and chrysene by synchronous spectrofluorometry in nonionic micellar media. **Talanta** 39: 1611-1617.

_____, J.H. Garcia, M.M.B. Suárez and A.B. Martin-Lázaro. 1993. Analysis of mixtures of polycyclic aromatic hydrocarbons in sea-water by synchronous fluorescence spectrometry in organized media. **Analyst** 118: 917-921.

Sánchez, F.G., A. Navas and M. Santiago. 1985. Synchronous scanning derivative spectrofluorimetry for the determination of cadmium with benzyl-2-pyridylketone-2-quinolylhydrazone. **Anal. Chim. Acta** 167: 217-223.

Sathish, R.S., U. Sujith, G.N. Rao and C. Janardhana. 2006. Fluoride ion detection by 8-hydroxyquinoline-Zr(IV)-EDTA complex. **Spectrochim. Acta Part A** 65: 565–570.

Skoog, D.A., F.J. Holler and T.A. Nieman. 1998. **Principles of Instrumental Analysis**, 5th ed. Brooks/Cole-Thomson Learning, Belmont.

Snell, F.D. 1978. **Photometric and Fluorometric Methods of Analysis**, **Metals Part I**. Wiley, New York.

Sommer, L. 1989. **Analytical Absorption Spectrophotometry in the Visible and Ultraviolet: The Principles**. Elsevier, Amsterdam.

Soroka, K., R.S. Vithanage, D.A. Phillips, B. Walker and P.K. Dasgupta. 1987. Fluorescence properties of metal complexes of 8-hydroxyquinoline-5-sulfonic acid and chromatographic applications. **Anal. Chem.** 59: 629-636.

Tabrizi, A. B. 2007. Cloud point extraction and spectrofluorimetric determination of aluminium and zinc in foodstuffs and water samples. **Food Chemistry** 100: 1698-1703.

Talsky, G. 1994. **Derivative Spectrophotometry: Low and Higher Order**. VCH, Weinheim.

Taylor, T.A. and H.H. Patterson. 1987. Excitation resolved synchronous fluorescence analysis of aromatic compounds and fuel oil. **Anal. Chem.** 59: 2180-2187.

Vilchez, J.L., M. del Olmo, R. Avidad and L.F. Capitán-Vallvey. 1994. Determination of polycyclic aromatic hydrocarbon residues in water by synchronous solid-phase spectrofluorimetry. **Analyst** 119: 1211-1214.

Vo-Dinh, T. 1978. Multi-component analysis by synchronous luminescence spectrometry. **Anal. Chem.** 50: 398-401.

_____ and P.R. Martinez. 1981. Direct determination of selected polynuclear aromatic hydrocarbons in a coal liquefaction product by synchronous luminescence techniques. **Anal. Chim. Acta** 125: 13-19.

Williams, R.J.P. 2002. Recent aspects of aluminium chemistry and biology: A survey. **Coordination Chem. Review** 228: 93-96.

Zhong, C., Q. Wu, R. Guo and H. Zhang. 2008. Synthesis and luminescence properties of polymeric complexes of Cu(II), Zn(II) and Al(III) with functionalized polybenzimidazole containing 8-hydroxyquinoline side group. **Optical material** 30: 870-875.

Zhu, R. and W. Th. Kok. 1998. Determination of trace metal ions by capillary electrophoresis with fluorescence detection based on post-column complexation with 8-hydroxyquinoline-5-sulphonic acid. **Anal. Chim. Acta** 371: 269-277.

APPENDICES

Appendix A

Scanning speeds

Appendix Table A1 Fluorescence intensity of Al(III)-HQS obtained at various scanning speeds.

Speed (nm min^{-1})	Wavelength range of peak maximum (nm)								Scan time (min)	Range
	494	495	496	497	498	499	500	501		
10	163.23	163.66	163.67	163.86	163.76	163.48	163.25	162.73	30.00	0.38
20	164.54	165.25	165.63	165.37	165.27	164.85	164.95	164.1	15.00	0.78
50	165.27	165.8	165.92	165.27	165.63	165.84	165.23	164.78	6.00	0.65
100	165.58	165.88	165.44	165.71	165.73	165.05	164.87	165.08	3.00	0.83
150	164.90	166.72	166.09	165.24	166.07	164.82	165.39	165.23	2.00	1.90
200	165.53	166.41	164.44	167.17	165.4	165.48	164.44	165.74	1.50	2.73
250	164.36	166.03	165.69	166.88	166.28	166.42	164.31	163.94	1.20	1.19
300	165.04	165.98	166.97	166.13	165.25	167.57	165.82	163.66	1.00	2.32
350	164.68	165.53	166.16	165.99	165.83	166.08	164.97	165.25	0.86	0.63
400	165.67	165.61	166.3	165.17	167.03	166.05	164.97	165.23	0.75	1.86
450	165.13	166.71	165.37	165.38	164.94	165.91	166.67	165.56	0.67	1.77
500	165.91	166.05	165.87	164.78	165.12	165.34	166.59	165.52	0.60	1.27
550	166.38	166.21	166.22	166.07	165.47	164.3	163.78	165.18	0.55	1.92
600	166.98	167.21	165.35	166.03	167	165.11	164.92	164.98	0.50	2.10
650	163.41	164.81	165.52	166.48	165.91	168.01	165.44	165.96	0.46	3.20
700	164.94	167.59	166.22	165.57	165.52	165.52	165.52	165.93	0.43	2.07
750	165.77	165.41	166.47	165.52	166.43	166.43	166.43	166.03	0.40	1.06
800	168.59	164.72	163.43	165.16	166.49	166.49	166.49	165.31	0.38	3.06
850	165.83	166.28	167.06	166.83	168.22	168.22	168.22	163.43	0.35	1.94
900	165.23	165.31	163.87	163.8	166.91	166.91	166.91	167.79	0.33	3.11
950	166.43	168.49	166.36	166.29	164.74	164.74	164.74	166.07	0.32	3.75
1000	166.98	166.19	166.46	167.91	165.12	165.12	165.12	162.19	0.30	2.79
1050	166.01	164.43	168.68	165.6	167.05	167.05	167.05	166.33	0.29	4.25
1100	166.07	166.04	166.97	164.71	167.09	167.09	167.09	164.57	0.27	2.38
1150	167.11	164.43	164.4	165.7	165.91	165.91	165.91	167.14	0.26	1.51
1200	163.95	165.44	165.78	166.39	163.89	163.89	163.89	168.01	0.25	2.50
1250	166.99	166.24	165.87	164.19	166.11	166.11	166.11	165.21	0.24	2.05
1300	166.01	164.65	170.13	164.9	166.98	166.98	166.98	164.85	0.23	5.48
1350	162.03	166.06	166.42	169.36	166.82	166.83	166.83	164.4	0.22	3.30
1400	162.52	167.94	166.07	165.22	167.47	167.47	167.47	166.62	0.21	2.72
1450	161.04	167.03	163.74	169.3	166.84	163	165.14	165.88	0.21	6.30
1500	167.81	165.19	166.13	164.22	163.85	164.13	165.77	165.99	0.20	2.28

Appendix B

Slit widths of excitation and emission monochromators

Appendix Table B1 Fluorescence intensity of Al(III)-HQS obtained at various slit widths of excitation and emission monochromators.

Ex Slit (nm)	**Em Slit** (nm)												
	3	**4**	**5**	**6**	**7**	**8**	**9**	**10**	**11**	**12**	**13**	**14**	**15**
3	7.71	17.05	34.82	50.89	79.15	103.40	132.00	171.19	207.15	251.18	290.29	333.33	375.28
4	8.51	18.51	35.42	57.07	84.36	111.21	141.45	178.44	215.49	262.34	299.95	346.05	387.18
5	9.60	20.37	37.28	56.48	84.02	111.49	144.61	184.26	219.10	266.25	303.58	342.43	380.64
6	5.90	12.77	26.50	37.13	53.46	72.42	94.11	119.16	143.31	173.08	197.32	223.10	247.72
7	6.22	12.86	24.44	37.02	54.36	74.44	97.71	120.32	144.44	172.59	199.35	228.45	253.22
8	6.24	13.11	24.82	39.06	55.93	75.24	99.26	120.49	145.85	176.23	201.77	233.12	257.90
9	6.30	13.43	25.46	39.02	57.46	76.75	100.99	127.20	153.06	184.25	212.30	241.45	266.16
10	6.48	14.17	26.11	40.56	59.65	79.61	106.30	131.23	157.65	189.68	217.63	248.84	277.25

Appendix Table B2 Fluorescence intensity of Cd(II)-HQS obtained at various slit widths of excitation and emission monochromators.

Ex Slit (nm)	**Em Slit** (nm)												
	3	**4**	**5**	**6**	**7**	**8**	**9**	**10**	**11**	**12**	**13**	**14**	**15**
3	203.42	428.46	803.65	999.9	999.9	999.9	999.9	999.9	999.9	999.9	999.9	999.9	999.9
4	193.49	441.65	810.67	999.9	999.9	999.9	999.9	999.9	999.9	999.9	999.9	999.9	999.9
5	195.76	441.99	816.76	999.9	999.9	999.9	999.9	999.9	999.9	999.9	999.9	999.9	999.9
6	119.76	260.78	480.97	758.81	999.9	999.9	999.9	999.9	999.9	999.9	999.9	999.9	999.9
7	119.87	257.26	487.64	761.67	999.9	999.9	999.9	999.9	999.9	999.9	999.9	999.9	999.9

Appendix C

Calculation of stability constants

Calculation of stability constant of Cd(II)-HQS complex

The stability constant, K_s of complex between cadmium(II) and HQS in NH_3-NH_4Cl buffer solution of pH 8.8 was determined. The formation reaction of complex, initial concentration and equilibrium concentration should be:

	Cd^{2+}	+	HQS	[Cd(HQS)]
Initial:	1×10^{-4}		1×10^{-4}	0
Equilibrium:	(1×10^{-4})-c		(1×10^{-4})-c	c

$$K_s = \frac{\text{[Cd-(HQS) complex]}}{\text{[Cd][HQS]}} \quad (1)$$

$$= \frac{c}{((1\times 10^{-4})-c))^2} \quad (2)$$

For the determination of stability constant, the equilibrium concentration, c, was observed from equation (3)

$$F = Kc \quad (3)$$

where F = The radiant power or intensity of emitted fluorescence at the optimum ratio

c = equilibrium concentration of Cd-(HQS) complex

The fluorescence intensity of complex was observed by continuous variation method from the optimum ratio of cadmium(II):HQS at 1:1 which yielded the maximum fluorescence of 311.10. The equilibrium concentration was calculated from the calibration curve of cadmium(II) complex which obtained from continuous variation method. The result is shown in Appendix Figure C1.

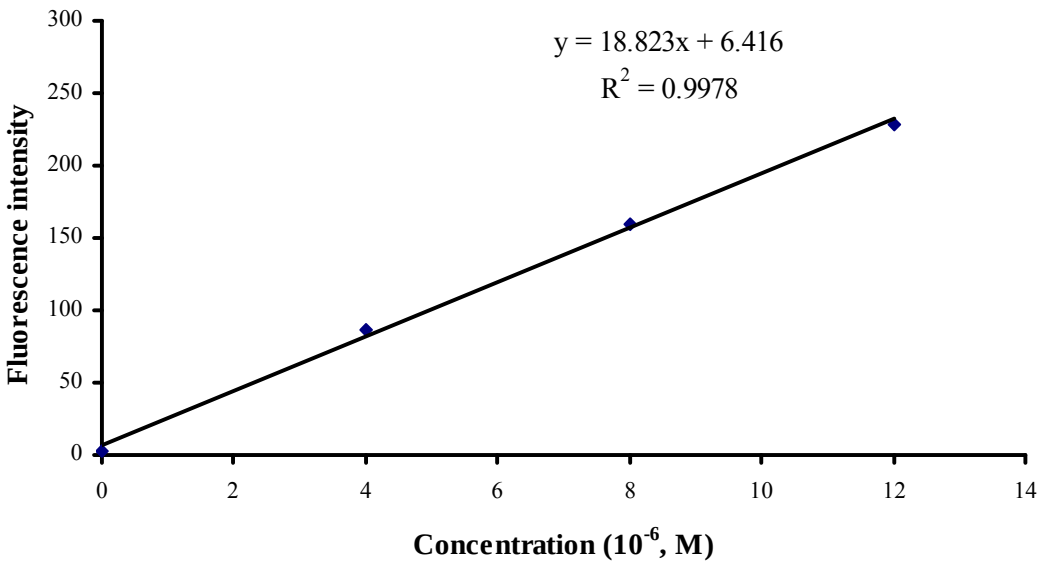

Appendix Figure C1 Calibration graph of Cd(II)-HQS.

The equilibrium concentration of complex was calculated from linear equation (4) of calibration curve as shown above.

$$y = 18.823x + 6.416 \quad (4)$$

where $y = F$ = The radiant power or intensity of emitted fluorescence at the optimum ratio

$x = c$ = equilibrium concentration of Cd-(HQS) complex

$$c = (311.10\text{-}6.416)/18.823$$
$$= 16.19\times10^{-6}\ \text{M}$$
$$= 1.62\times10^{-5}\ \text{M}$$

The stability constant, K_s of equation (2) is

$$K_s = \frac{1.62\times10^{-5}}{((1\times 10^{-4}) - 1.62\times10^{-5}))^2}$$
$$= \frac{1.62\times10^{-5}}{(8.38\times10^{-5})^2}$$
$$= 2314.29$$

Calculation of stability constant of Al(III)-HQS complex

The stability constant, K_s of complex between aluminium(III) and HQS in CH_3COOH-CH_3COONa buffer solution of pH 4.0 was determined. The reaction of complex formation, initial concentration and equilibrium concentration should be:

	Al^{3+}	+	HQS	[Al-(HQS)]
Initial:	1×10^{-4}		1×10^{-4}	0
Equilibrium:	(1×10^{-4})-c		(1×10^{-4})-c	c

$$K_s = \frac{\text{[Al-(HQS) complex]}}{\text{[Al][HQS]}} \quad (1)$$

$$= \frac{c}{((1\times 10^{-4})-c))^2} \quad (2)$$

For the determination of stability constant, the equilibrium concentration, c, was observed from equation (3)

$$F = Kc \quad (3)$$

where F = The radiant power or intensity of emitted fluorescence at the optimum ratio

c = equilibrium concentration of Al(III)-(HQS) complex

The fluorescence intensity of complex was observed by continuous variation method from the optimum ratio of aluminium(III):HQS at 1:1 which yielded the maximum fluorescence of 268.37. The equilibrium concentration was calculated from the calibration curve of aluminium(III) complex which obtained from continuous variation method. The result is shown in Appendix Figure C2.

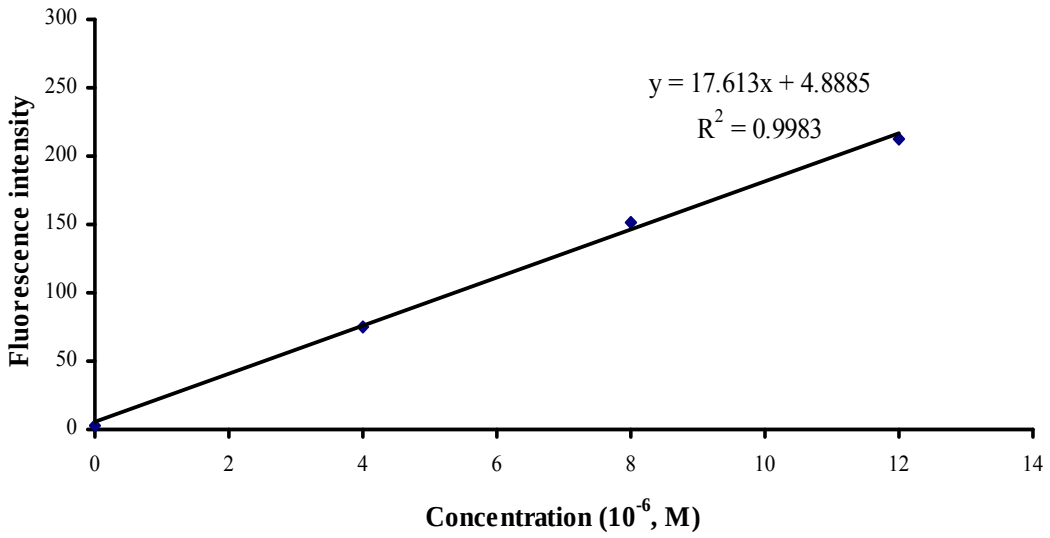

Appendix Figure C2 Calibration graph of Al(III)-HQS.

The equilibrium concentration of complex was calculated from linear equation (4) of calibration curve as shown above.

$$y = 17.613x + 4.8885 \quad (4)$$

where $y = F$ = The radiant power or intensity of emitted fluorescence at the optimum ratio

$x = c$ = equilibrium concentration of Al(III)-HQS complex

$$c = (268.37\text{-}4.8885)/\ 17.613$$
$$= 14.96\times10^{-6}\ \text{M}$$
$$= 1.50\times10^{-5}\ \text{M}$$

The stability constant, K_s of equation (2) is

$$K_s = \frac{1.50\times10^{-5}}{((1\times 10^{-4}) - 1.50\times10^{-5}))^2}$$
$$= \frac{1.50\times10^{-5}}{(8.5\times10^{-5})^2}$$
$$= 2076.12$$

Appendix D

SSF spectra of Cd(II)-HQS, Al(III)-HQS, and binary mixture at various Δλs

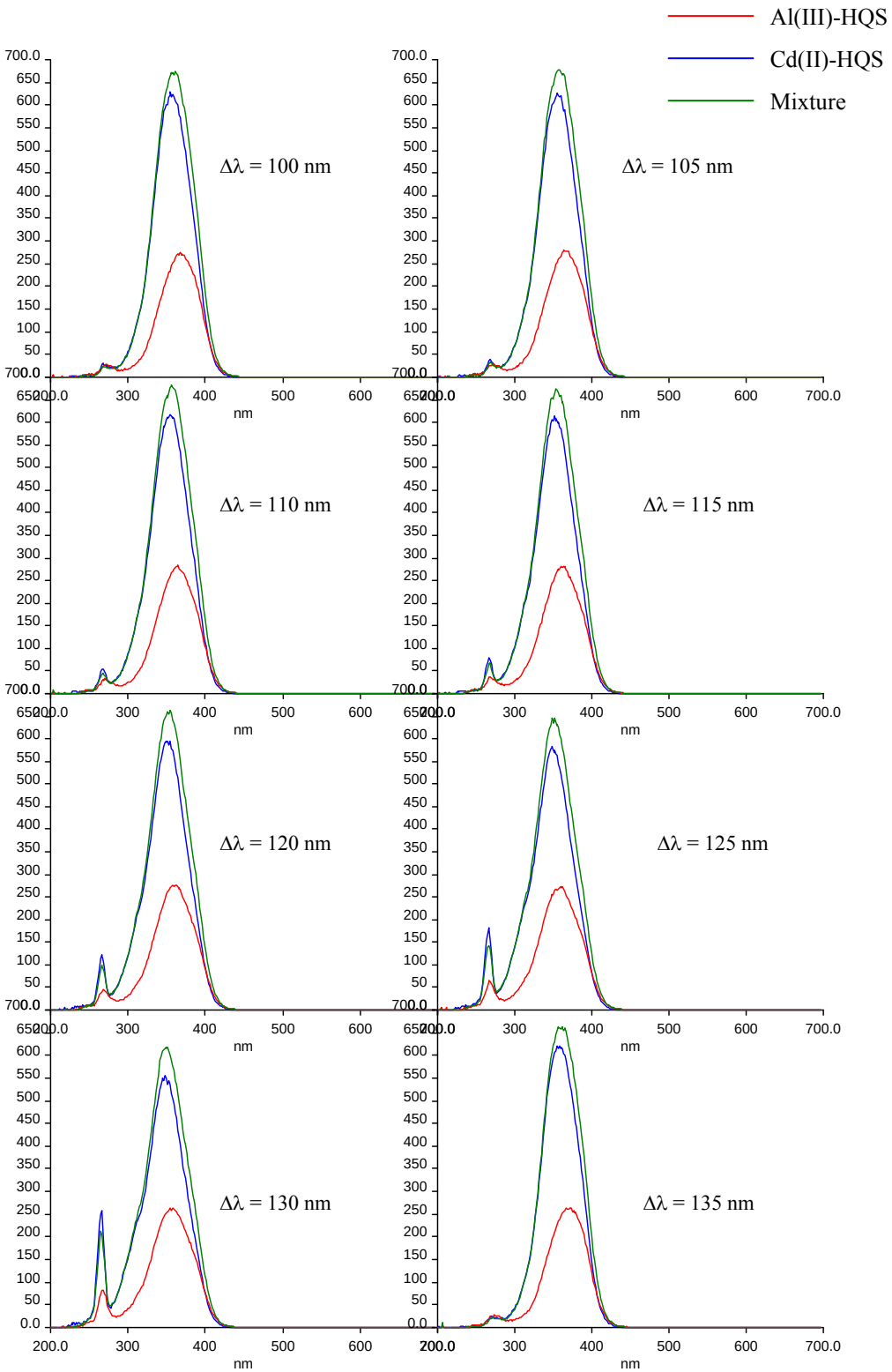

Appendix Figure D1 SSF spectra of Cd(II)-HQS, Al(III)-HQS, and binary mixture, buffered to pH 8.8, at various Δλs.

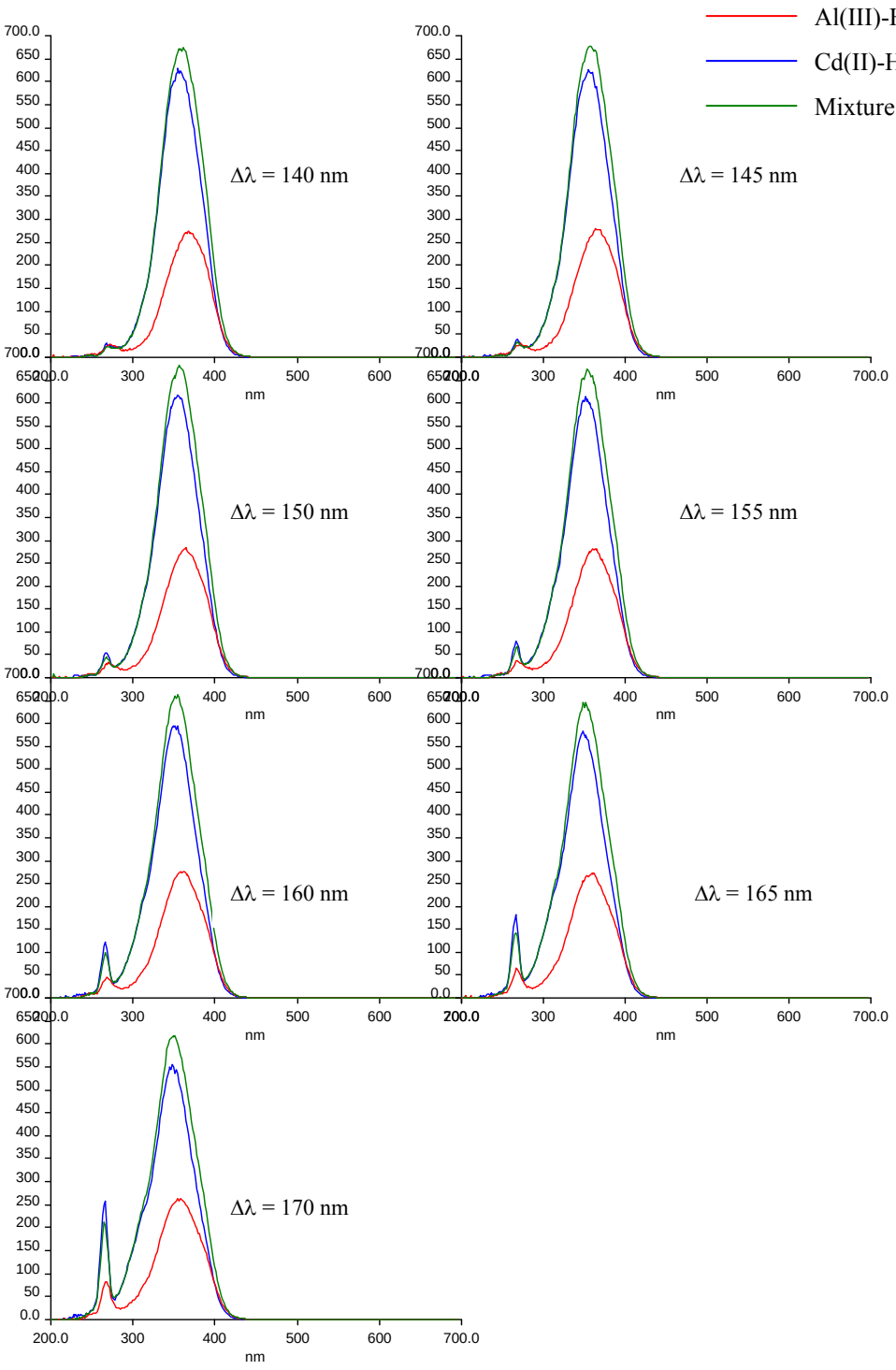

Appendix Figure D1 (Continued)

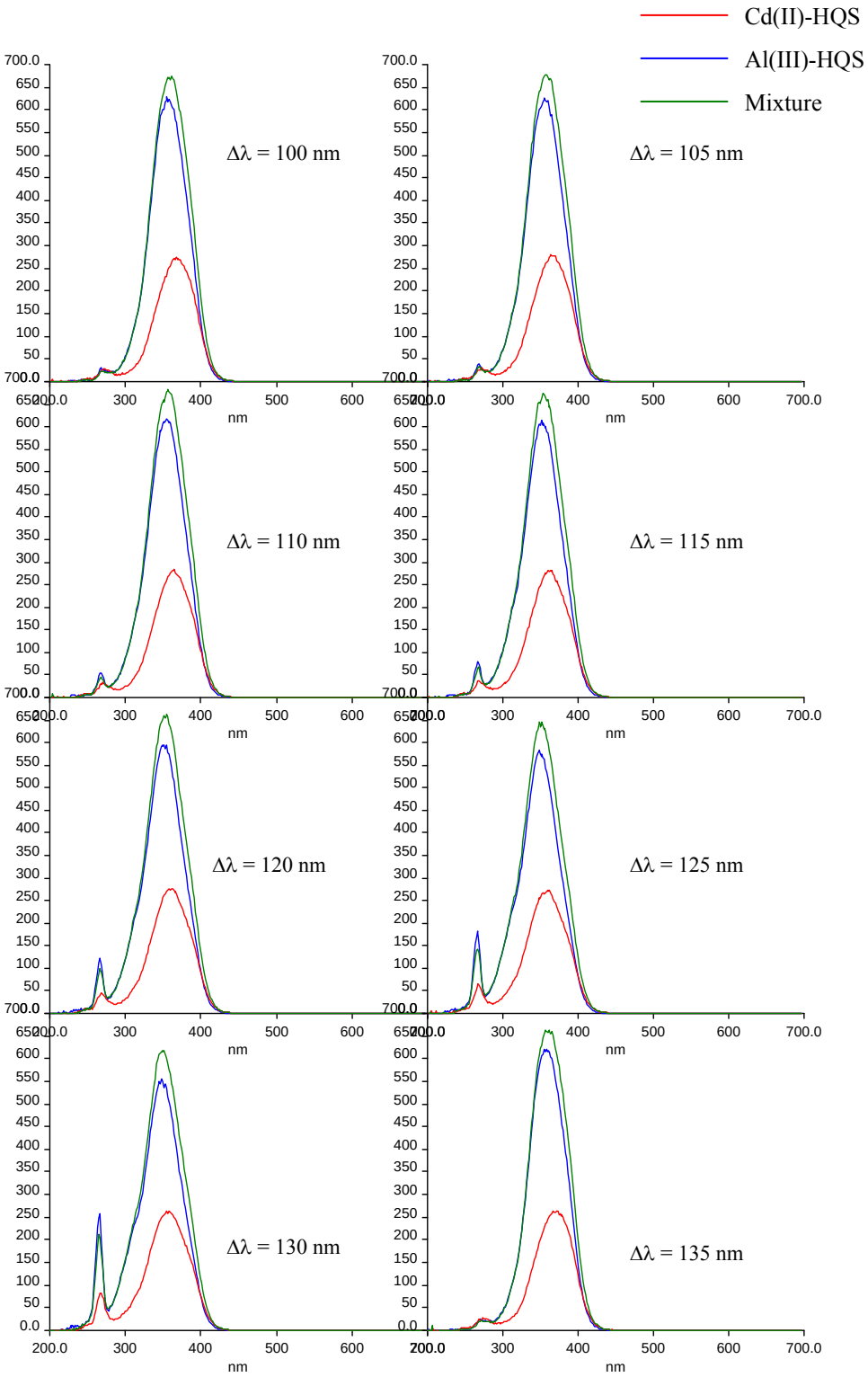

Appendix Figure D2 SSF spectra of Cd(II)-HQS, Al(III)-HQS, and binary mixture, buffered to pH 4.0, at various Δλs.

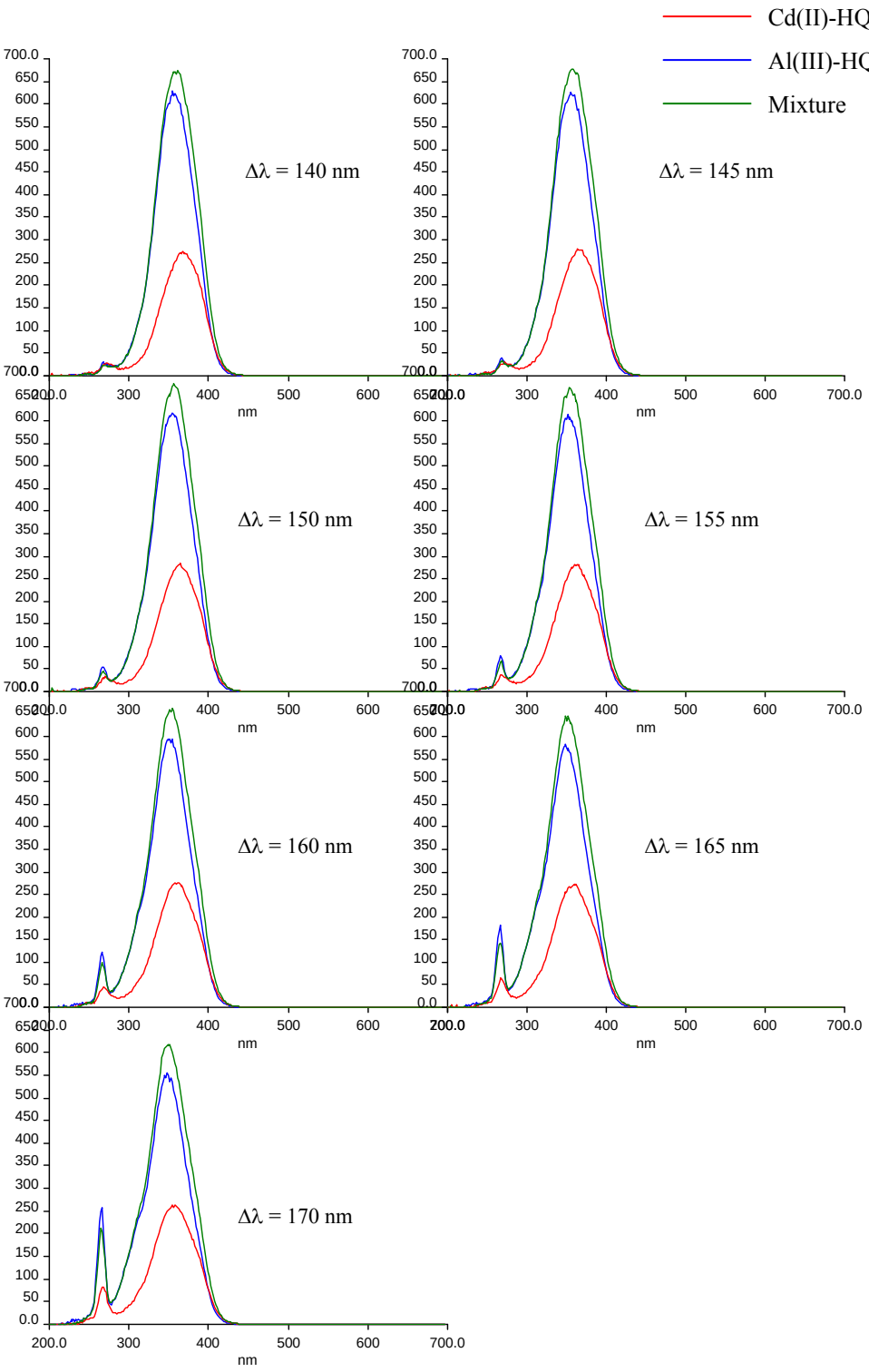

Appendix Figure D2 (Continued)

Appendix E

FL-WinLab Programme for calculation of D1SSF and D2SSF spectra

First- and second-derivative calculation of SSF spectrum by the FL WinLab

1. Doubly click on the **FL-WinLab** shortcut icon.

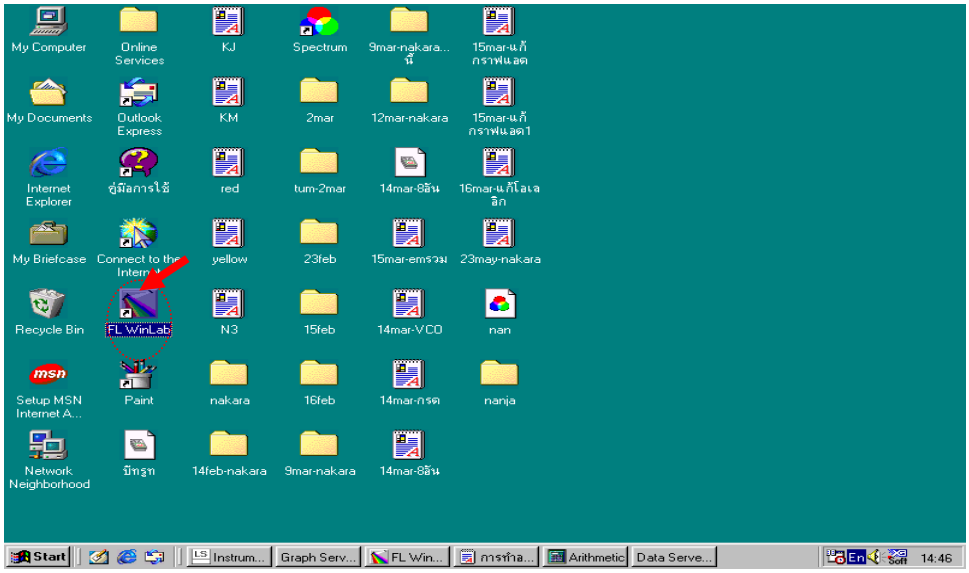

The FL WinLab application is displayed.

2. Select **Arithmetic** from the *Data Handling* menu.

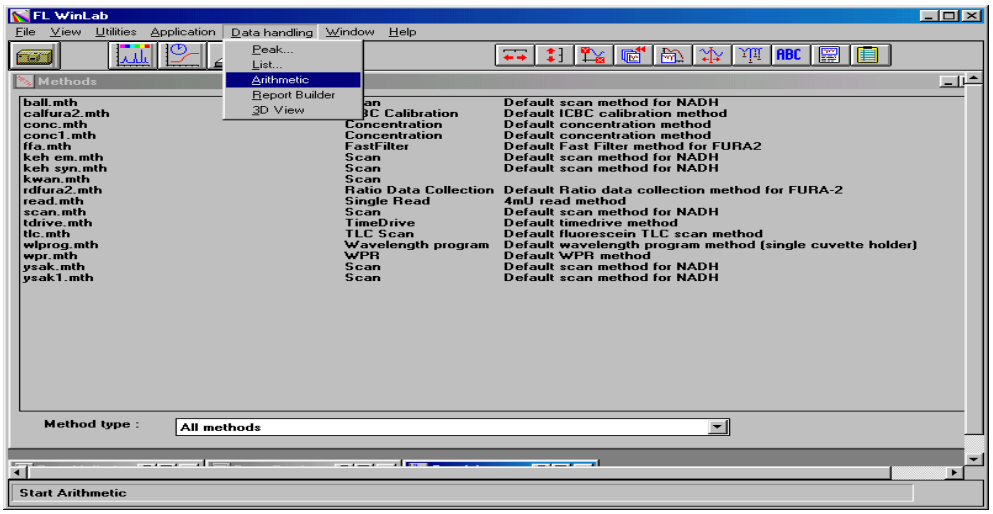

The Arithmetic-[Graph Window] application is displayed.

3. Select **Open** from the File menu, or click on  icon.

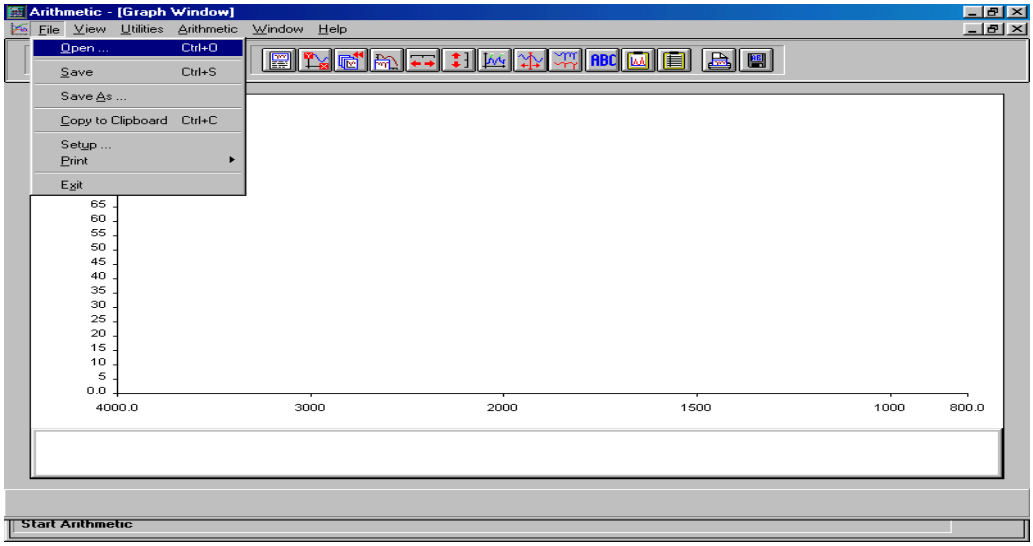

4. Select the spectrum (or spectra) wished to perform the calculation.

The spectrum is displayed in the Arithmetic-[Graph Window].

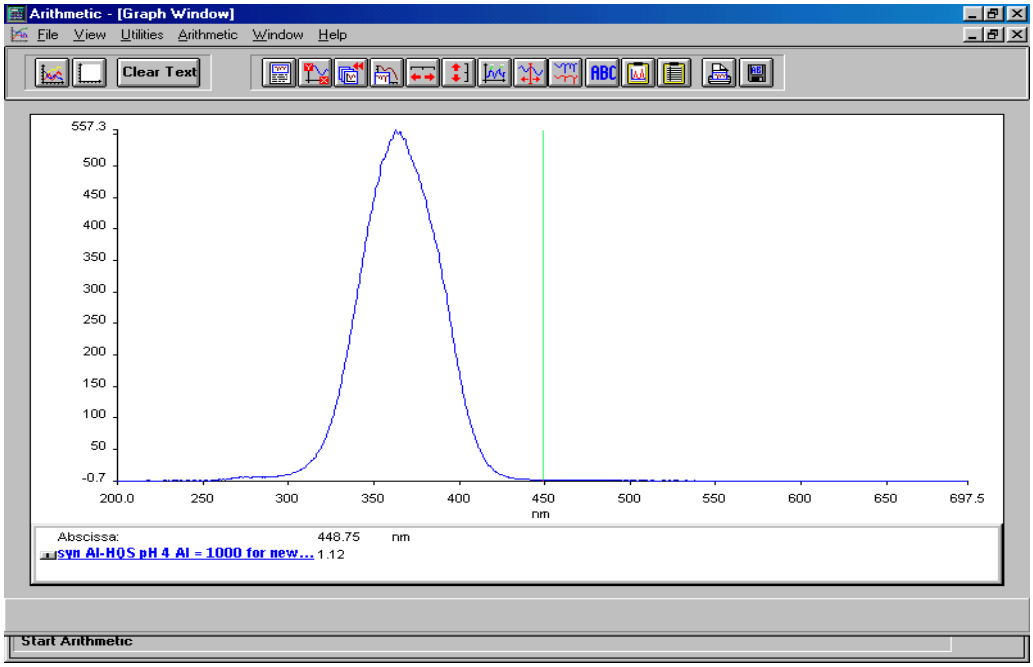

5. Select **Arithmetic** and click **Derivative** from the drop-down list.

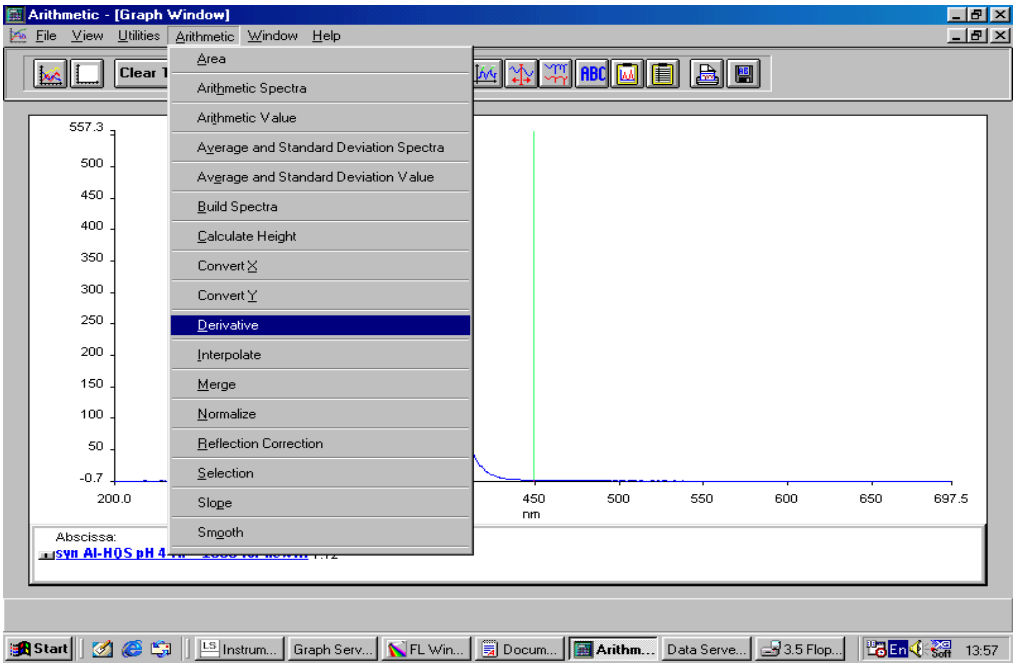

Two windows, *i.e.* Graph and Result windows, are displayed.

6. Select the **Derivative Order**, under Graph Window, wished to apply to the spectrum from the drop-down list.

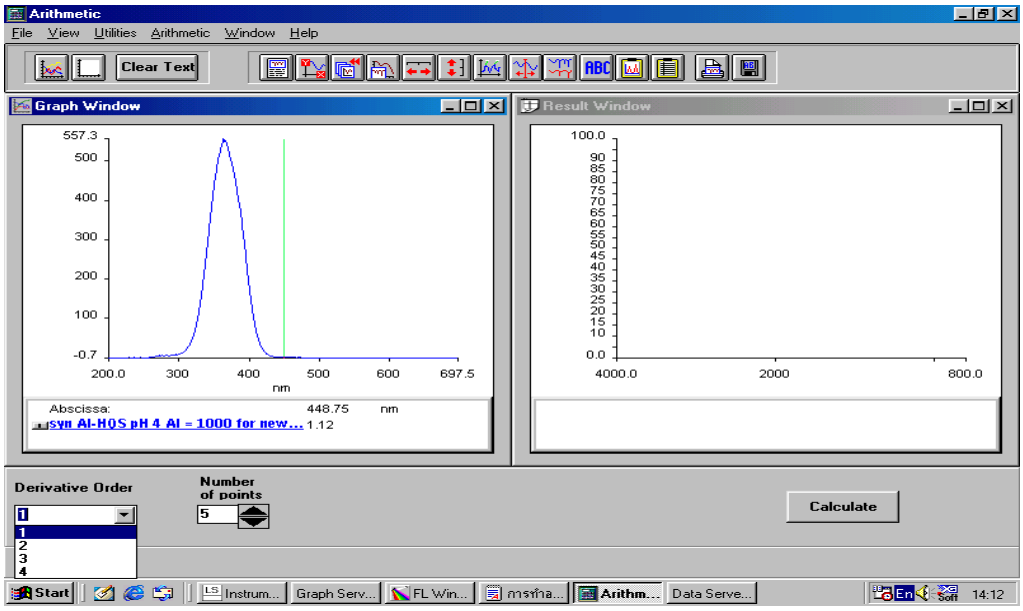

7. Select the **Number of points** required.
8. Click **the Calculate** function key.

   The derivative spectrum is calculated and then displayed in the Result Window.

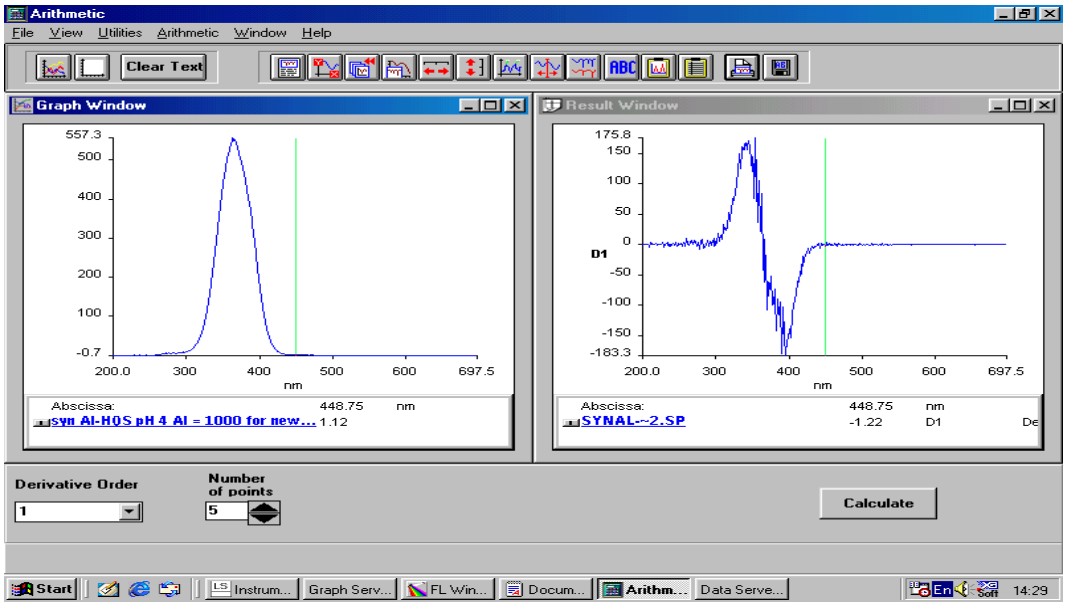

9. To save the result spectrum, activate the Result Window and click Save as from the File menu.

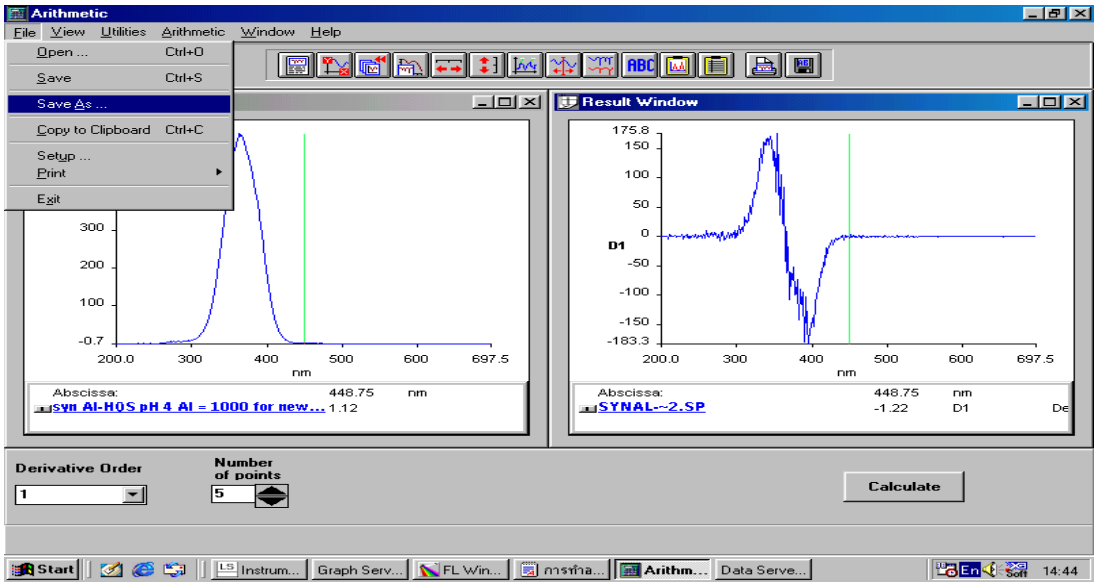

CURRICULUM VITAE

NAME : Miss Nisa Nauangchamnong

BIRTH DATE : January 14, 1983

BIRTH PLACE : Chonburi, Thailand

EDUCATION

: YEAR	**INSTITUTION**	**DEGREE/DIPLOMA**
2004	Thammasat Univ.	B.Sc. (Chemistry)

POSITION/TITLE : -

WORK PLACE : -

SCHOLARSHRIP : Center for Innovation in Chemistry: Postgraduate Education and Research Program in Chemistry (PERCH-CIC)